Jagiellonian University
in Kraków
Faculty of Biochemistry, Biophysics, and Biotechnology

Małgorzata Kajstura

Effects of Geldanamycin, a Ligand of Heat Shock Protein 90, on Cell Cycle Progression and Induction of Apoptosis in Human Lymphocytes and Jurkat Cells

Ph.D. Thesis

The experimental work was performed at the Brander Cancer Research Institute, New York Medical College, Valhalla, New York, USA

Thesis Advisor: Professor Jerzy Dobrucki, Ph.D., D.Sc.

Kraków, 2018

I am immensely indebted to Professor Zbigniew Darzynkiewicz, M.D., Ph.D, for introducing me to the fascinating world of flow cytometry.

ABSTRACT

Heat shock protein 90 (HSP90), which is implicated in post-translational folding, stability, and maturation of proteins, controls several key cell cycle regulators. Thus, the hypothesis was raised that geldanamycin, a specific and potent inhibitor of HSP90 function, may have pronounced effects on cell cycle progression. The objective of this study was to test this hypothesis in normal and cancer cells of human origin.

The experiments performed on human lymphocytes mitogenically stimulated by phytohemagglutinin (PHA) indicated that 100 nM or 150 nM geldanamycin induces transition of cells to the G0 state of cell cycle. This was documented utilizing acridine orange, a metachromatic dye which differentially stains DNA versus RNA. The same experimental protocol allowed demonstration that geldanamycin is a potent inducer of apoptosis in PHA-activated cells. Importantly, both the block in G0 and induction of apoptosis were reversible and returned to control values upon removal of geldanamycin. Similar conclusions were reached when cell number in cultures was analyzed, excluding the possibility that a relevant fraction of cells was disintegrated during the incubation period.

Experiments on Jurkat line of acute T-cell leukemia were performed next. Jurkat cells were used here as a model system in which the cytostatic and cytotoxic properties of geldanamycin on cancer cells can be tested. Initial experiments determined the time course and concentration-dependence of geldanamycin-induced alterations in cell cycle distribution and apoptosis. In contrast to human lymphocytes, geldanamycin did not induce G0 arrest in Jurkat cells, but inhibited them initially in the G2 phase, and at later time points in the G1 phase. The G2 was distinguished from mitosis by the absence of phosphorylation of histone H3, a specific marker of mitotic cells. The inhibition of Jurkat cells in G1 was linked to a decrease in phosphorylation of retinoblastoma protein. Finally, the exposure of Jurkat cells to geldanamycin resulted in induction of apoptosis, predominantly in cells being arrested in G1 and G2/M phases of the cell cycle.

Finally, to address the possibility that stimulation of nuclear factor kappa-B (NF-κB), downstream of HSP90, modulates the effects of geldanamycin on cancer cells, Jurkat IκBαM line was employed. These cells cannot activate their NF-κB-mediated responses

because of the mutation in its inhibitory protein, IκB. In the absence of functional NF-κB, geldanamycin-mediated induction of apoptosis and loss of cycling cells were markedly higher than when NF-κB was functional. These results were further corroborated by experiments in which parthenolide, a plant-derived inhibitor of NF-κB was employed. Geldanamycin-treated Jurkat cells responded to the parthenolide challenge by partial arrest in S phase and increased cell death by apoptosis.

In conclusion, inhibition of HSP90 by geldanamycin blocks cell cycle progression and induces apoptosis of Jurkat cells, and NF-κB mediates these effects. The newly identified network of interactions may facilitate understanding of the mechanism of cytostatic and cytotoxic action of geldanamycin derivatives used currently in clinical trials.

ABBREVIATIONS

AO: acridine orange

AHBA: 3-amino-5-hydroxybenzoic acid

bcr-Abl: breakpoint cluster region - Abelson

BSA: bovine serum albumin

Cdk: cyclin-dependent kinase

CTD: C-terminal domain

DAPI: 4',6-diamidino-2-phenylindole

DMSO: dimethyl sulfoxide

EGFR: epidermal growth factor receptor

ErbB: erythroblastic leukemia viral oncogene B

FITC: fluorescein isothiocyanate

Grp94: glucose-regulated protein

HBSS: Hanks' balanced salt solution

HSP: Heat shock protein

HER-2: human epidermal growth factor receptor 2

IGF1R: insulin-like growth factor 1 receptor

I-κB: inhibitor of NF-κB

IKK: I-κB kinase

MMP2: matrix metalloproteinase 2

MHC: major histocompatibility complex

MD: middle domain

Myt1: myelin transcription factor 1

NF-κB: nuclear factor κB

NTD: N-terminal domain

PBS: phosphate buffered saline

PDGFR: platelet-derived growth factor receptor

PHA: phytohaemagglutinin

PI: propidium iodide

PKS: polyketide synthase

pRb: hyperphosphorylated retinoblastoma protein

PTEN: phosphatase and tensin homolog

Rb: retinoblastoma protein

Trap1: TNF Receptor-Associated Protein 1

Wee1: nuclear protein kinase belonging to the Ser/Thr family

TABLE OF CONTENT

INTRODUCTION

Structure and synthesis of geldanamycin

Geldanamycin is a benzoquinoid ansamycin antibiotic which has profound effects on eukaryotic cells. It was isolated for the first time from the actinomycete, *Streptomyces hygroscopicus* var. *geldanus* var. *nova* in 1970 [DeBoer *et al.* 1970]. Similarly to other ansamycins, geldanamycin is composed of an aromatic moiety bridged by an aliphatic chain. The structure of geldanamycin is illustrated in **Figure 1**.

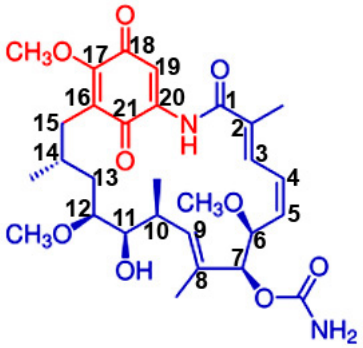

Figure 1. The molecule of geldanamycin. The aromatic part is shown in red, while the aliphatic bridge is depicted in blue. The numbering of carbon atoms is indicated. Molecular weight of geldanamycin is 561.

The biosynthesis of ansamycins begins with the assembly of 3-amino-5-hydroxybenzoic acid [He *et al.,*2006; Lee *et al.*, 2006; Chang *et al.*,2014; Li *et al.*, 2015]. Next, a set of polyketide synthases catalyzes the sequential addition of extender units: acetate, propionate, and glycolate, resulting in the formation of progeldanamycin (**Figure 2**). This initial product is subsequently processed to form geldanamycin by a series of addition reactions: C-17 hydroxylation, C-17 O-methylation, C-21 oxidation, C-7 carbamoylation, and C-4,5 oxidation (**Figure 2**).

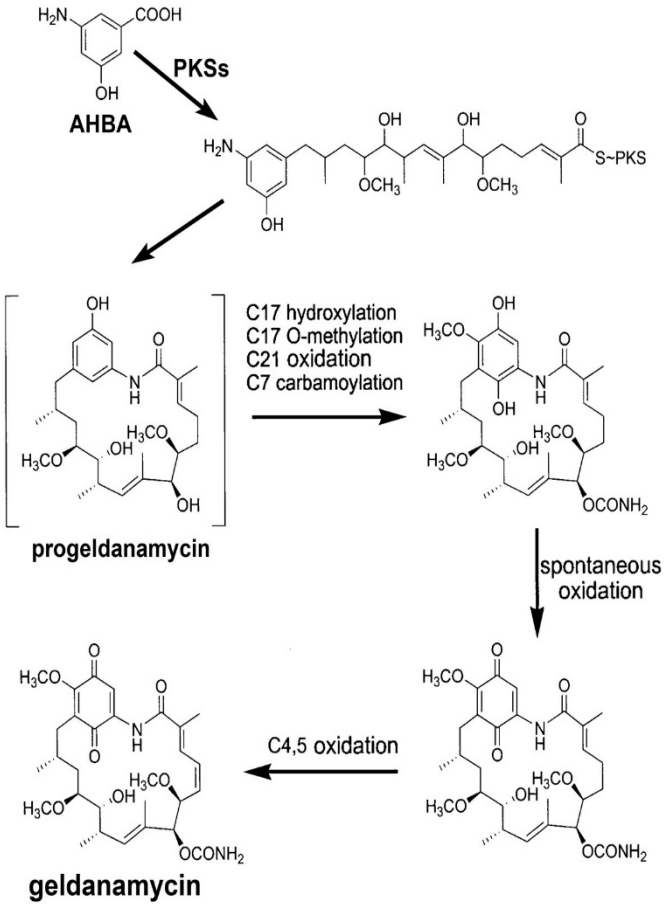

Figure 2. Geldanamycin synthesis pathway. Multiple steps leading to the formation of geldanamycin are illustrated. AHBA: 3-amino-5-hydroxybenzoic acid; PKSs: polyketide synthases. For the numbering of carbon atoms see Figure 1. Adapted from [Lee *et al*., 2006].

Geldanamycin is a potent antibiotic and antifungal agent [Piper and Millson, 2012; Hill *et al*., 2013]. However, it was only after the

demonstration of its interaction with the heat shock protein 90 (HSP90) that a great interest in geldanamycin has developed.

HSP 90

Heat shock proteins (HSPs) were so named because they were observed for the first time in cells exposed to elevated temperature. The evidence of heat shock response was initially documented by Ferruccio Ritossa in puffs of the salivary glands of *Drosophila* [Ritossa, 1962; Ritossa, 1996] after the temperature of an incubator housing the flies was incidentally increased. To date, multiple HSPs have been identified; they differ in size and are named according to their molecular weight. The HSP superfamily comprises five well-conserved families of proteins: HSP33, HSP60, HSP70, HSP90, and HSP100, the names are derived from their molecular weights, which are 33, 60, 70, 90 and 100 kDa, respectively [Erlejman *et al*., 2014, Wu *et al*., 2017].

The 90 kDa member of the HSPs family, HSP90, is a protein that was highly conserved in the evolution. There is approximately 50% similarity of the protein chain sequence between *Escherichia coli*, yeast, fruit fly, trypanosomes, and mammals, including humans [Borkovich *et al.*, 1989]. Most organisms contain two cytosolic isoforms of HSP90, which exhibit 85% homology in mammalian cells [Chen *et al*., 2006]. They correspond to a stress-inducible isoform HSP90α and a constitutively expressed isoform HSP90β [Hickey *et al.*, 1989]. Additionally, a mitochondrial form of HSP90, Trap1, and a form localizing to the endoplasmic reticulum, Grp94, are expressed in mammals [Sreedhar and Csermely, 2004].

HSP90 is ubiquitously expressed in the cytosol of eukaryotic and prokaryotic cells [Erlejman *et al*., 2014]. In unstressed cells, HSP90 accounts for 1-2% of all cell proteins, while induction of stress increases its cellular content to 4-6% [Messaoudi *et al*., 2011]. A small fraction of this protein, 2-3%, exhibits nuclear localization [Sawarkar and Paro, 2013], and this fraction can also increase under stressful conditions [Katschinski *et al.*, 2002; Lamoth *et al*., 2012]. There are only two known exceptions to the intracellular localization of HSP90. The isoform HSP90α, which is typically present in the cytoplasm, was also identified as an extracellular chaperone of matrix metalloproteinase 2 (MMP2) [Eustace *et al*., 2004]. It also serves extracellularly as a chaperone of HER-2, a member of the ErbB family of receptor tyrosine kinases [Sidera *et al*., 2008]. Given these

extracellular functions, it was not a surprise that HSP90 could be found on the external surface of the cell membrane [Sidera and Patsavoudi, 2008]. The association of HSP90 with receptors affecting cytoskeletal rearrangements implicates its involvement in cell motility, invasion, and metastasis, essential features of cancer cells [Sidera *et al*., 2008; Sidera and Patsavoudi, 2008; Tsutsumi *et al*., 2008, Jurczyszyn *et al*., 2014].

The structural and functional studies of HSP90 have proven to be an arduous endeavor. One of the reasons for this complexity is the broad range of cellular processes in which HSP90 is involved. Moreover, the function of HSP90 often relies on binding of various co-chaperones at the same time. In unstressed cells, HSP90 takes part in nascent protein folding, as well as in maintenance, degradation, and activation of proteins. HSP90 prevents the formation of protein aggregates, regulates intracellular transport, cell signaling, DNA replication and repair, gene transcription, telomere maintenance, and antigen processing for presentation by MHC class I and II antigens [Rajagopal *et al*., 2006; Richter *et al*., 2007; DeZwaan and Freeman, 2008; DeZwaan and Freeman, 2010; Eckl and Richter, 2013; Barrott and Haystead., 2013; Hu *et al*., 2015]. The number of proteins with diverse functions for which HSP90 is a molecular chaperone is continuously growing. An up-to-date list of molecules with which HSP90 interacts, co-chaperones as well as client proteins, is compiled and maintained by D. Picard on his website [http://www.picard.ch/downloads/Hsp90interactors.pdf]. As of now (December 2017), this list comprises over 700 entries.

Structure of HSP90 and its interaction with geldanamycin

At physiologic temperatures, HSP90 exhibits a structure of a homodimer [Wandinger *et al*., 2008] with each protomer comprised of three domains, N-terminal (NTD), middle (MD) and C-terminal domain (CTD) (**Figure 3**). The N-terminal domain contains an ATP binding site, while the C-terminal domain is responsible for dimerization of the chaperone and also serves as a binding site for co-chaperons containing a tetratricopeptide repeat (TPR) structural motifs. TPRs consist of a sequence of 34 amino acids; this sequence is conserved between proteins and across the species. TPRs are found in tandem arrays of 3–16 motifs which provide the structural basis for protein-protein interactions including the formation of multiprotein complexes, such as chaperone/co-chaperone/client protein [Spelt *et al*., 2015].

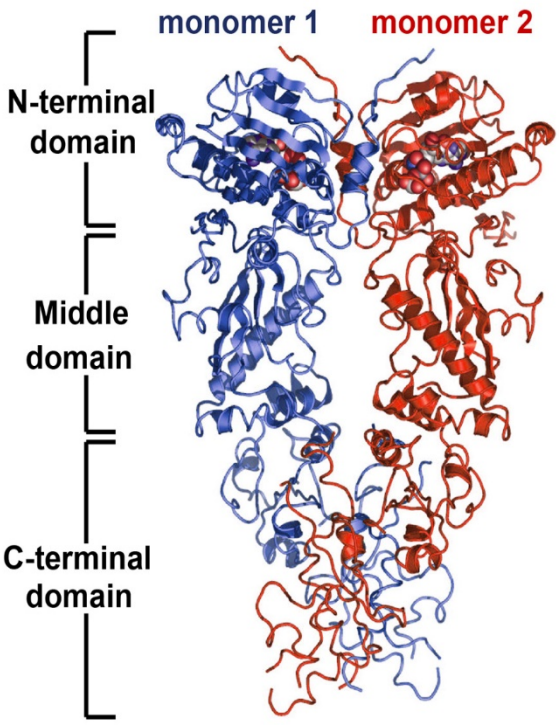

The middle domain is believed to be the binding site of client substrates. Analysis of HSP90 interactions with its client substrates through small-angle X-ray scattering [Street *et al.*, 2011], crystal structure analysis [Pearl and Prodromou, 2006], electron microscopy and cryo-EM [Southworth and Agard, 2011] revealed client-induced changes in the conformation of the complex and its structural flexibility. Specifically, it has been proposed that binding of the client protein to HSP90 induces conformational changes in this molecule by bringing the NTDs closer together [Street *et al*., 2011; Krukenberg *et al*., 2011].

Figure 3. Three-dimensional structure of an HSP90 dimer. The two monomers are illustrated by blue and red color, respectively. The location of the three major domains of HSP90 is also indicated. Modified from [Pearl and Prodromou, 2006].

Additionally, dramatic changes in the conformation of dimerized HSP90 occur upon binding the molecule of ATP, and following hydrolysis of this nucleotide (**Figure 4**). These conformational changes in HSP90 are believed to be relevant in the process of activation and stabilization of the client proteins [Pearl and Prodromou, 2006; Southworth and Agard, 2011; Krukenberg *et al*., 2011; Seo, 2015; Flynn *et al*., 2015].

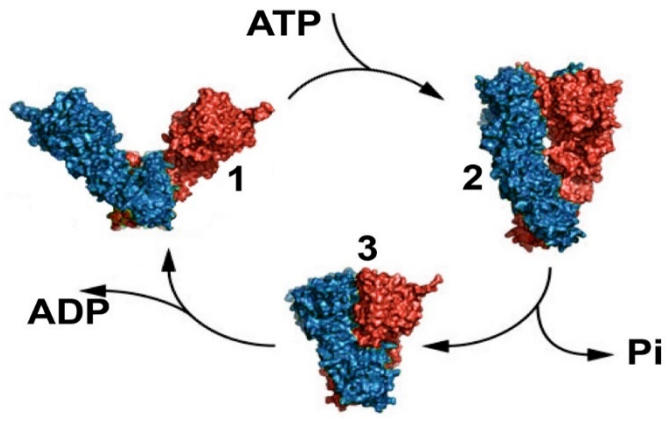

Figure 4. Conformational changes of HSP 90. During the ATP-dependent conformational cycle, binding of the nucleotide alters the conformation from an open structure of dimerized HSP90 (1) to more closed configuration (2). Hydrolysis of ATP and release of P_i results in a further compaction of the protein (3). Dissociation of ADP restores the open conformation and restarts the conformational cycle. The two monomers are illustrated by blue and red color, respectively. Modified from [Krukenberg *et al*., 2011].

A crucial feature of the ATP binding site, which is located in a hydrophobic pocket within the NTD, is its ability to bind geldanamycin with high affinity despite the structural differences between this antibiotic and ATP. Mechanistically, binding of geldanamycin to HSP90 prevents ATP-mediated conformational changes in the protein, disrupting the complexes between the chaperone and its client proteins [An *et al*., 2000, Seo, 2015]. This mode of action is consistent with the result of the classic experiment of Whitesell and collaborators on the effect of geldanamycin on 3T3 fibroblasts expressing v-src kinase [Whitesell *et al*., 1994]. They noted a stark contrast between the ability of geldanamycin to inhibit v-src kinase activity in intact cells and its inability to act as an inhibitor of the kinase in an *in vitro* assay. In the search for the reason for this discrepancy, the crucial role of HSP90 in cancer cell signaling was established for the first time [Dai and Whitesell, 2005; Cullinan and Whitesell, 2006; Whitesell and Lin, 2012].

HSP90, the cell cycle, and cancer

Several lines of evidence point to the critical role of HSP90 in cell cycle progression [reviewed in Burrows *et al*., 2004; Sankhala *et al*., 2011; Jackson, 2013]. The mRNA encoding HSP90 is markedly upregulated at the G1-S phase transition [Jérôme *et al*., 1993]. Moreover, specific blockade of HSP90 mRNA by the introduction of an expression vector containing anti-sense cDNA for HSP90 results in a decreased proliferation in human cells in vitro [Galea-Lauri *et al*., 1996]. Consistent with the role of HSP90 in the control of cell cycle, a small but measurable fraction of this protein is compartmentalized in the nucleus, and during mitosis remains associated with centromeres [Lange *et al*., 2000; Sawarkar and Paro, 2013].

HSP90, as a molecular chaperone, is implicated in post-translational folding, stability, and maturation of hundreds of different proteins. It is therefore conceivable that HSP90 may affect the progression through the cell cycle by interacting with cell cycle-regulating client proteins. In fact, it is well recognized that, in addition to upstream effects, HSP90 directly controls many critical cell cycle regulators [Neckers and Ivy, 2003, Zhang and Burrows, 2004; Burrows *et al*., 2004]. Table I lists the most important examples in this category.

Table I: Cell cycle regulators associated with HSP90

Client Protein	Function	Reference
Cdk1	regulator of G2 checkpoint	[Zhang and Burrows, 2004]
Cdk2	regulator of G1/S and G2/M transitions	[Burrows *et al.*, 2004]
Cdk4	partner of cyclin E, phosphorylation of Rb	[Munoz and Jimenez, 1999]
Cdk6	essential for the initiation of S phase	[Bedin *et al.*, 2004]
Cyclin B	G2 checkpoint, initiation of mitosis	[Zhang and Burrows, 2004]
Cyclin D	regulator of G1/S transition	[Stepanova *et al.*, 1996]
Cyclin E	entry into S phase	[Burrows *et al.*, 2004]
c-Myc	protooncogene	[Mahony *et al.*, 1998]
DNA polymerase α	DNA synthesis	[Munster *et al.*, 2001]
IGF1R	receptor of growth factor	[Munster *et al.*, 2001]
PDGFR	receptor of growth factor	[Munster *et al.*, 2001]

In addition to cell cycle regulators, the clientele of HSP90 involves *bona fide* oncoproteins implicated in several types of cancers [Workman *et al.*, 2007; Neckers and Workman, 2012; Chatterjee *et al.*, 2016]. These targets include a wide range of oncogenic kinases, such as ErbB2 (Her2) [Jeong *et al.*, 2017], EGFR [Yang *et al.*, 2016], B-Raf [Eckl *et al.*, 2016], c-Raf [Mitra *et al.*, 2016], Akt [Ke *et al.*, 2017], Met [Karkoulis *et al.*, 2013], and Bcr-Abl [Kancha *et al.*, 2013]. HSP90 interacts with the estrogen receptor, a transcription factor essential for the development of breast cancer [Chang *et al.*, 2014], and with the androgen receptor, a transcription factor essential for the development of prostate cancer [Uo *et al.*, 2017]. Other transcription factors implicated in oncogenesis, such as p53 and HIF-1α, require HSP90 for the maintenance of their stability [Li and Marchenko, 2017; Zhang *et al.*, 2017]. Finally, HSP90 activates the catalytic subunit of telomerase [DeZwaan and Freeman, 2010], permitting unlimited proliferation of cells and their evolution into a fully transformed cancerous state [Martínez and Blasco 2017].

Geldanamycin and the cell cycle

The ability of HSP90 to function as a chaperone of multiple cell cycle-related proteins strongly suggests that geldanamycin, a potent inhibitor of HSP90, can have significant consequences on cell cycle progression. Surprisingly, in spite of numerous clinical trials testing geldanamycin and its derivatives as anti-cancer drugs [Nowakowski *et al.*, 2006; Lancet *et al.*, 2010; Vaishampayan *et al.*, 2010; Siegel et al., 2011; Gartner *et al.*, 2012; Iyer *et al.*, 2012; Barrott and Haystead, 2013; Kim *et al.*, 2013; Modi *et al.*, 2013; Wagner

et al., 2013; Saif *et al*., 2013; Schenk *et al*., 2013; Walker *et al*., 2013; Bhat *et al*., 2014; Pedersen *et al*., 2015; see also unpublished trials listed at *ClinicalTrials.gov*: NCT00079404, NCT00088374, NCT00093405, NCT00098423, NCT00118092, NCT00118248, NCT01228435, NCT01427946], the information available on the impact of geldanamycin on cell growth and death is manifestly scant.

Short-term studies indicated a reduction in the proportion of cells in S phase in one line of urinary bladder cancer cells, but not in another [Karkoulis *et al*., 2013]. Human gastric carcinoma MGC803 cells responded to the geldanamycin treatment by a decrease in proliferation rate, but whether this was due to cell cycle inhibition or activation of cell death remains unknown [Wang *et al*., 2014]. Similar results were obtained in a study of U266 myeloma cell line [Jurczyszyn *et al*., 2014], but again the distinction between the effect of geldanamycin on cell cycle and cell death could not be established. Malignant cells of the small cell lung cancer were reported to experience inhibition of proliferation at low doses of geldanamycin, and cell death at high doses, but the latter outcome was considered an off-target effect, unrelated to inhibition of HSP90 [Restall and Lorimer, 2010]. Another study, which utilized human hepatocellular carcinoma cells grown *in vitro* and *in vivo* has shown that geldanamycin induced cell cycle arrest in G2 or mitosis, and a claim was made that the mitotic block might be responsible for triggering apoptosis. However, apoptosis was not observed in the *in vivo* setting, raising doubts on the relevance of this form of cell death [Watanabe *et al*., 2009]. The paucity of basic research on the impact of geldanamycin on cancer-related cellular activities necessitates further research in this area.

Nuclear factor-κB and HSP90

Attenuation of HSP90 function has been shown to induce apoptosis in various types of cancer cells: breast cancer cells [Huang *et al*., 2014], colorectal cancer cells [Kinzel *et al*., 2016], T-cell acute lymphoblastic leukemia [Akahane *et al*., 2016], thyroid cancer cells [Belalcazar *et al*., 2017], ovarian cancer cells [Lee *et al*., 2017], nasopharyngeal carcinoma [Ye *et al*., 2017], and Burkitt lymphoma [Walter *et al*., 2017]. This property appears to be mediated by the interaction of the chaperone with nuclear factor-κB (NF-κB) [Chen *et al*., 2002; Bai *et al*., 2011, Wang *et al*., 2013]. NF-κB, originally identified as a regulator of expression of immunoglobulin κ-light chain in B lymphocytes [Sen and Baltimore, 1986], is a eukaryotic transcription factor controlling a large number of normal

cellular processes, including proliferation [Wan and Leonardo, 2010; Lorenz *et al*., 2016], and apoptosis [Baldwin, 2012; Gasparini *et al*., 2014].

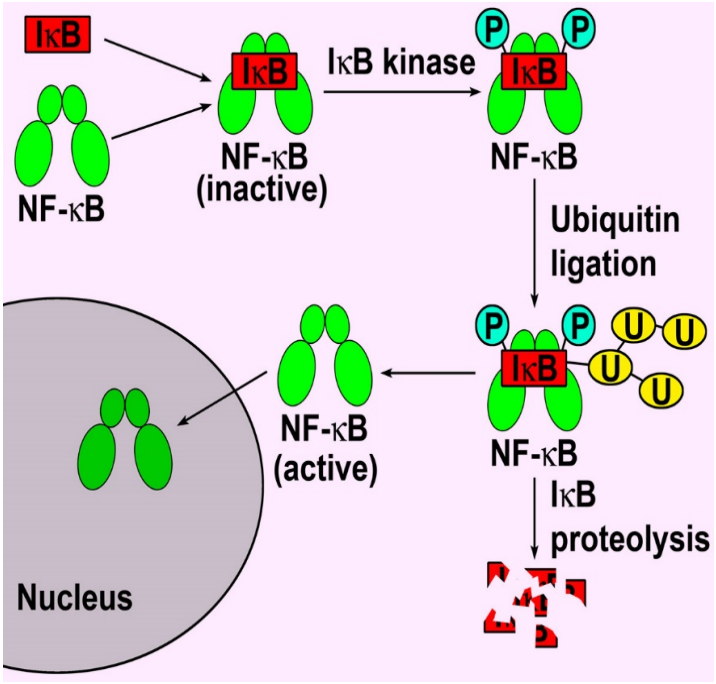

The regulation of the activity of NF-κB is illustrated in **Figure 5**. Cytoplasmic NF-κB binds its inhibitor, I-κB, forming an inactive complex that can only be disrupted when I-κB kinase, IKK, is activated. When the phosphorylated I-κB is marked by ubiquitination for degradation in the proteasome pathway, the active molecule of NF-κB translocates to the nucleus where it acts as a transcription factor.

Figure 5. NF-κB signaling pathway. See text for description.

The transcription factor NF-κB was shown to be activated in a wide range of human cancers [Karin and Greten, 2005; Jin *et al*., 2008; Prasad *et al*., 2010; Arkan and Greten, 2011; Wu *et al*., 2015; Cahill *et al*., 2016; Durand and Baldwin, 2017]. Moreover, it is well-established that NF-κB functions to block cell death through transcriptional induction of genes encoding anti-apoptotic and anti-oxidant proteins [Baldwin, 2012]. The mechanism by which HSP90 promotes the pro-survival action of NF-κB has been elucidated in recent years [Neckers, 2007; Baldwin, 2012]. Specifically, IKK, a molecule critical for the activation of NF-κB [Napetschnig and Wu, 2013], is degraded upon inhibition of HSP90 [Broemer *et al*., 2004]; loss of IKK inactivates NF-κB and inhibits NF- κB-dependent pro-survival pathways [Lewis *et al*., 2000; Wang *et al*., 2006; Baldwin, 2012].

The role of NF-κB in the HSP90 function can be studied by employing Jurkat-IκBαM cells which are stably transfected with a dominant-negative IκB gene, IκBαM. Its protein product

cannot be phosphorylated by IKK and marked for degradation and, therefore, remains permanently attached to NF-κB, blocking its function [Duckett *et al*., 1993]. Thus, although Jurkat-IκBαM cells express normal amounts of NF-κB, its role as a transcription factor is abolished, and NF-κB-dependent signaling pathways are inhibited.

An alternative approach to probing the function of NF-κB in HSP90 signaling is the use of pharmacologic inhibitors of this transcription factor. An example of such a drug is parthenolide (**Figure 6**), a sesquiterpene lactone which occurs naturally in the plant feverfew (*Tanacetum parthenium*). Parthenolide is a specific inhibitor of NF-κB [Wen *et al*., 2002; Pozarowski *et al*., 2003; Sun *et al*., 2007]. However, notably when present at higher concentrations, it may induce necrosis in an NF-κB-independent manner [Pozarowski *et al*., 2003], requiring simultaneous determination of apoptosis and necrosis.

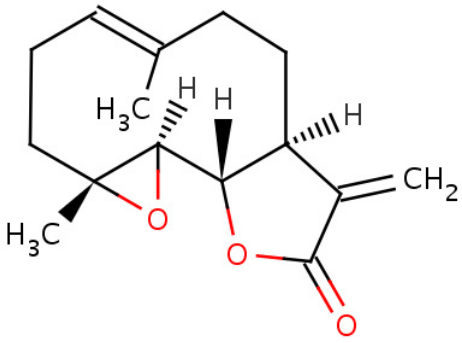

Figure 6. Molecular structure of parthenolide.

Jurkat-IκBαM cells and parthenolide were utilized as two independent strategies to elucidate the role of NF-κB in downstream events of HSP90 signaling.

MATERIALS AND METHODS

Cells and cell treatment

All experiments were performed utilizing phytohaemagglutinin (PHA)-stimulated human peripheral blood lymphocytes, immortalized human T-cell leukemia cell line Jurkat, and Jurkat IκBαM cells.

Lymphocyte cultures

Human peripheral blood lymphocytes were obtained from healthy male volunteers by venipuncture and isolated by density gradient centrifugation using Ficol-Hypaque as previously described [Halicka *et al*., 2002]. The cells were washed twice with Hanks' Balanced Salt Solution with calcium and magnesium (HBSS) and resuspended in RPMI-1640 medium. The medium was supplemented with 10% fetal bovine serum, 100 units/ml penicillin, 100 μg/ml streptomycin and 2mM L-glutamine (all from GIBCO/BRL Life Technologies, Inc., Grand Island, NY). Cells were maintained at a density approximately $5x10^5$ cells/ml. Except for control conditions, the cells were cultured in the presence of 10μg/ml PHA (Sigma Chemical, St. Louis, MO). The cell cultures were incubated at 37.5°C in 25 ml (12.5 cm^2) Falcon flasks placed vertically, or in 48 multi-well trays (both from Becton Dickinson Co., Franklin, LA) in a mixture of 95% air and 5% carbon dioxide.

Jurkat and Jurkat IκBαM cell cultures.

Parental Jurkat cell line and Jurkat IκBαM cells [Van Antwerp *et al*., 1996] were kindly provided by Dr. Douglas R. Green of La Jolla Institute for Allergy and Immunology, San Diego, CA. The cells were grown in RPMI-1640 medium supplemented with 10% fetal bovine serum, 100 units/ml penicillin, 100 μg/ml streptomycin and 2mM L-glutamine (all from GIBCO/BRL Life Technologies, Inc., Grand Island, NY). Twenty-five ml (12.5 cm^2) Falcon flasks or in 48 multi-well trays (both from Becton Dickinson Co., Franklin, LA) were used for the cultures. At the beginning of experiments, the cells density was adjusted to approximately $3x10^5$ cells/ml. During the assays, the cells were in an exponential and asynchronous phase of growth.

Treatment with geldanamycin

Cultures of lymphocytes, Jurkat and Jurkat IκBαM cell were treated with various concentrations of geldanamycin derived from *Streptomyces hygroscopicus* (Sigma

Chemical, St. Louis, MO). Geldanamycin was administered at concentrations from 5nM to 250nM for different periods of time: 8h, 12h, 24h, 36h, 48h, 72h, and 96h, as indicated in the Results section. The stock solution of geldanamycin (1mM) was prepared in dimethyl sulfoxide (DMSO; Sigma Chemical, St. Louis, MO) and stored at -20°C. The working solution was prepared freshly before treatment of the culture by diluting the stock solution with the culture medium. Control cultures were treated with corresponding concentrations of DMSO alone.

Evaluation of cell cycle distribution and induction of apoptosis

Acridine Orange

Staining of permeabilized cells with metachromatic dye acridine orange (AO) allowed the quantification of apoptotic cells, characterized by fragmented DNA, and simultaneously measure the cell cycle distribution based on bivariate differential staining of cellular DNA and RNA. Simultaneous differential staining of DNA versus RNA with AO was performed according to the procedure developed by Dr. Darzynkiewicz [Darzynkiewicz *et al*., 2004]. Briefly, 0.2 ml of cell suspension in culture medium was transferred to a 5 ml Falcon tube, placed on ice, and gently mixed with 0.4 ml of ice-cold Solution A containing 0.1% Triton X-100 (Sigma), 0.08 M HCl and 0.15 M NaCl. After 15 seconds of incubation on ice, 1.2 ml of ice-cold Solution B, containing 6μg/ml of AO (Invitrogen, Eugene, OR), 1 mM EDTA-Na, and 0.15 M NaCl in the phosphate-citric acid buffer, pH 6.0, was gently dispensed into each tube. Incubation was then continued under darkness on ice for 10 minutes. Under these conditions, cultured cells are permeabilized by the action of the non-ionic detergent at low pH. In permeabilized cells, the DNA stains with AO orthochromatically, i.e., preserving the color of the dye, emitting green fluorescence (~530 nm), while double-stranded RNA undergoes denaturation to single-stranded RNA, which stains with AO by precipitation, emitting red fluorescence (630-644 nm). A FACScan flow cytometer (Becton Dickinson, San Jose, CA), equipped with 488 nm argon-ion laser and with standard settings for detecting green fluorescence in FL1 and red fluorescence in FL3 channels, was used to measure the intensity of green and red AO signals.

Propidium Iodide

Propidium iodide (PI) is an intercalating dye binding specifically to double-stranded nucleic acids. It is used for staining of DNA in fixed, permeabilized cells. An enzymatic removal of RNA is necessary during staining process prior to DNA analysis. PI can be used as a

single staining agent allowing univariate analysis of cellular DNA and detection of apoptotic cells, or in combination with fluorochrome-labeled antibodies directed against cellular proteins, especially cell cycle and apoptosis-associated proteins [Juan and Darzynkiewicz, 2001; Darzynkiewicz *et al*., 2001a; Pozarowski *et al*., 2004]. When indicated in staining protocols, cellular DNA was counterstained with 10 μg/ml PI (Invitrogen-Molecular Probes, Eugene, OR) in a solution of PBS containing 100 μg/ml of DNase-free RNase A (Sigma Chemical Co., St. Louis, MO). The staining was performed for 30 minutes at room temperature in the dark. Cell analysis was accomplished using FACScan flow cytometer equipped with an argon-ion laser.

DAPI

4',6-diamidino-2-phenylindol (DAPI) is a DNA-specific fluorochrome that requires UV excitation [Darzynkiewicz *et al*., 2001a]. Because DAPI binds externally to the double helix and does not require unwinding of the DNA, staining by DAPI is - among all DNA staining fluorochromes - the least affected by chromatin structure [Darzynkiewicz *et al*., 1984]. Therefore DAPI is a preferred DNA stain for quantitative analysis. The cells were incubated in the dark for 15 minutes at room temperature with DAPI solution containing 2 μg/ml of DAPI in a PIPES/Triton X-100 buffer. The pattern of staining was evaluated by epifluorescence microscopy.

Activation of caspase 3

During activation of apoptosis, pro-caspase 3 is proteolytically cleaved to yield the active enzyme, caspase 3 [Shalini *et al.*, 2015]. Cleaved caspase 3 was detected following fixation of 5 x 10^5 cells/ml in 1% formaldehyde for 15 minutes on ice. Subsequently, cells were stored until use in 70% ethanol at -20°C. For staining, cells were washed twice to remove ethanol and incubated for 2 hours at room temperature with an antibody against cleaved caspase 3-Asp 175 (Cell Signaling Technology, Beverly, MA), diluted 1:100 in PBS containing 1% BSA [Pozarowski *et al.*, 2003]. FITC-conjugated swine polyclonal anti-rabbit IgG (DAKO, Carpinteria, CA), diluted 1:30 in PBS was used as a secondary antibody. DNA content was detected by incubation with PI and RNase for 30 minutes at room temperature. Cell analysis was performed using FACScan flow cytometer equipped with an argon-ion laser.

Phospho-histone H3

The effect of geldanamycin on mitotic sub-population of cells was evaluated by measurement of phosphorylated histone H3. Phosphorylation of a highly conserved serine residue (Ser10) in histone H3 is required for the entry of cells into mitosis [Xie *et al*., 2013], making it a highly specific marker of this phase of the cell cycle. Phospho-histone H3 was detected following fixation of 5 x 10^5 cells/ml in 1% formaldehyde for 15 minutes on ice and storage in 70% ethanol at -20°C. For staining, cells were washed twice to remove ethanol and incubated for 2 hours at room temperature with an antibody against phospho-histone H3 (Cell Signaling Technology, Beverly, MA) [Juan *et al*., 1998]. FITC-conjugated goat polyclonal anti-mouse IgG (DAKO, Carpinteria, CA) diluted 1:30 was used as a secondary antibody. To measure the DNA content, cells were incubated with PI and RNase for 30 minutes at room temperature. Cell analysis was performed using FACScan flow cytometer equipped with an argon-ion laser.

Retinoblastoma protein

The detection of hyper-phosphorylated retinoblastoma protein (pRb) was performed since this posttranslational modification of Rb is a characteristic feature of cycling cells. pRb was detected by fixation of cells (5 x 10^5 cells/ml) in 1% formaldehyde for 15 minutes on ice. Fixed cells were stored in 70% ethanol at -20°C. For staining, cells were washed twice to remove ethanol and incubated for 2 hours room temperature with an antibody against phospho-retinoblastoma (Cell Signaling Technology, Beverly, MA) [Juan *et al*., 1998]. FITC-conjugated swine polyclonal anti-rabbit IgG (DAKO, Carpinteria, CA), diluted 1:30 in PBS, was used as a secondary antibody. DNA content was detected by incubation with PI and RNase for 30 minutes at room temperature. Cell analysis was performed using FACScan flow cytometer equipped with an argon-ion laser.

Cell number calculation

The time, T, necessary to run a sample is directly proportional to the number of events to be acquired, N_E, and the volume of cell suspension, V, and is inversely proportional to the rate of flow, R, and the number of cells, N_C:

$$T = (N_E \times V) / (R \times N_C).$$

Thus,

$$N_C = (N_E \times V) / (R \times T).$$

If the variables N_E, V, and R are kept constant, N_C is inversely related to T:

$$N_C = k / T.$$

The relative change in cell number between time 1 and time 2, N_{C2} / N_{C1}, can be derived from

$$N_{C1} = k / T_1$$

and

$$N_{C2} = k / T_2$$

to yield

$$N_{C2} / N_{C1} = T_1 / T_2. \qquad \text{(equation 1)}$$

Therefore, in measurements aiming at the determination of the rate of cell growth, the number of events, volume of cell suspension, and rate of flow were kept constant, and the change in cell number was calculated from equation 1.

Flow cytometric analysis

Cellular fluorescence was measured using the FACScan flow cytometer (Becton Dickinson, San Jose, CA) equipped with a 488nm argon-ion laser. The green and red emissions from each cell were divided optically and quantitated by separate photomultipliers. Background fluorescence was subtracted automatically. The measurements were filed by computer for further analysis. The histograms were deconvoluted using CellQuest (Becton Dickinson) software.

Statistics

The number of replicates for each experiment is listed in the Results section. The significance ($P<0.05$) of differences in quantitative results among multiple groups was calculated by analysis of variance with Bonferroni correction.

RESULTS

Geldanamycin affects the cell cycle of human lymphocytes

The objective of this initial study was to determine the time course and dose-dependency of the impact of geldanamycin on cell cycle progression. Experiments were performed utilizing human lymphocytes; quiescent cells served as a negative control, and phytohemagglutinin (PHA)-stimulated cells as a positive control. The distribution of cells between G0, G1, S and G2/M phases was probed with the use of acridine orange (AO). AO is a cell-permeable, nucleic acid-selective, metachromatic dye. Under stringent conditions of pH and high ionic strength, AO intercalates into DNA and also binds to RNA by electrostatic forces. When bound to DNA, it emits green light at 525 nm, while in association with RNA it fluoresces in red with maximum emission at 650 nm. Bivariate analysis of the fluorescence spectra permits the distinction between G0 and G1 cell populations. Both populations exhibit the same DNA content (green fluorescence) but differ in RNA content (red fluorescence); the G1 cells possess dramatically higher RNA levels than G0 cells withdrawn from the cell cycle. This difference is due to the fact that transition of cells from G0 to G1 is associated with a many-fold increase in cellular RNA, primarily rRNA, content (Darzynkiewicz *et al*., 1976). An example of this assay and its interpretation is shown in **Figure 7**.

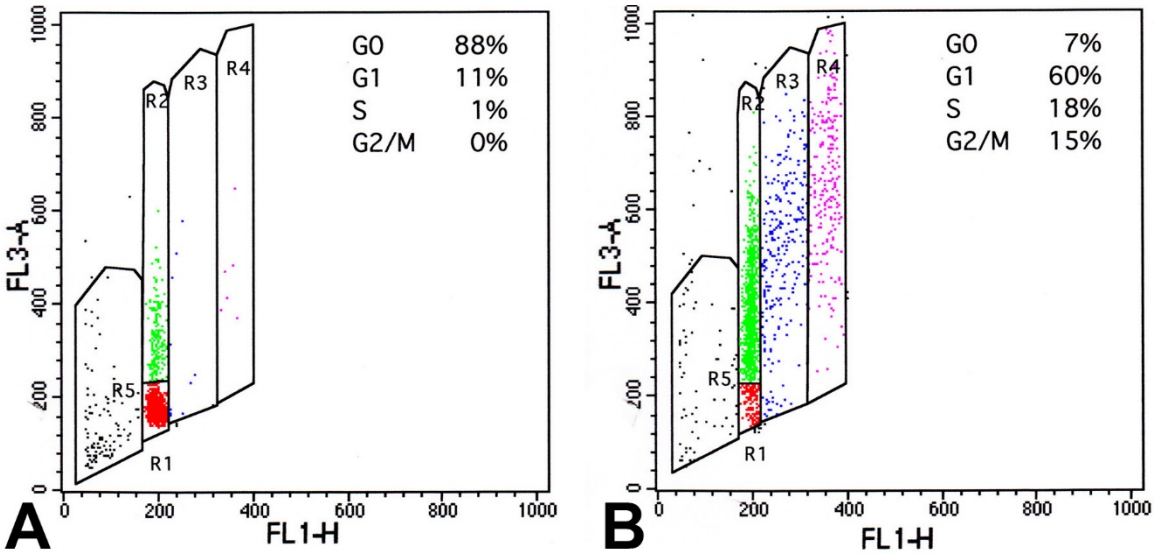

Figure 7. Bivariate analysis of AO staining of non-stimulated (A) and PHA-stimulated (B) human lymphocytes. The PHA stimulation lasted 48 hours. FL1-H represents the green fluorescence and FL3-A represents the red fluorescence. Red dots in gate R1 correspond to cells with diploid DNA content and low RNA level, i.e., G0 cells. Green events in gate R2 correspond to cells with diploid DNA content and high RNA level, i.e., G1 cells. Blue (gate R3) and magenta (gate R4) dots reflect cells in S and G2/M, respectively. Black dots in gate R5 indicate sub-G0/G1 DNA content and correspond to cells undergoing apoptosis. Note the decrease in quiescent G0 cells and a corresponding increase in cycling G1, S, and G2/M cells upon PHA stimulation (B).

In order to analyze the impact of geldanamycin on the distribution of human lymphocytes in the cell cycle, the cells were exposed to PHA, and at the same time the drug was administered at concentrations 5, 10, 25, 50, 100, and 150 nM. Lymphocytes were analyzed by flow cytometry at 24, 48, and 72 hours after initiation of the treatment. The results of these experiments are summarized in **Figure 8.**

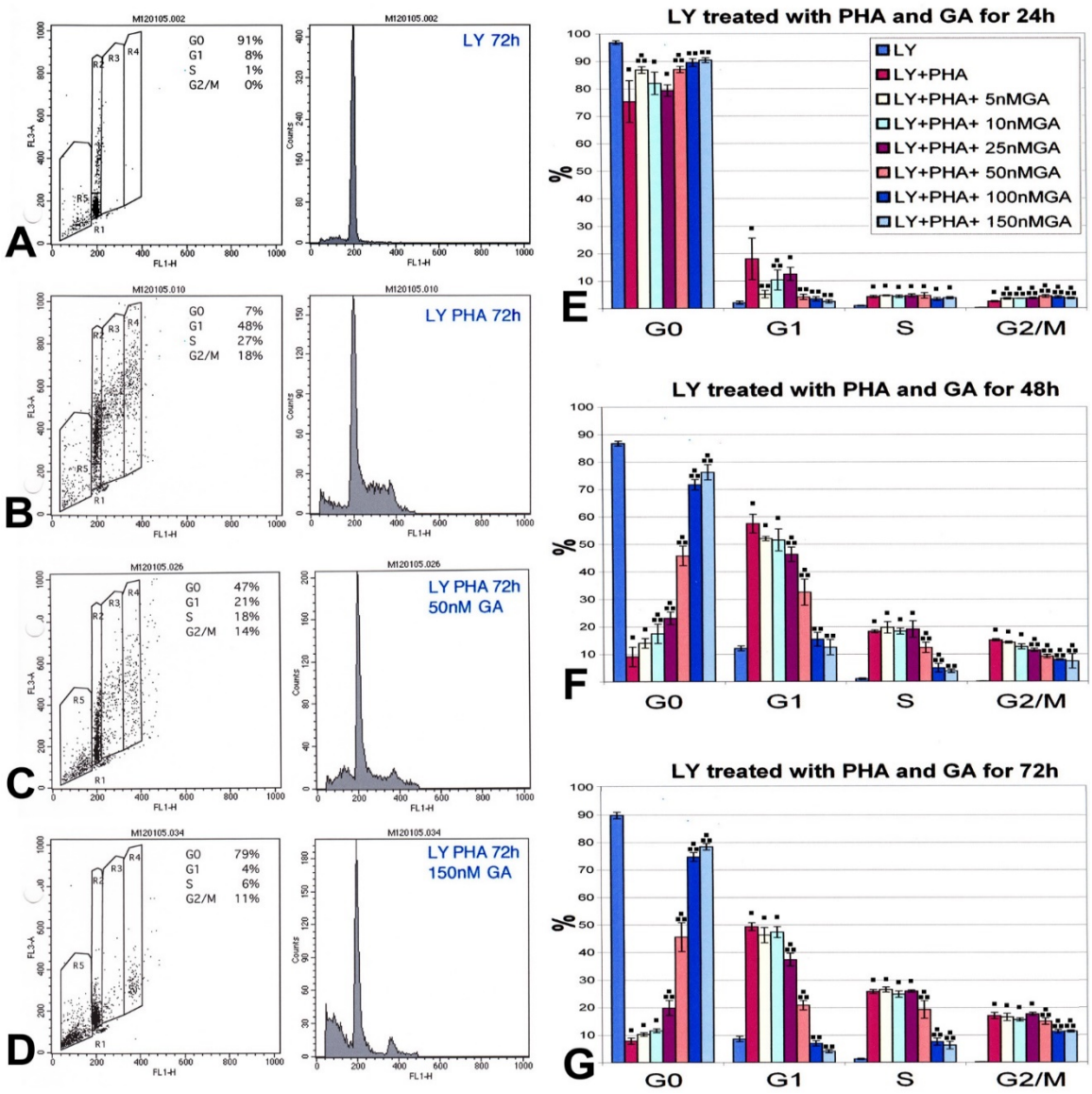

Figure 8. Time- and dose-dependent impact of geldanamycin on cell cycle progression in human lymphocytes. A-D illustrate examples of bivariate analysis (left panels) of AO staining at 72 hours of treatment of control lymphocytes (A), and lymphocytes stimulated by PHA in the absence (B) and the presence of 50 nM (C) and 150 nM (D) geldanamycin. Right panels in A-D show corresponding frequency histograms of DNA content distribution. Bar graphs depict the impact of increasing concentrations of geldanamycin on the distribution of cells in each phase of the cell cycle at 24 hours (E), 48 hours (F), and 72 hours (G). ■ and ■■ indicate, respectively, statistically significant ($P<0.05$) difference versus non-stimulated lymphocytes and lymphocytes stimulated by PHA only. LY, lymphocytes; GA, geldanamycin.

As expected, stimulation of cells with PHA for 72 hours resulted in an 11-fold decrease in G0 population, and a 6-fold, 20-fold, and 85-fold increase in G1, S and G2/M populations, respectively. The effect of geldanamycin on PHA-stimulated cells was rather modest at 24 hours (**Figure 8E**) but was visibly pronounced at 48 and 72 hours of incubation (**Figure 8F, G**). Specifically, in comparison with lymphocytes treated with PHA only, 150 nM geldanamycin at 72 hours resulted in a 10-fold increase in the frequency of G0 cells, and a 12-fold, 4-fold, and 1.5-fold decrease in frequency of G1, S, and G2/M lymphocytes, respectively. Comparable values were noted in the presence of 100 nM geldanamycin. The drug had no significant impact on cell cycle distribution at 5 and 10 nM, and intermediate effects were observed at 25 and 50 nM concentrations. Thus, geldanamycin inhibits the cell cycle traverse of human lymphocytes by blocking the recruitment of cells from G0 into the cell cycle.

Simultaneous detection of apoptotic cells by counting nuclei with sub-G0/G1 DNA content, representing cells with fragmented DNA, (see gate R5 in **Figure 7**) allowed the assessment of the magnitude of apoptosis induced by geldanamycin (**Figure 9**). It should be emphasized that the methodology employed in this work did not involve any of the steps (trypsinization, density gradient separation, centrifugation) that commonly contribute to cell loss-related errors in quantitation of apoptosis by flow cytometry, [Darzynkiewicz *et al*., 2001b]. In this quantitative analysis, the pool of cells in G0 was excluded since quiescent cells are not susceptible to apoptotic stimuli [Helbing *et al*., 1998; Naderi *et al*., 2003]. Stimulation by PHA did not affect the baseline magnitude of apoptosis at any time interval examined. Additionally, there was no increase in this parameter at any concentration of geldanamycin at 24 hours. However, at 48 and 72 hours, a 3-5-fold increase in the

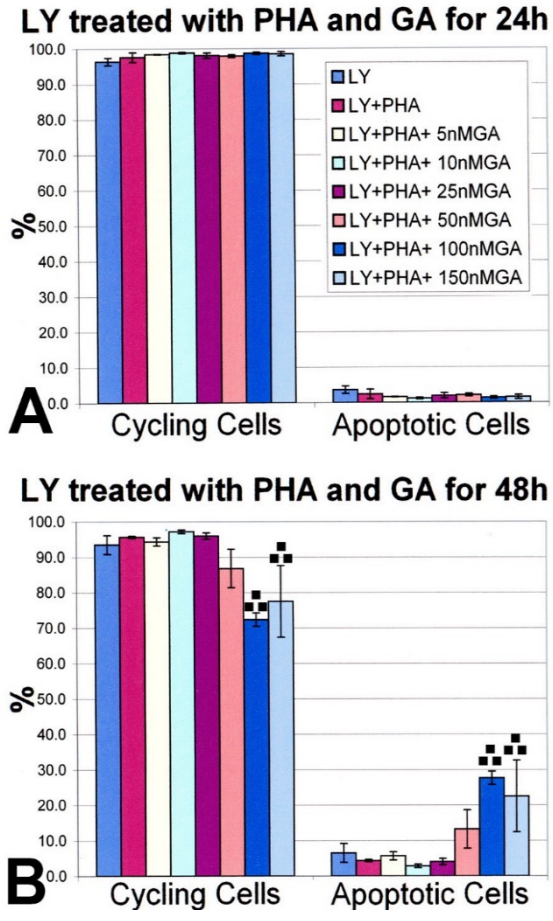

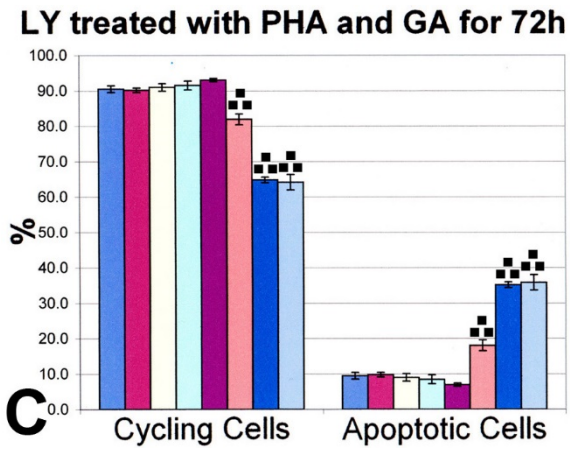

incidence of cell death was present at the highest geldanamycin concentrations, i.e., 100 and 150 nM (**Figure 9**). A less pronounced activation of cell death was seen at 50 nM geldanamycin, and it reached statistical significance only at the longest time interval examined.

Figure 9. Time- and dose-dependent impact of geldanamycin on apoptosis of human lymphocytes. Bar graphs depict the effect of increasing concentrations of geldanamycin on the fraction of cycling and apoptotic cells at 24 hours (A), 48 hours (B), and 72 hours (C). ■ and ■■ indicate, respectively, statistically significant ($P<0.05$) difference versus non-stimulated lymphocytes and lymphocytes stimulated by PHA only. LY, lymphocytes; GA, geldanamycin.

The presence of apoptosis was also observed morphologically. **Figure 10** shows shrinkage of nuclei and condensation of chromatin; these structural alterations are typical of apoptosis. This image corresponds to human lymphocytes exposed to 150 nM geldanamycin for 72 hours.

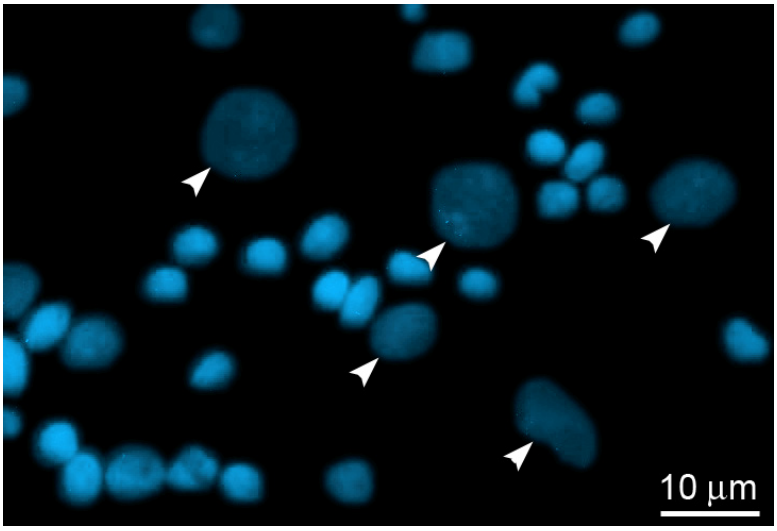

Figure 10. Morphology of nuclei of apoptotic human lymphocytes. Nuclei were stained with DAPI. Nuclei of remaining 5 live lymphocytes are indicated by arrowheads. Chromatin condensation, indicative of apoptosis, is evident in the remaining cells.

The question was then whether the observed actions of geldanamycin were related to the recruitment of lymphocytes into the cell cycle by PHA, or could be reproduced in already actively cycling cells. This is a relevant issue, since forcing the entry of quiescent cells into the cell cycle can itself result in the initiation of the apoptotic pathway [Agah *et al*., 1997]. To address this problem, human lymphocytes were first treated with PHA for 72 hours to promote their exit from G0 (as shown in **Figure 8E-G**) and then exposed to geldanamycin

for an additional interval of 8 and 24 hours. PHA was present throughout the experiment. **Figure 11** shows that already at 8 hours of incubation with geldanamycin the fraction of lymphocytes in S phase was decreased significantly. The impact of geldanamycin on cycling lymphocytes became more evident at 24 hours. The fraction of cells in G0 increased by 66-70%, while the population in the S phase decreased by 59-67% and in G2/M by 23-38%. These changes were independent of geldanamycin concentration, which ranged from 100nM to 250nM. A small but statistically significant increase, 9%, in G1 lymphocytes was noted, possibly reflecting a slow-down in the rate of the cell cycle traverse.

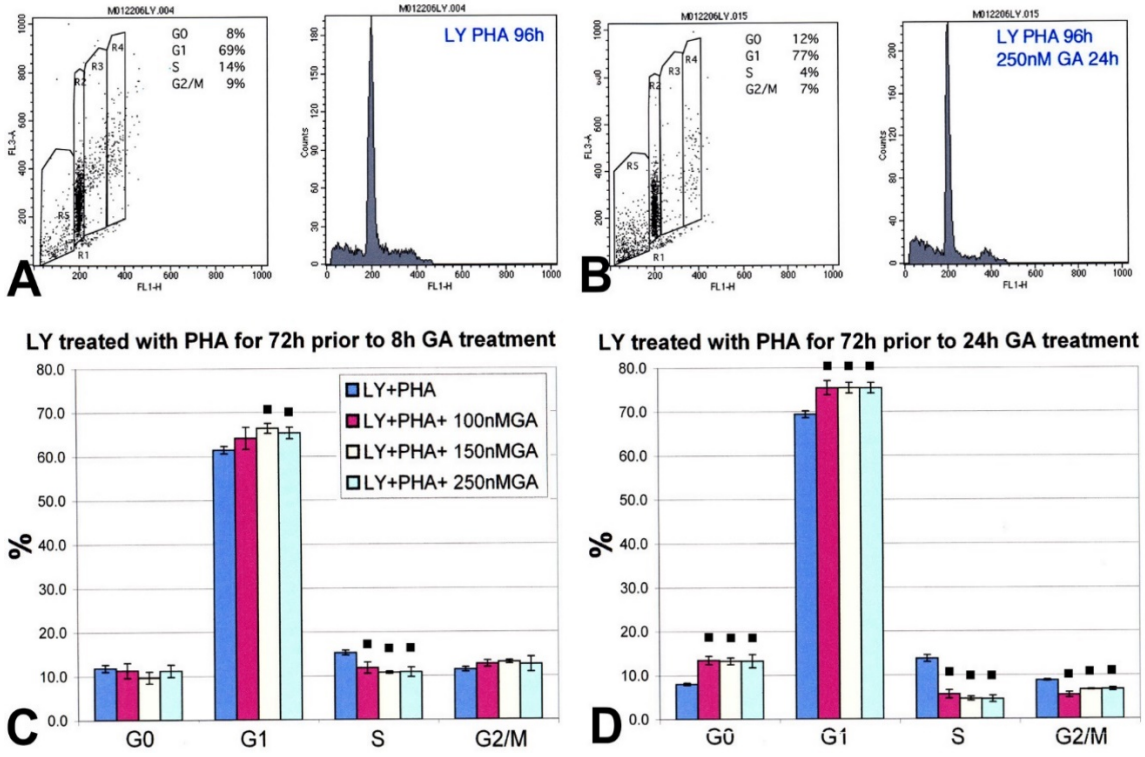

Figure 11. Impact of geldanamycin on cell cycle progression in human lymphocytes pre-activated by PHA. A and B illustrate examples of bivariate analysis (left panels) of AO staining of lymphocytes stimulated by PHA for 96 hours (A) and PHA-stimulated lymphocytes exposed for 24 hours to 250 nM geldanamycin (B). Right panels in A and B show corresponding frequency histograms of DNA content distribution. Bar graphs depict the impact of increasing concentrations of geldanamycin on the distribution of cells in each part of the cell cycle at 8 hours (C) and 24 hours (D). ■ Indicates statistically significant ($P<0.05$) difference versus lymphocytes stimulated by PHA only. LY, lymphocytes; GA, geldanamycin.

Analysis of lymphocytes with sub-G1 DNA content provided information on the extent of apoptosis in cycling lymphocytes exposed to geldanamycin. As explained previously, only the non-G0 population of cells was included in the quantitation.

Geldanamycin did not affect cell death at 8 hours, but its impact became apparent at 24 hours, when an average 76% increase in frequency of apoptosis occurred (**Figure 12**). Again, this change did not depend on the geldanamycin concentration in the range examined, from 100 to 250nM.

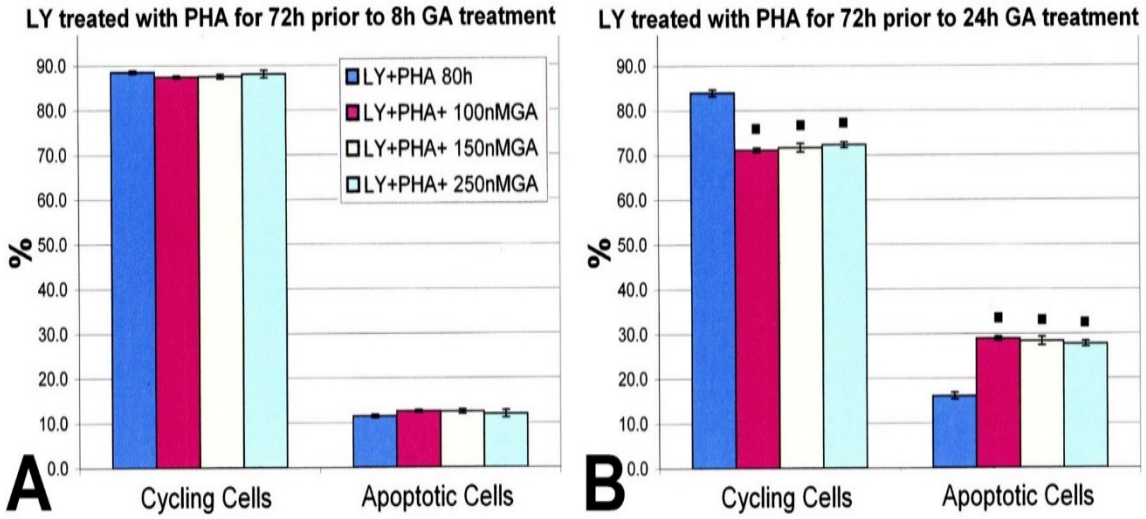

Figure 12. Impact of geldanamycin on apoptosis in human lymphocytes activated by PHA. Bar graphs depict the impact of increasing concentrations of geldanamycin on the fraction of apoptotic cells at 8 hours (A) and 24 hours (B). ■ Indicates statistically significant ($P<0.05$) difference versus lymphocytes stimulated by PHA only. LY, lymphocytes; GA, geldanamycin.

Finally, whether the effect of geldanamycin on cell cycle of human lymphocytes is reversible was determined. It is a relevant question since an affirmative answer would exclude a non-physiological generalized toxic action as the mechanism underlying the inhibition of cell cycle progression. To test the reversibility of cell cycle inhibition, lymphocytes were incubated with both PHA and geldanamycin for 48, 72 and 96 hours, or geldanamycin was present only for initial 24 hours, and the remaining 24, 48 and 72 hours of incubation were carried out in the presence of PHA only (**Figure 13**). In these experiments, geldanamycin was used at concentrations ranging from 25 to 150 nM.

As expected on the basis of experiments discussed above, geldanamycin, when present throughout the incubation period, resulted in a striking decrease in cycling cells in G1 and S phase, with a simultaneous increase in non-cycling G0 cells (**Figure 13A, C, and E**). This inhibitory impact of geldanamycin was reversed after the removal of the drug: the fraction of lymphocytes in G1 and S phase increased in a time-dependent manner (**Figure 13B, D, and F**). For example, with 150 nM geldanamycin, a 1.5-fold, 3.4-fold and 2.7-fold increase in S phase cells was seen, respectively, at 24, 48, and 72 hours after the removal of the drug from the incubation medium. Corresponding increases for G1 lymphocytes

were 4.3-fold, 6.6-fold and 9.3-fold. Conversely, a decrease in the fraction of G0 lymphocytes was noted following the withdrawal of geldanamycin after 24 hours; subsequent 24, 48, and 72-hour incubations yielded 16%, 50% and 67% reduction in this parameter, respectively. Thus, geldanamycin-induced G0 arrest in human lymphocytes is reversible.

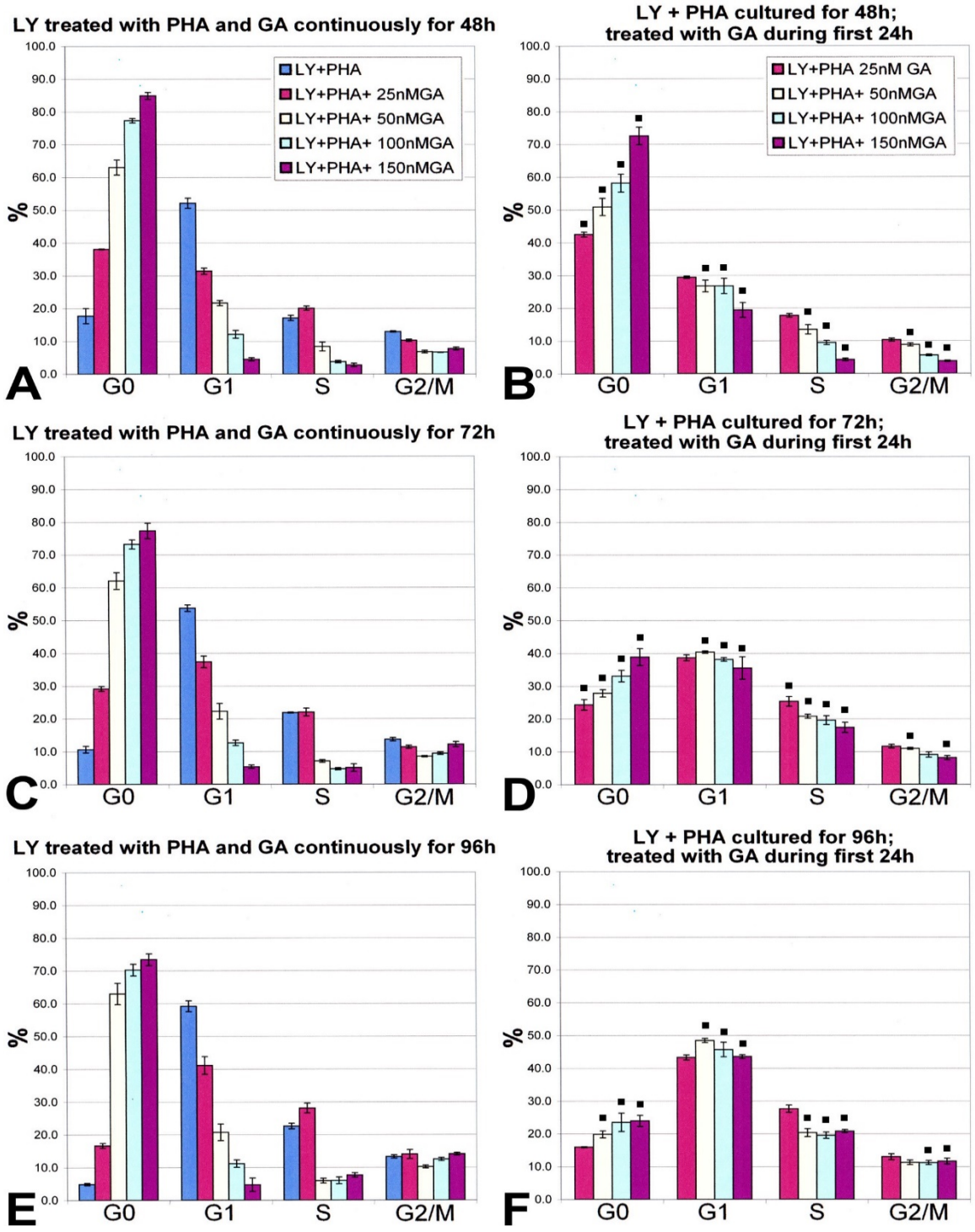

Figure 13. Reversibility of the effect of geldanamycin on cell cycle progression in human lymphocytes. A, C, and E depict the impact of continuously present geldanamycin at various concentrations on the distribution of cells in each part of the cell cycle at 48 hours (A), 72 hours (C), and 96 hours (E). B, D, and F show the results of an analogous experiment, in which geldanamycin was present only for the first 24 hours. ■ Indicates statistically significant ($P<0.05$) difference versus lymphocytes exposed continuously to geldanamycin. LY, lymphocytes; GA, geldanamycin.

The fraction of lymphocytes with fragmented DNA, the sub-G1 population, was used to estimate the magnitude of apoptosis in these experiments. As indicated previously, only the non-G0 cells were considered in this analysis. **Figure 14** illustrates that the impact of geldanamycin was almost entirely reversible. For example, with 150 nM geldanamycin, a 43%, 63%, and 56% smaller fraction of apoptotic lymphocytes was detected at, respectively, 24, 48, and 72 hours after the removal of the drug from the medium.

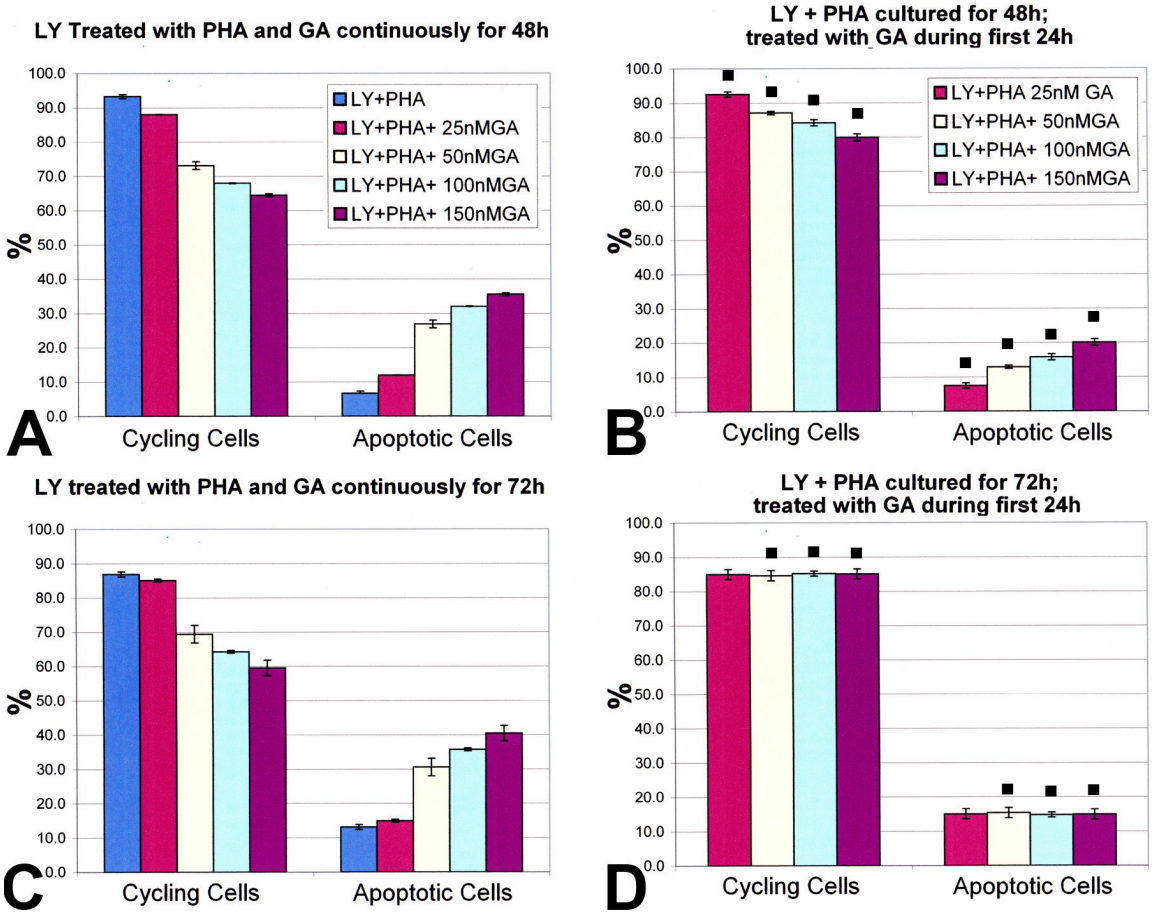

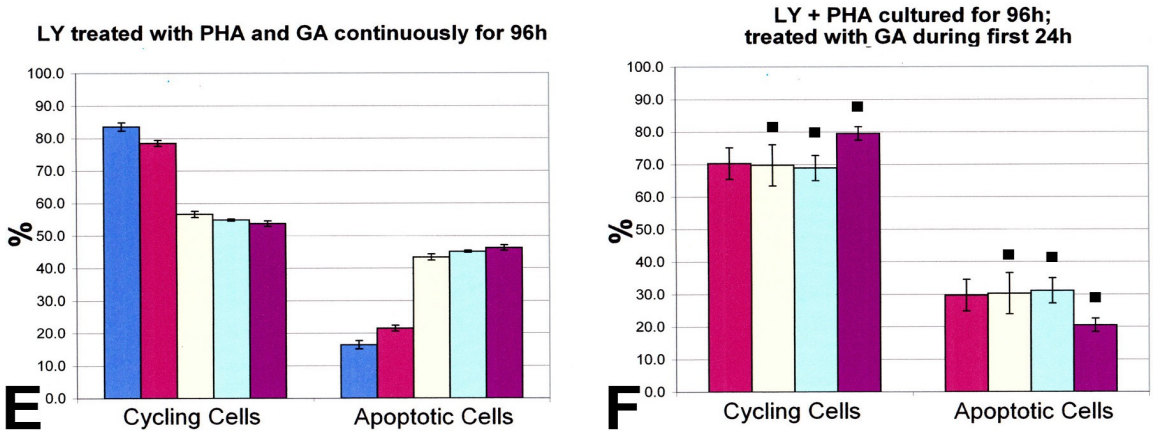

Figure 14. Reversibility of the effect of geldanamycin on apoptosis of human lymphocytes activated by PHA. A, C, and E depict the impact of continuously present geldanamycin at various concentrations on the fraction of cycling and apoptotic cells at 48 hours (A), 72 hours (C), and 96 hours (E). B, D, and F show the results of an analogous experiment, in which geldanamycin was present only for the first 24 hours. ■ Indicates statistically significant ($P<0.05$) difference versus lymphocytes exposed continuously to geldanamycin. LY, lymphocytes; GA, geldanamycin.

Thus, geldanamycin reversibly blocks PHA-induced cell cycle progression of human lymphocytes, inducing their transition into the G0 phase and activating apoptosis.

The knowledge of the rate of data acquisition by the flow cytometer, and of the volume of the samples, allowed the computation of the total number of cells arrested in G0, cycling cells, and apoptotic cells in the sample. It was essential to complement the data on relative fractions with actual counts of cells since it is impossible to exclude *a priori* the possibility that a relevant fraction of cells was lost during the incubation period, or that changes in the duration of specific phases of the cell cycle occur under experimental conditions. For example, an increase in the fraction of apoptotic cells may reflect a higher rate of cell death, but may also be alternatively explained by an elongation of the time necessary for the disintegration of apoptotic cells.

The methodology to obtain cell counts was implemented *post hoc* and therefore the experiments did not involve the use of fluorescent microspheres [Schlenke *et al.*, 1998]. Admittedly, the inclusion of fluorescent microspheres in the tested sample has the advantage of accounting for cell loss during sample preparation and standardizing the performance of the instrument [Brando *et al.*, 2000]. However, it has been demonstrated that with a constant rate of flow, typical of bench-top flow cytometers, reliable cell counts can be obtained despite the above-indicated limitations [Storie *et al.*, 2003]. Moreover, as

discussed earlier, loss of cells in the protocols used in the present work is negligible. Importantly, any systematic error that might have occurred would have no impact on the relative changes in cell number which were the basis for the conclusions reached here.

The quantitative data on cell number are shown in **Figures 15 and 16**. As expected, upon stimulation with PHA the total number of lymphocytes increased 1.8-fold from 48 to 96 hours. This rate of cell proliferation corresponds to a population doubling time of 56 hours and is within the range reported in the literature [Rubini *et al*., 1990; Zhang *et al*., 2013]. At 96 hours, continuous treatment with 150 nM geldanamycin resulted in a 35-fold decrease in the number of lymphocytes in G1, an 8.1-fold decrease in the number of lymphocytes in S, and a 2.3-fold decrease in the number of lymphocytes in G2/M. Conversely, the number of lymphocytes in G0 increased 5.4-fold, and the number of apoptotic lymphocytes increased 1.6-fold (**Figures 15 and 16**). When geldanamycin was removed from the medium at 24 hours, allowing 72 hours of recovery, the number of G1 lymphocytes increased 14-fold. Corresponding values for S and G2/M cells were 6.9-fold and 1.3-fold, respectively. Consequently, the number of lymphocytes arrested in G0 decreased 2-fold, and the number of apoptotic lymphocytes decreased 2.2-fold after geldanamycin removal (**Figures 15 and 16**).

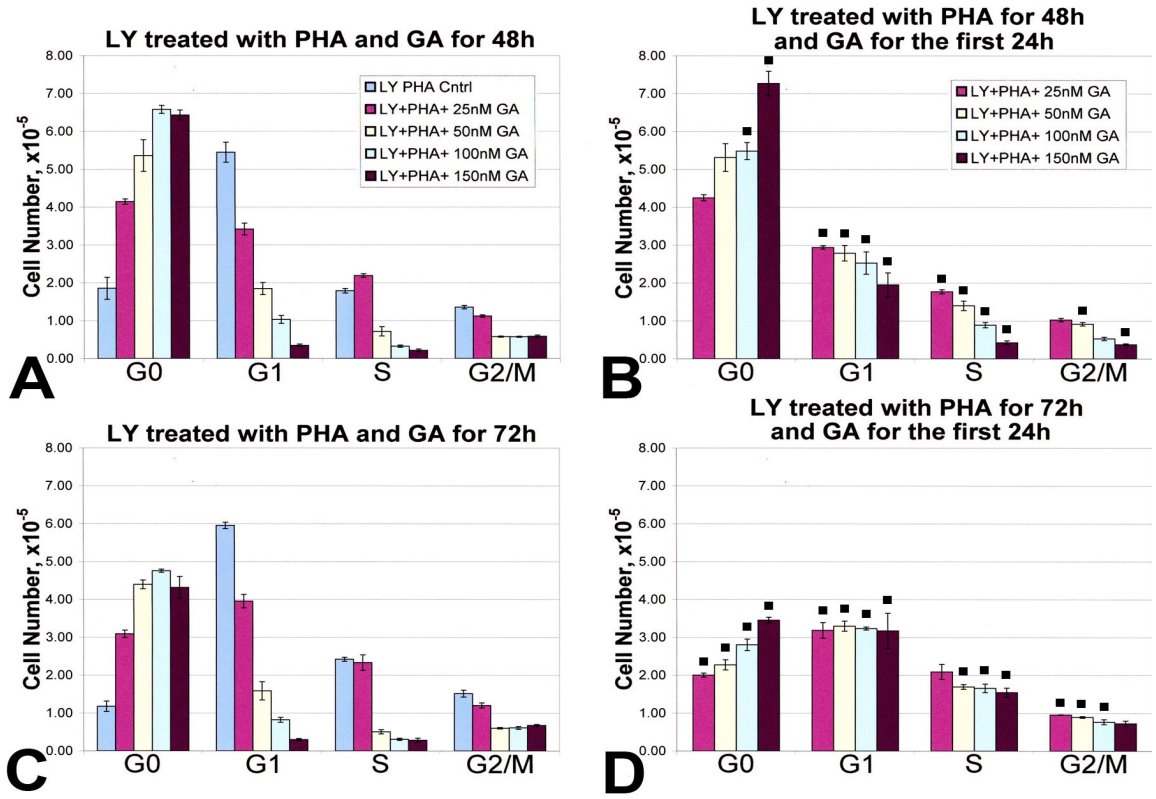

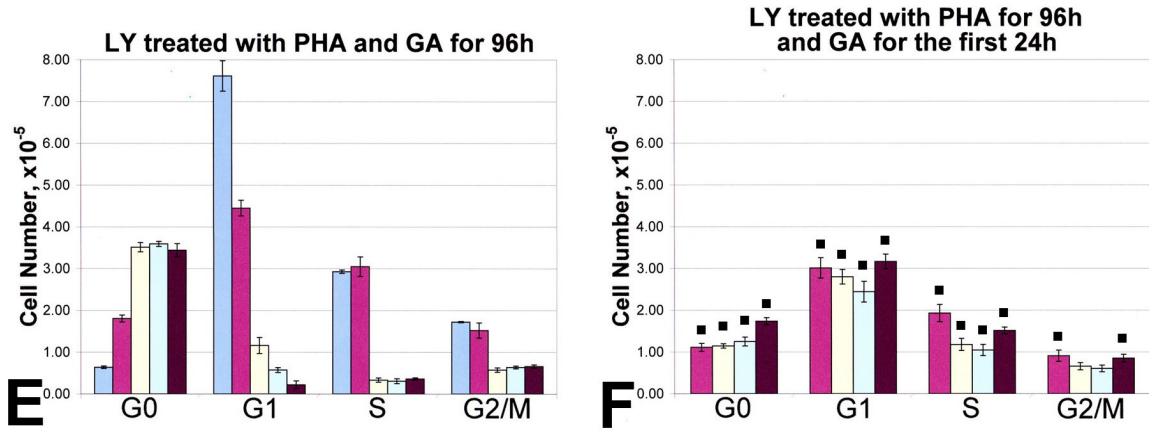

Figure 15. Reversibility of the effect of geldanamycin on the number of human lymphocytes traversing the cell cycle. A, C, and E depict the impact of continuously present geldanamycin at various concentrations on the number of cells in each phase of the cell cycle at 48 hours (A), 72hours (C), and 96 hours (E). B, D, and F show the results of an analogous experiment, in which geldanamycin was present only for the first 24 hours. ■ Indicates statistically significant ($P<0.05$) difference versus lymphocytes exposed continuously to geldanamycin. LY, lymphocytes; GA, geldanamycin.

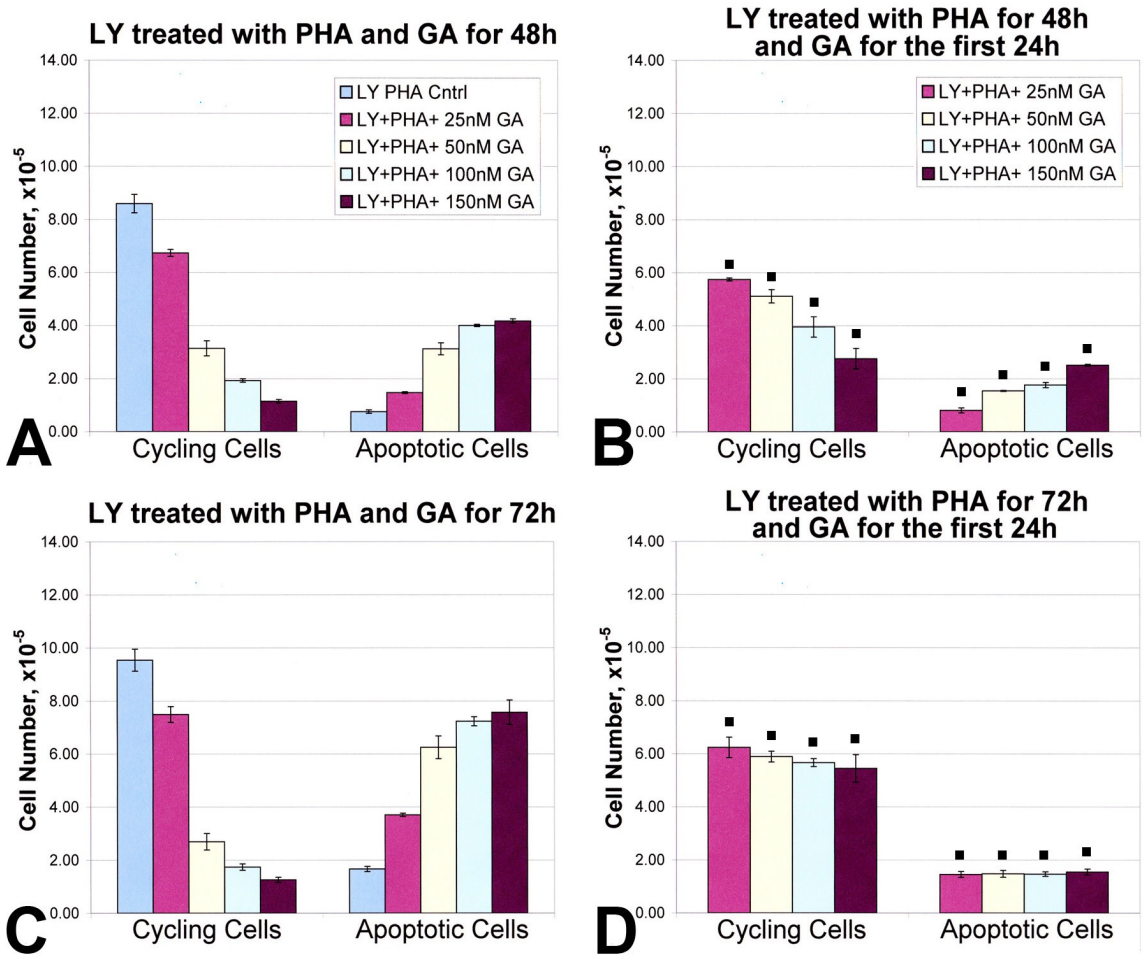

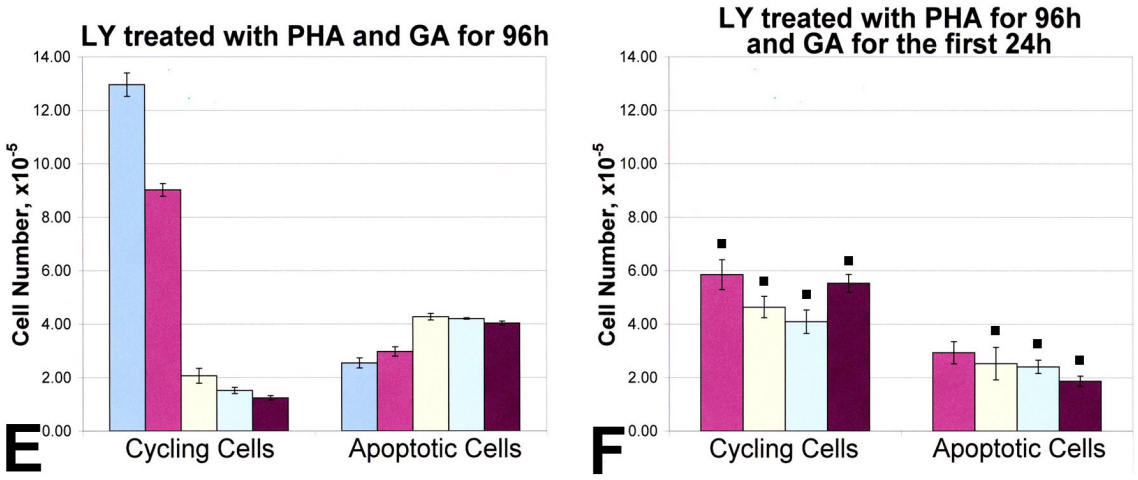

Figure 16. Reversibility of the effect of geldanamycin on the number of cycling and apoptotic human lymphocytes activated by PHA. A, C, and E depict the impact of continuously present geldanamycin at various concentrations on the number of cycling and apoptotic cells at 48 hours (A), 72 hours (C), and 96 hours (E). B, D, and F show the results of an analogous experiment, in which geldanamycin was present only for the first 24 hours. ■ Indicates statistically significant ($P<0.05$) difference versus lymphocytes exposed continuously to geldanamycin. LY, lymphocytes; GA, geldanamycin.

Together, the accumulated data indicate that the impact of geldanamycin on cell cycle progression and apoptosis of human lymphocytes is mostly reversible, with regard to both the fraction and the number of cycling, resting, and dying cells.

Geldanamycin affects the cell cycle of Jurkat cells

The Jurkat cell line (called initially JM) was established in the late 1970s from the peripheral blood of a 14 years old boy with T cell leukemia [Schneider *et al*., 1977]. This immortalized cell line has been used to investigate acute T cell leukemia, T cell signaling, and the expression of receptors implicated in the entry of viruses, particularly HIV [Du *et al*., 2011; Ren *et al*., 2014]. The most commonly, however, these cells are used to examine the mechanisms of susceptibility of cancer cells to chemotherapeutic compounds [Umezawa and Chaicharoenpong, 2002; Elia *et al*., 2014] and apoptosis-inducing signals [Du *et al*., 2011; Beyer and Pisetsky, 2013]. For these reasons, the Jurkat cells were chosen for this study as a model system to test the cytostatic properties of geldanamycin.

Initial experiments consisted of the determination of the time course and concentration-dependence of geldanamycin-induced alterations in cell cycle distribution and apoptosis. Based on the results with human lymphocytes discussed above, the duration of exposure to geldanamycin was restricted to 48 hours. This corresponded to the earliest time point

at which geldanamycin reached maximal effect. The low, ineffective concentrations of geldanamycin were omitted from the protocol, and the drug was administered at 100, 150, and 250 nM.

Quantitative analysis of the impact of geldanamycin on Jurkat cells is shown in **Figure 17**. At 8 hours, there was a transient inhibition of cells in G2/M, with a corresponding decrease in the G1 subpopulation (**Figure 17A**). However, four hours later the fraction of G1 cells increased while the fraction of cells in S phase decreased (**Figure 17C**). These changes were even more apparent at 24 (**Figure 17E)** and 48 hours (**Figure 17G**), so that at the latter time point the proportion of G1 cells increased on average by 28%, while the proportion of S and G2/M decreased by 30% and 34%, respectively. Even higher were the effects of geldanamycin on apoptosis of Jurkat cells. This parameter was found to increase by 1.6-fold, 1.7-fold, 3.4-fold, and 12.0-fold at 8, 12, 24, and 48 hours, respectively (**Figure 17B, D, F,** and **H**). All observed effects were largely independent of the concentration of geldanamycin in the range tested. Moreover, in control cells all tested parameters remained essentially unchanged with time, indicating a stable cell culture system.

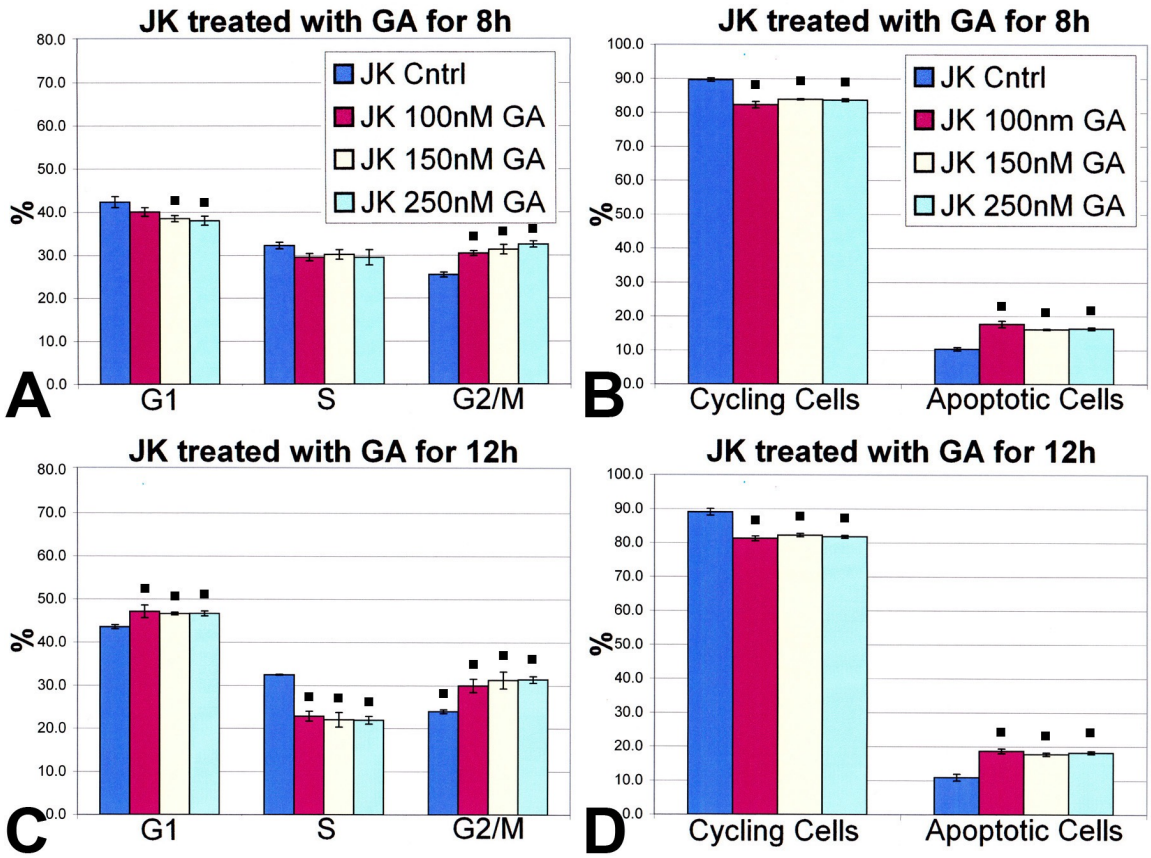

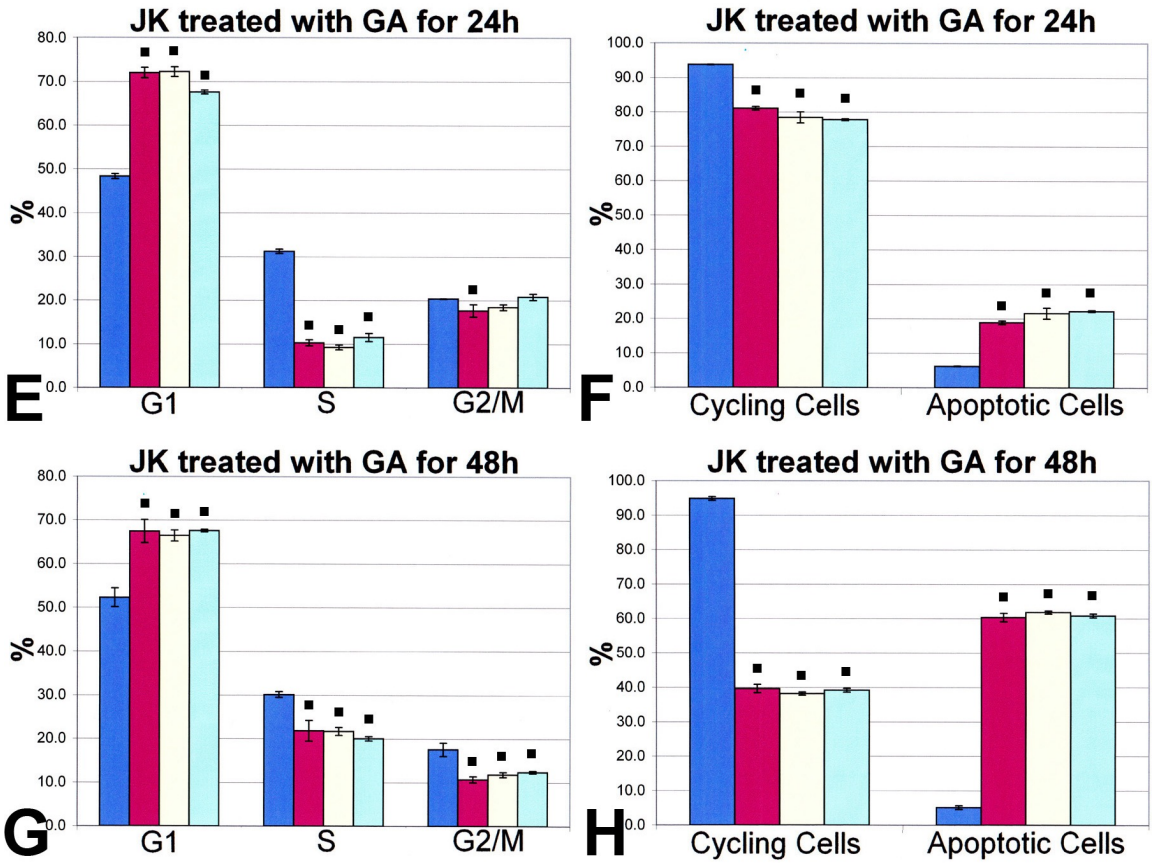

Figure 17. Time-dependent impact of geldanamycin on cell cycle and apoptosis of Jurkat cells. Bar graphs depict the impact of increasing concentrations of geldanamycin on the distribution of cells in each phase of the cell cycle (A, C, E, and G) and on apoptotic cell death (B, D, F, and H). The measurements were performed at 8 hours (A and B), 12 hours (C and D), 24 hours (E and F), and 48 hours (G and H). ■ Indicates statistically significant ($P<0.05$) difference versus control conditions (Cntrl). JK, Jurkat cells; GA, geldanamycin.

To discriminate whether the subpopulation of cells transiently inhibited in G2/M (**Figure 17A and C**) experienced a block in the G2 phase of the cell cycle or during mitosis, control and geldanamycin-treated cells were stained with an antibody against phospho-histone H3. Histone H3 is phosphorylated only at the onset of mitosis and this post-translational modification it is not present in cells traversing or inhibited in the G2 phase [Tetzlaff *et al*., 2013; Banerjee *et al*., 2014]. This experiment was performed at 24 hours after administration of 250 nM of geldanamycin. As shown in **Figure 18**, a small but distinct population of cells with G2 DNA content and strongly positive for phospho-histone H3 was seen both in control cultures and in cells treated with geldanamycin (dots in the green oval). Importantly, the size of this subpopulation did not vary markedly with the geldanamycin treatment, indicating that the block in the cell cycle occurred actually in the G2 phase, and not during mitosis. The presence of G2 arrest in this experiment is

confirmed by the presence of a higher G2/M peak in histograms of DNA distribution (**Figure 18, right panels**).

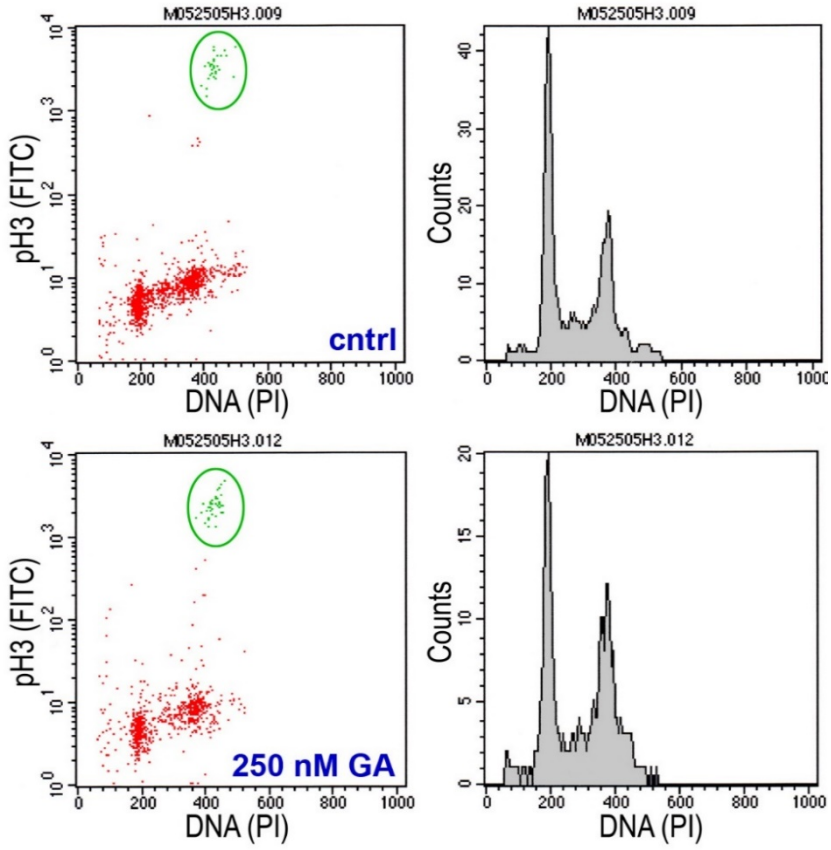

Figure 18. Impact of geldanamycin on phosphorylation of histone H3. Upper panels represent control conditions, and lower panels show cells treated with 250 nM geldanamycin. Left panels show the bivariate distribution of DNA and phosphorylated histone H3 (pH3) labeling. The mitotic cells with high levels of phospho-histone H3 are included in the green ovals. Right panels show respective frequency distribution histograms of DNA content. Cntrl, control medium; GA, geldanamycin.

To evaluate whether inhibition of cell cycle was accompanied by changes in phosphorylation state of retinoblastoma (Rb) protein, labeling was performed with an antibody recognizing its hyperphosphorylated form, pRb. Hyperphosphorylated pRb is essential for the transition through each phase of the cell cycle [Dick and Rubin, 2013; Indovina *et al.*, 2013], and the observed inhibition of cycling by geldanamycin could be associated with a decrease in the level of pRb. Experiments addressing this question were performed at 8 and 24 hours after administration of the drug. As illustrated in **Figure 19**, Jurkat cells grown in control conditions showed robust expression of pRb in all phases of the cell cycle (green dots). However, exposure of cells to geldanamycin resulted in a time-dependent loss of hyperphosphorylated pRb and an increase in the subpopulation of cells exhibiting hypophosphorylated Rb (red dots). Importantly, changes in the state of phosphorylation of Rb correlated in time with alterations in cell cycle distribution (compare the timing of changes in Figures 17 and 19).

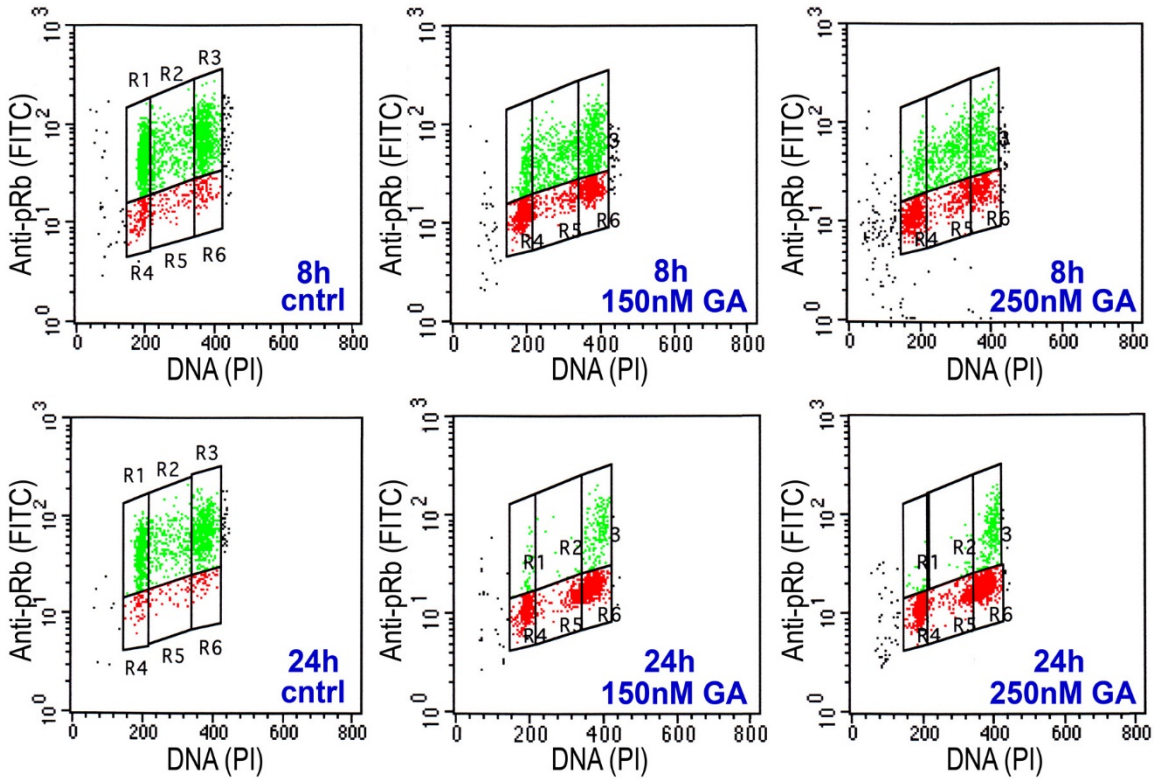

Figure 19. Impact of geldanamycin on phosphorylation of Rb protein. Cells with a high level of Rb protein phosphorylation are indicated by green dots, while those with hypophosphorylated Rb by red dots. Based on the DNA content, regions R1 and R4 correspond to cells in G1, regions R2 and R5 to cells in S, and regions R3 and R6 to cells in G2/M. pRb, hyperphosphorylated retinoblastoma protein; cntrl, control medium; GA, geldanamycin.

To obtain further evidence of the activation of apoptotic cell death by geldanamycin, the presence of activated caspase-3, a marker of early stages of apoptosis [Lavrik *et al*., 2005; Fang *et al*., 2006] was determined. The activation of caspase-3 was tested at 8, 12 and 24 hours after addition of 250 nM geldanamycin (**Figure 20**). Minimal amounts of caspase-3-positive cells (green dots) were noted in control conditions at all three time intervals. However, a noticeable increase in caspase-3 activation was observed already at 8 hours after administration of geldanamycin, and the percentage of these cells increased significantly at 12 and 24 hours. Majority of cells with activated caspase-3 had clearly defined G1 and G2/M DNA content, without evidently delineated sub-G1 population. The absence of the latter population was due to multiple washing steps required in the staining protocol; this led to the loss of fragmented or shrunk cells at advanced stages of apoptosis.

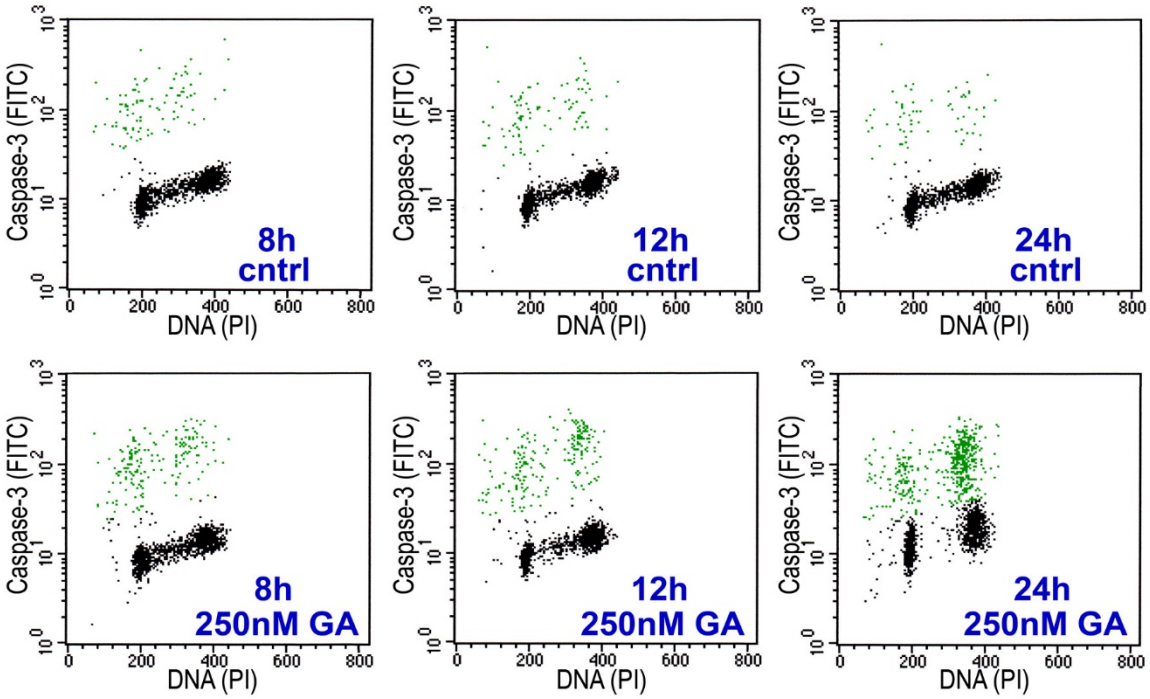

Figure 20. Effect of geldanamycin on activation of caspase-3. Cells with activated caspase-3 are indicated by green dots. Cntrl, control medium; GA, geldanamycin.

To determine whether the changes in cell cycle distribution and cell death affected the population dynamics, changes in cell number under the various experimental conditions were evaluated. Approach identical to that used for lymphocytes, described earlier, was employed. The quantitative data are summarized in **Figure 21**. Jurkat cells cultured under control conditions were characterized by a high rate of growth, with an average population doubling time of 16.7 hours. From 8 to 48 hours, the number of control cells increased 5.2-fold, while during the same time interval the number of cells treated with 100 nM, 150 nM, and 250 nM geldanamycin decreased by 37%, 38%, and 40%, respectively. The decrease in the number of cells in the presence of the drug was the result of two factors: arrest of cells in G1 (see **Figure 17C, E, and G**) and increase in the number of cells dying by apoptosis (**Figure 21B, D, F, and H**). The latter parameter was increasing with time at all concentrations and was, on average, 40%, 41%, 56% and 133% higher in the presence of geldanamycin than under control conditions at 8, 12, 24, and 48 hours, respectively. When the number of cells in each phase of the cell cycle was considered, the data indicated that essentially no change occurred in the number of G1 cells (a 6.7% increase), but an average 2.3-fold decrease in the number of cells in S phase and a 4.4-fold decrease in the number of cells in G2/M took place with geldanamycin (compare **Figure 21A** with

21G). This result further confirms the existence of a geldanamycin-induced block in the G1 phase of the cell cycle of Jurkat cells.

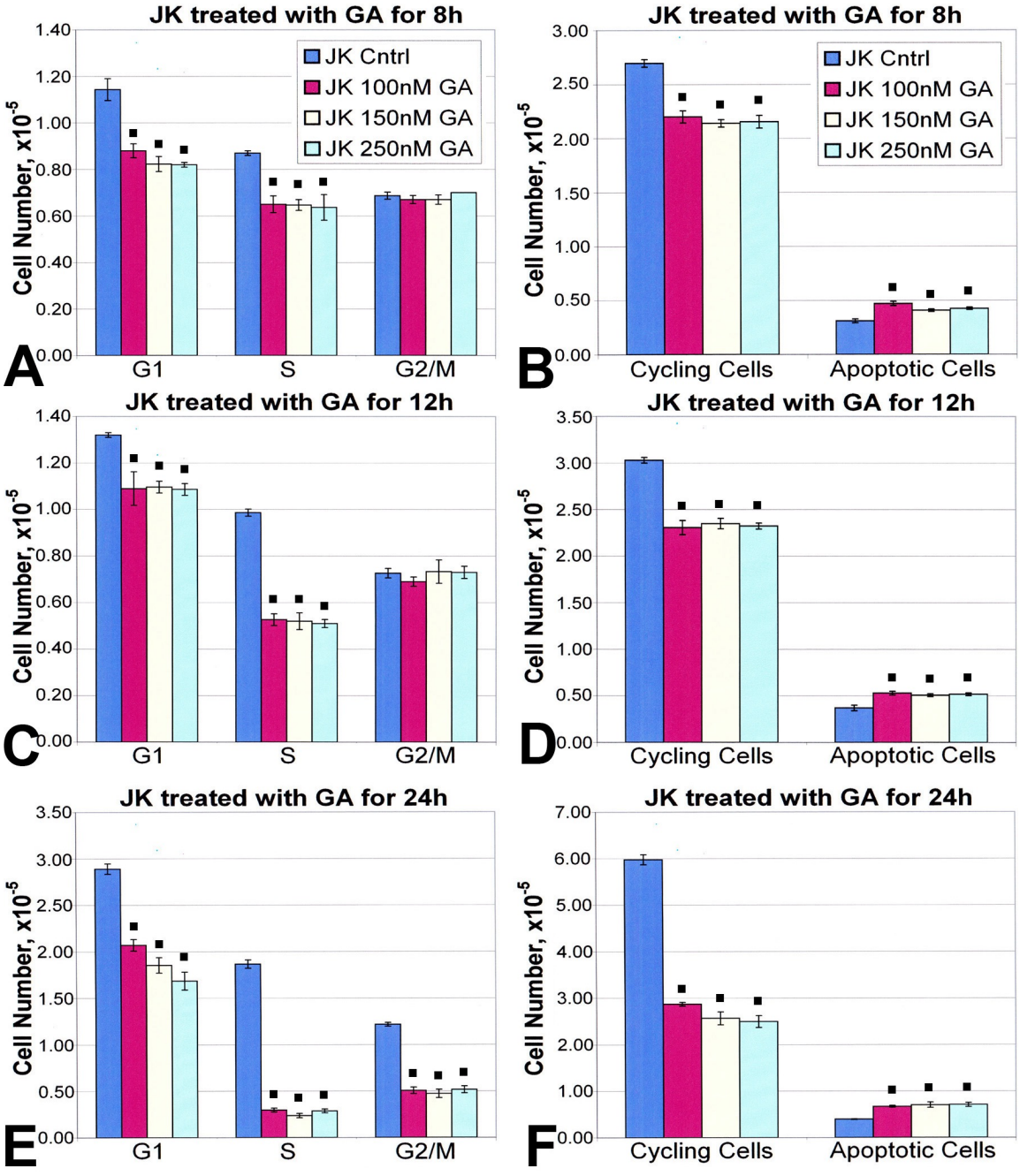

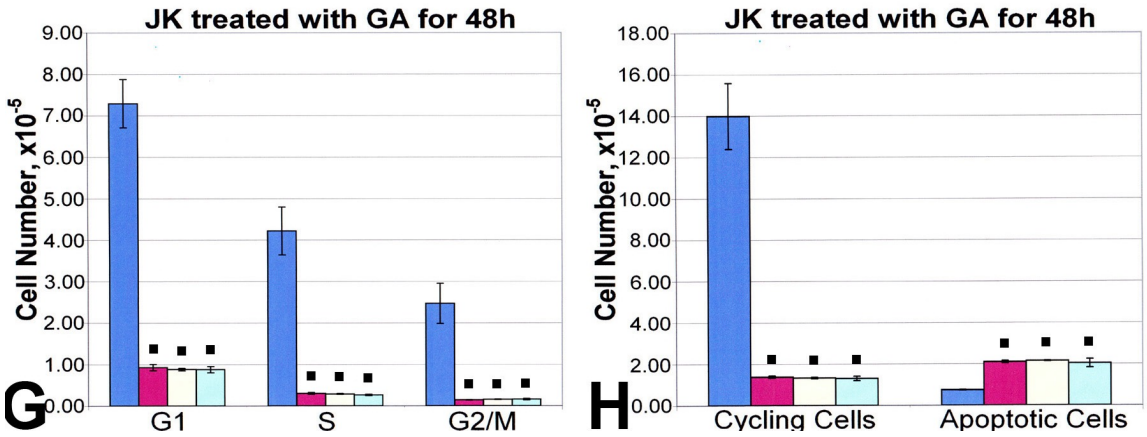

Figure 21. Time-dependent impact of geldanamycin on number of cycling and apoptotic Jurkat cells. Bar graphs depict the effect of increasing concentrations of geldanamycin on the number of cells in each phase of the cell cycle (A, C, E, and G) and undergoing apoptosis (B, D, F, and H) at 8 (A and B), 12 (C and D), 24 (E and F), and 48 (G and H) hours. ■ Indicates statistically significant ($P<0.05$) difference vs. control conditions (Cntrl). JK, Jurkat cells; GA, geldanamycin.

Geldanamycin and cell cycle and apoptosis in Jurkat IκBαM cells

As discussed earlier, Jurkat IκBαM cells cannot activate their NF-κB-mediated responses because of the mutation in the inhibitory subunit of NF-κB, IκB (see **Figure 5** in the Introduction). Therefore, these cells were utilized in experiments aiming at evaluation of the role of NF-κB in the response of cells to geldanamycin (**Figure 22**). All experiments were performed under conditions identical to those employed for the parental Jurkat cell line, shown in **Figures 17** and **18**. Importantly, the behavior of these two lines was indistinguishable under control conditions without geldanamycin.

The impact of geldanamycin on the distribution of Jurkat IκBαM cells in the cell cycle was, in some aspects, comparable to that seen in the parental Jurkat cell line (compare left panels in **Figure 22** with left panels in **Figure 17**), but a few essential differences were noted. The treatment with geldanamycin increased the fraction of Jurkat IκBαM cells in G1 at 24 and 48 hours by 69% and 44% (**Figure 22E and G**), values comparable to those observed for parental Jurkat cells (**Figure 17E and G**). The early increase in G2/M cells was also observed in both cell lines, although it was more apparent in Jurkat IκBαM, where it reached 65% and 83% at 8 and 12 hours, respectively (**Figure 22A and C**). The most apparent difference between Jurkat IκBαM cells and their parental line was the dramatic reduction in the fraction of cells in the S phase. When compared to control cultures untreated with geldanamycin, at 48 hours this fraction decreased 6-fold in Jurkat IκBαM

cells (**Figure 22G**) and only 2-fold in parental cells (**Figure 17E and G**). This 3-fold difference in response to geldanamycin was statistically significant (P<0.0001).

More striking were the differences between the fraction of cycling and apoptotic cells (compare right panels in **Figure 22** with right panels in **Figure 17**). The effect of the inactivation of NF-κB was most apparent at 48 hours, when the fraction of surviving, cycling Jurkat IκBαM was 2-fold, 3-fold and 6-fold lower than that of parental Jurkat cells at 100 nM, 150 nM, and 250 nM geldanamycin, respectively (**Figure 22H**). This decrease was accompanied by nearly doubling of the fraction of apoptotic cells. Thus, in the absence of activity of NF-κB, geldanamycin-mediated stimulation of apoptosis and loss of cycling cells are much more pronounced than when NF-κB is active. This result points to the growth-promoting and anti-apoptotic function of NF-κB in Jurkat cells.

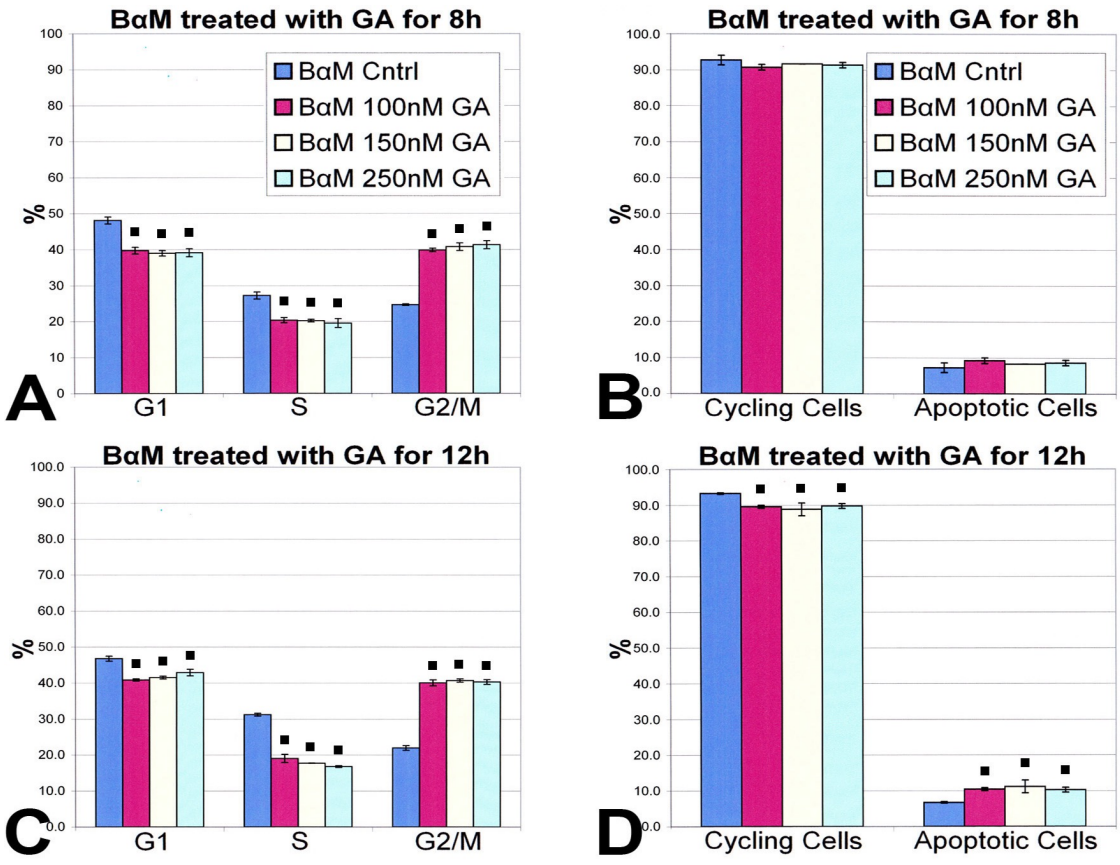

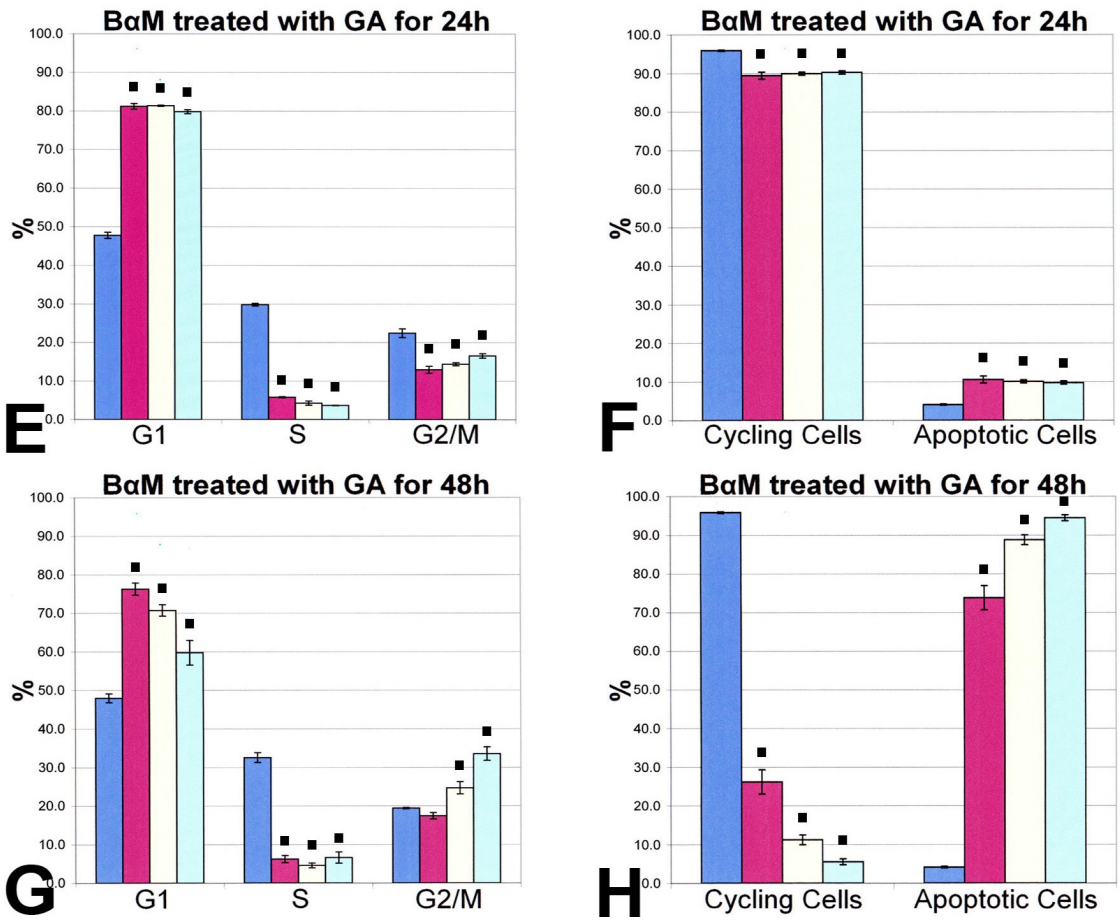

Figure 22. Time-dependent impact of geldanamycin on cell cycle and apoptosis of Jurkat IκBαM cells. Bar graphs depict the impact of increasing concentrations of geldanamycin on distribution of cells in each phase of the cell cycle (A, C, E, and G) and apoptotic cell death (B, D, F, and H) at 8 hours (A and B), 12 hours (C and D), 24 hours (E and F), and 48 hours (G and H). ■ Indicates statistically significant ($P<0.05$) difference versus control conditions (Cntrl). BαM, Jurkat IκBαM cells; GA, geldanamycin.

The above conclusions were confirmed when the changes in the number of cells were analyzed (**Figure 23**). Under control conditions, i.e., in the absence of geldanamycin, the population doubling time of Jurkat IκBαM was 16.9 hours, comparable to that measured for the parental line, 16.7 hours. Thus, when not challenged by geldanamycin, the population dynamics of both cell lines were comparable. However, an increase in the number of apoptotic cells became first apparent at 24 hours of incubation with the drug and became even more pronounced at 48 hours. Activation of apoptosis resulted in a significant loss of living cells. In comparison with untreated controls, the decrease in the

number of cells was 14-fold, 33-fold, and 71-fold after 48 hours of exposure of cells to 100 nM, 150 nM, and 250 nM geldanamycin, respectively (**Figure 23**).

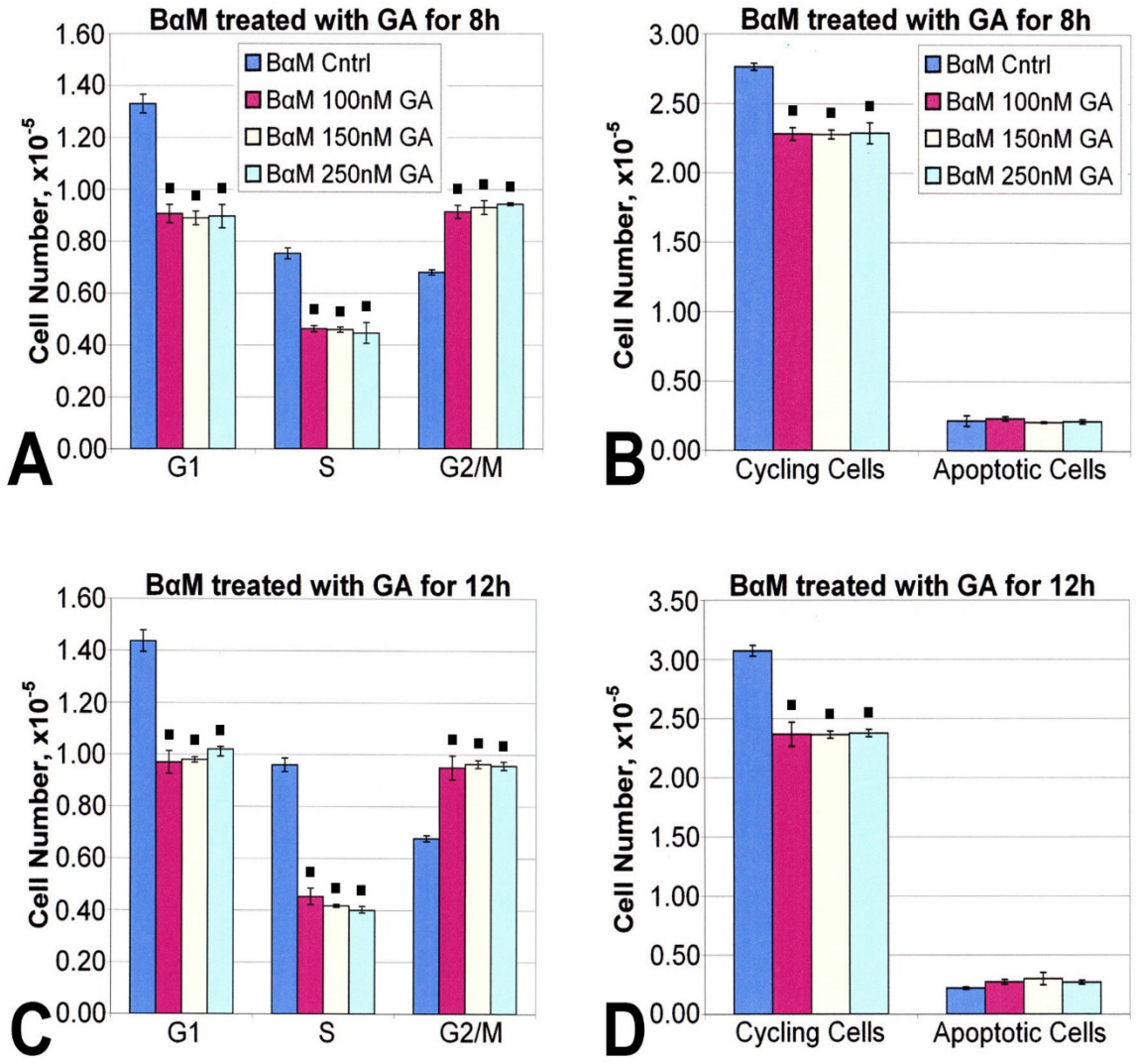

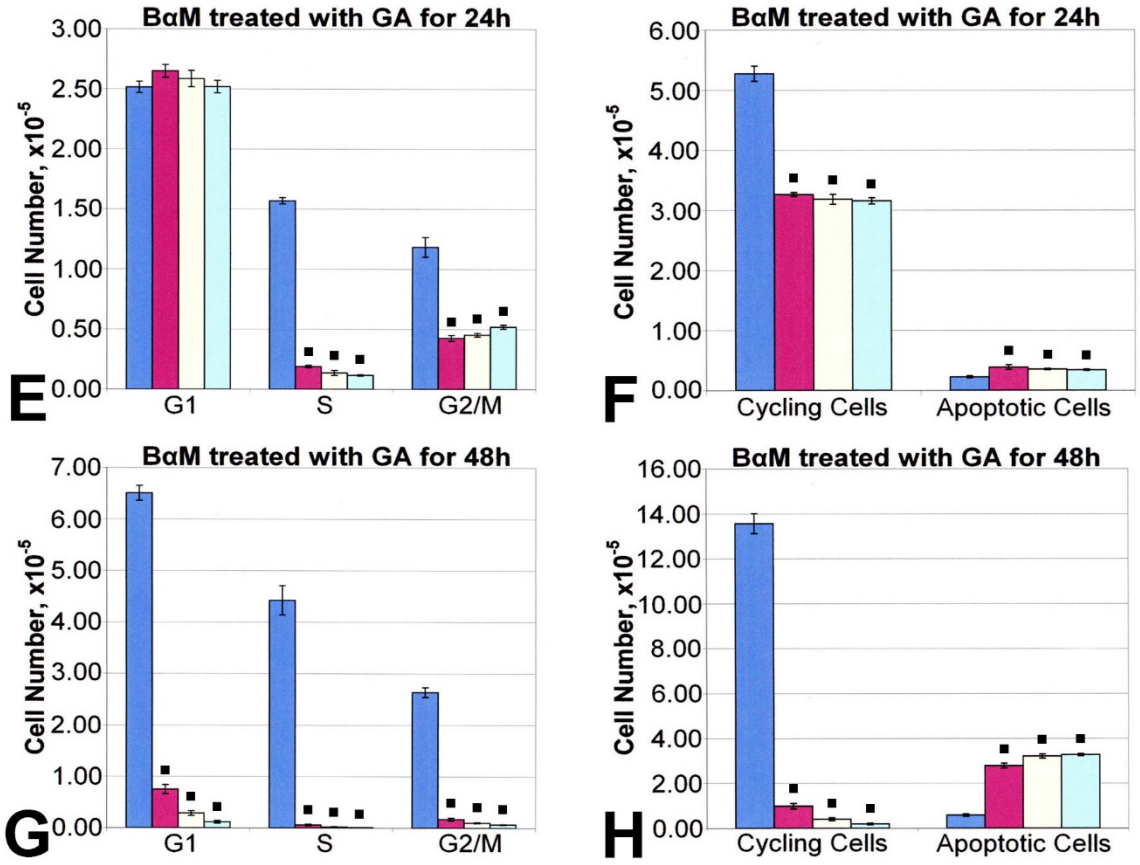

Figure 23. Time-dependent impact of geldanamycin on the number of cycling and apoptotic Jurkat IκBαM cells. Bar graphs depict the effect of increasing concentrations of geldanamycin on number of cells in each phase of the cell cycle (A, C, E, and G) and undergoing apoptosis (B, D, F, and H) at 8 (A and B), 12 (C and D), 24 (E and F), and 48 (G and H) hours. ■ Indicates statistically significant ($P<0.05$) difference vs. control conditions (Cntrl). BαM, Jurkat IκBαM cells; GA, geldanamycin.

Geldanamycin, cell cycle, and apoptosis in parthenolide-treated Jurkat cells

The work described above, performed with Jurkat IκBαM cells, was complemented by experiments in which parthenolide, a plant-derived inhibitor of NF-κB [64, 65], was employed. In initial studies, the drug was utilized at concentrations ranging from 5 to 20 μM. Examples of these results are presented in **Figure 24**. The illustrated experiment corresponds to 8 hours of exposure to parthenolide alone (**Figure 24A-D**) or parthenolide together with geldanamycin (**Figure 24E-H**). The use of acridine orange in this assay permitted visualization of not only apoptotic cells (black points in dot plots) but also necrotic or very late apoptotic cells (magenta points in dot plots). The necrotic cells were recognized by having a markedly decreased RNA content (red fluorescence of acridine orange in channel FL3). The reduction in RNA was most likely the result of loss of integrity

of their plasma membrane and consequent outflux of cytoplasmic components [Blagosklonny, 2000; Lockshin *et al.*, 2002; Pozarowski *et al.*, 2003]. Of note, in contrast to apoptotic cells, the DNA content in necrotic cells (green fluorescence in channel FL1) did not change markedly.

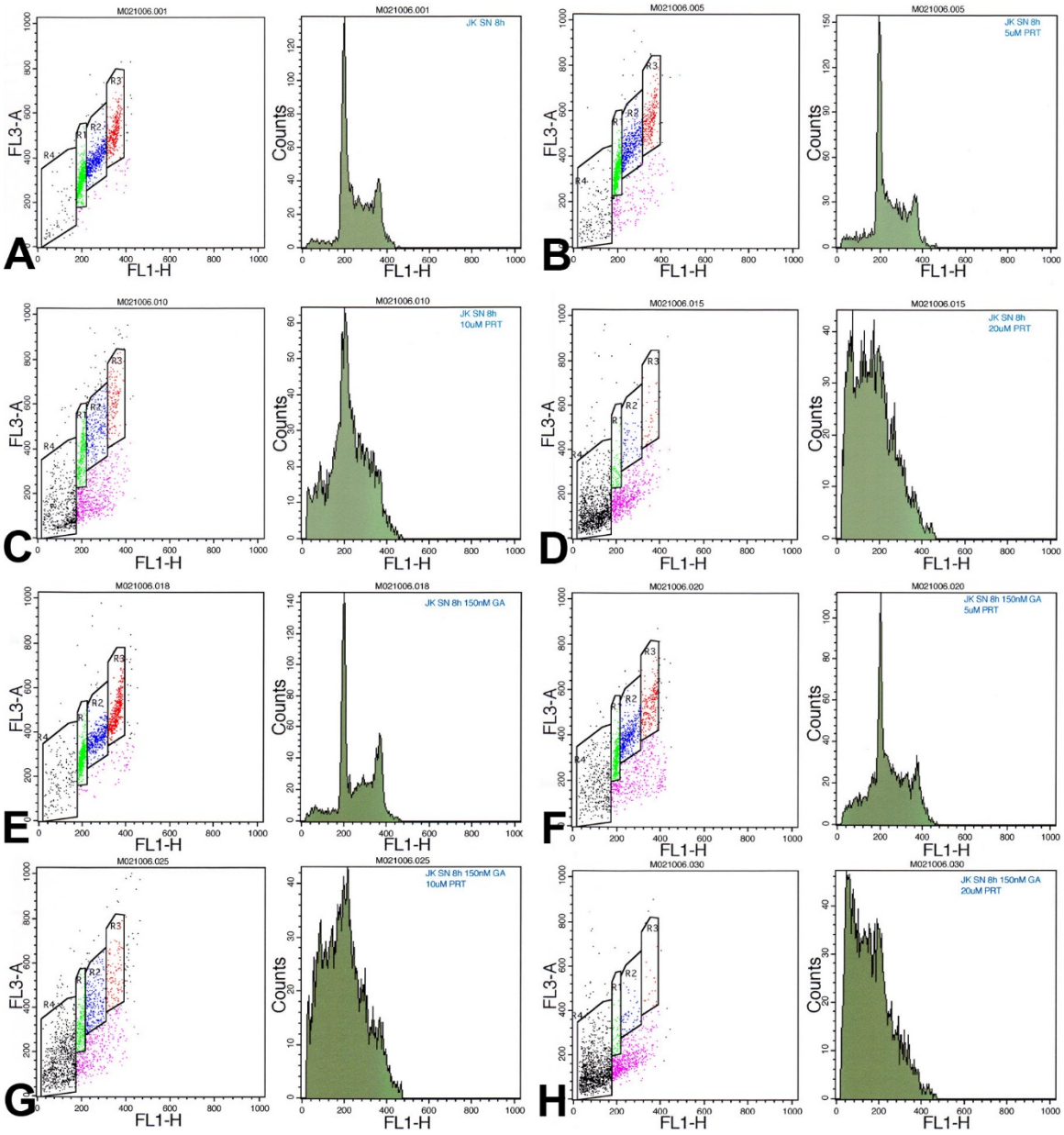

Figure 24. Parthenolide, geldanamycin, and apoptotic and necrotic cell death. Jurkat cells were incubated with parthenolide alone (A-D) or parthenolide and 150 nM geldanamycin (E-H) for 8 hours. A and E: no parthenolide (control); B and F: 5 μM parthenolide; C and G: 10 μM parthenolide; D and H: 20 μM parthenolide. In dot plots, green points correspond to cells in G1, blue dots to cells in S, red dots to cells in G2/M, black dots to apoptotic cells and magenta dots to necrotic cells. FL1: fluorescence channel 1 reflecting green fluorescence of acridine orange, i.e., DNA; FL3: fluorescence channel 3 reflecting red fluorescence of acridine orange, i.e., RNA.

The quantitative data from experiments with parthenolide are shown in **Figure 25**. Cells dying by necrosis were excluded from this analysis. The impact of parthenolide on Jurkat cells was apparent already at 8 hours after administration of the drug. Parthenolide alone only modestly affected the relative distribution of cells within the cell cycle (**Figure 25A**). However, it had a significant impact on the magnitude of apoptosis and, by extension, on the fraction of live cycling cells (**Figure 25B**). In comparison with control cultures, apoptosis increased 2.3-fold, 5.0-fold, 9.2-fold, and 18-fold in the presence of 5, 7.5, 10, and 20 μM parthenolide, respectively (**Figure 25B**).

Importantly, when parthenolide was administered together with geldanamycin (150 nM), its impact on the cell cycle distribution was more apparent. There was a 48%, 55%, 69%, and 56% increase in cells in S phase at 5, 7.5, 10, and 20 μM parthenolide, respectively (**Figure 25C**). This was accompanied by a 29%, 46%, 45%, and 51% reduction in cells in G2/M at corresponding parthenolide concentrations. Increase in the fraction of apoptotic cells and loss of viable cycling cells was also higher in the presence of geldanamycin than when parthenolide alone was used (**Figure 25D**). Thus, geldanamycin-treated cells respond rapidly to the parthenolide challenge by inhibition in S phase and increased apoptotic cell death.

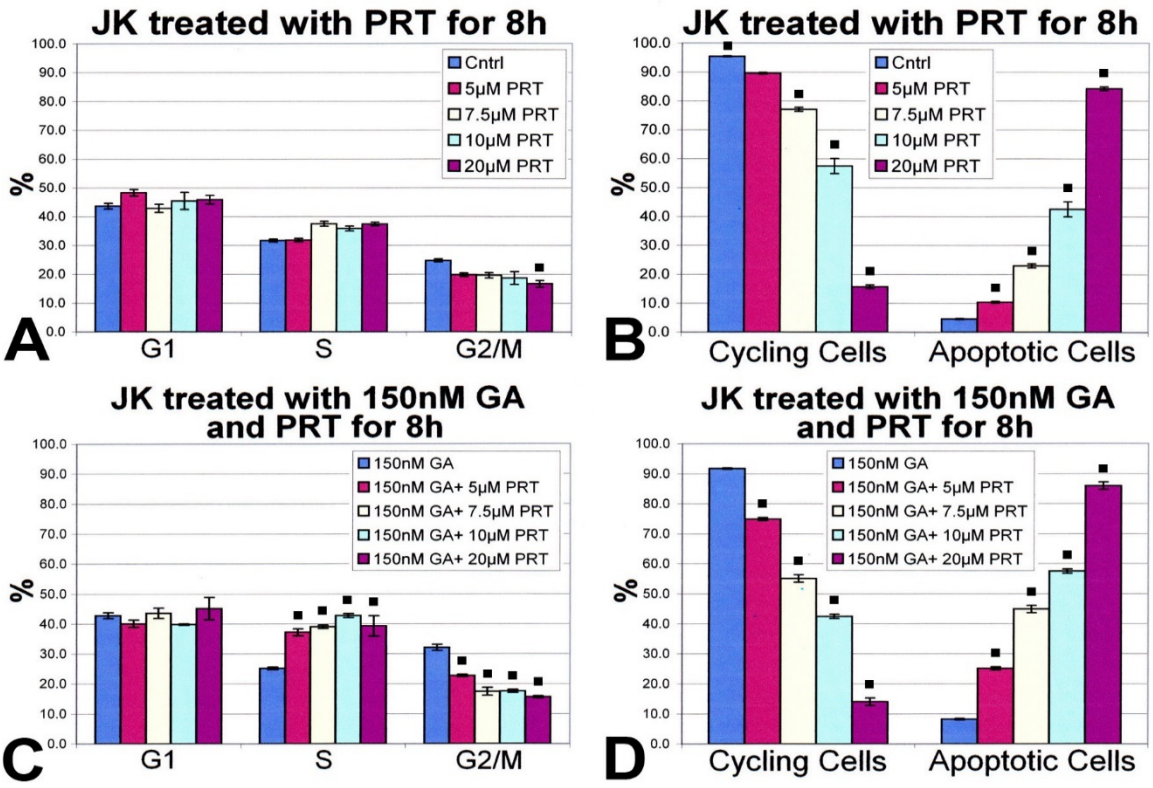

Figure 25. Short-term effects of parthenolide on Jurkat cells. Cells were cultured in the absence (A and B) or the presence (C and D) of 150 nM geldanamycin. Bar graphs illustrate the distribution of viable cells in the cell cycle (A and C) and the proportion of cells undergoing apoptosis (B and D). ■ Indicates statistically significant ($P<0.05$) difference vs. control conditions (Cntrl). PRT, parthenolide; GA, geldanamycin.

Because of high levels of necrosis associated with exposure of cells to 20 μM of parthenolide (see **Figure 24D** and **24H**), this dose of the drug was not utilized in subsequent protocols. These experiments analyzed the effect of blocking NF-κB on the response of Jurkat cells to geldanamycin at later time points, 12 and 24 hours. The quantitative results are summarized in **Figure 26**. Inhibition of NF-κB resulted in an accumulation of cells in S-phase at both time intervals (**Figure 26A and C**). At 24 hours, the increase in the fraction of cells in the S phase was 3.1-fold, 4.1-fold, and 3.8-fold with 5, 7.5, and 10 μM parthenolide, respectively. It was accompanied, respectively, by a 49%, 47%, and 41% decrease in the fraction of G1 cells (**Figure 26C**). Increase in the fraction of apoptotic cells and loss of viable cycling cells was also apparent (**Figure 26B and D**).

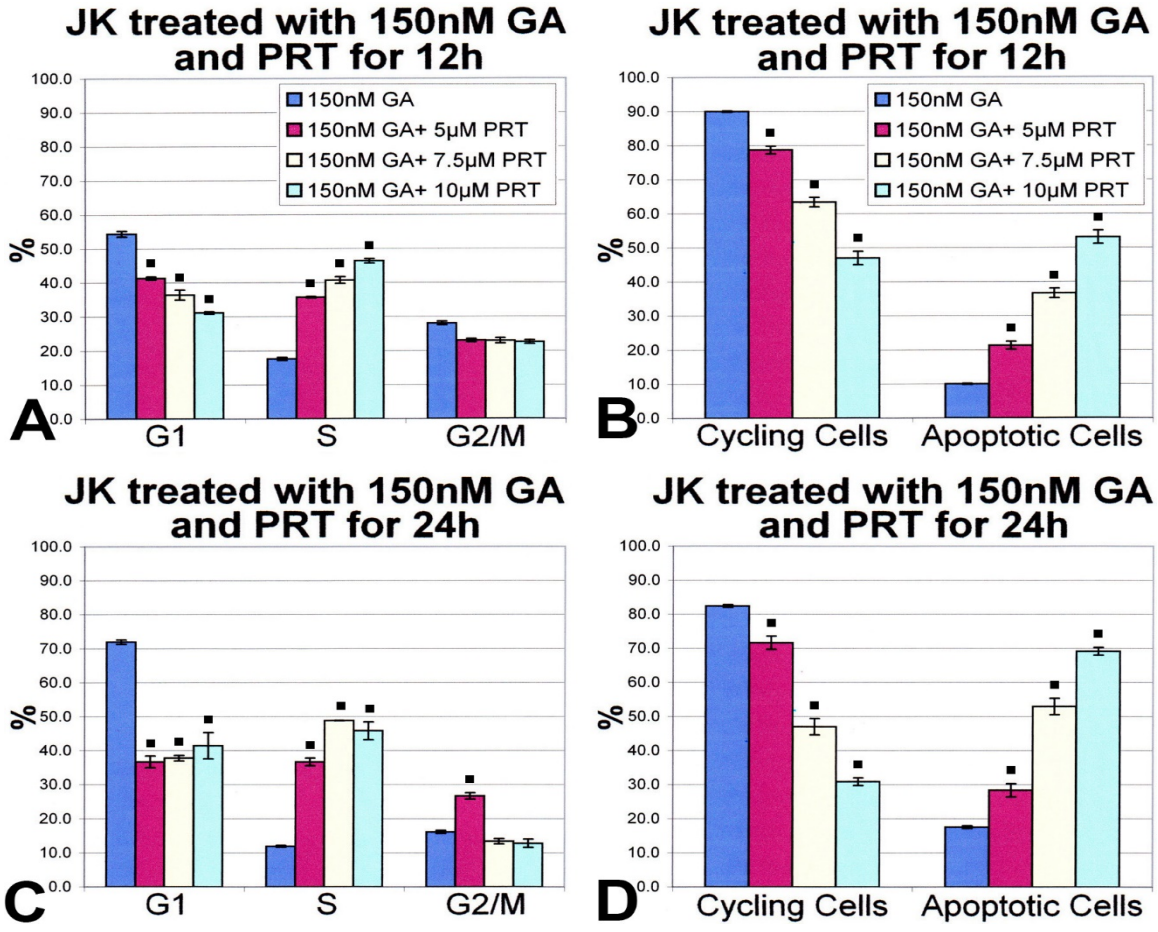

Figure 26. Long-term effects of parthenolide on Jurkat cells. Cells were cultured in the presence of 150 nM geldanamycin. Bar graphs illustrate the distribution of viable cells in the cell

cycle (A and C) and the proportion of cells undergoing apoptosis (B and D). ■ Indicates statistically significant (P<0.05) difference vs. control conditions (150 nM geldanamycin). PRT, parthenolide; GA, geldanamycin.

Similar conclusions were reached when the number of cells was analyzed (**Figure 27**). The number of cells in G1 was decreasing progressively with time and, in comparison to control conditions, was diminished 8.1-fold at 24 hours of exposure to 10 μM parthenolide. At the same time point, the number of all cycling cells decreased 4.5-fold, and the number of apoptotic cells increased 2.4-fold (**Figure 27**). Because of the diminished total number of cells in the presence of parthenolide and geldanamycin, the increase in the fraction of cells in S phase did not translate into an increase in their number, which remained essentially constant.

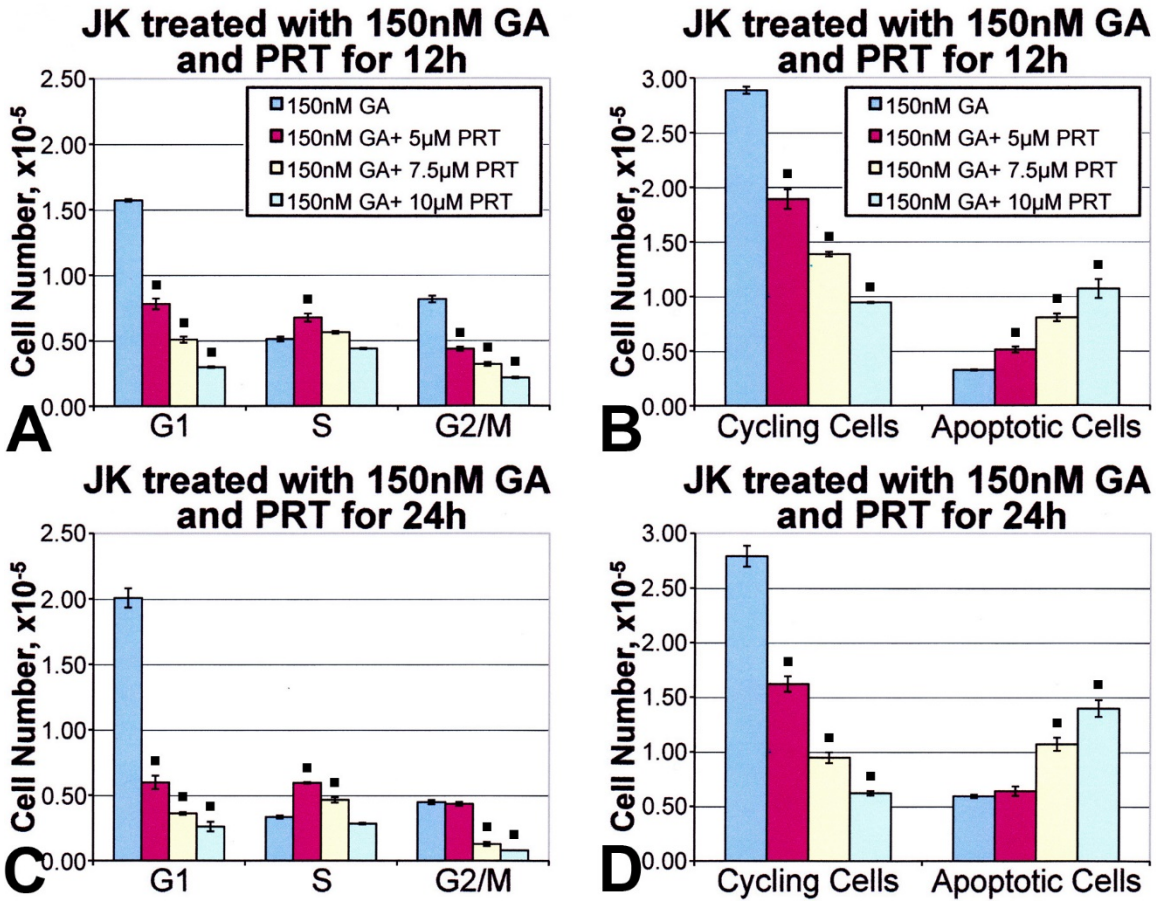

Figure 27. Long-term effects of parthenolide on the number of Jurkat cells. Cells were cultured in the presence of 150 nM geldanamycin. Bar graphs illustrate the number of cells in each phase of the cell cycle (A and C) and the number of cells undergoing apoptosis (B and D). ■ Indicates statistically significant (P<0.05) difference vs. control conditions (150 nM geldanamycin). PRT, parthenolide; GA, geldanamycin.

Alternative geldanamycin treatment protocols

Supplementary experiments were performed to ensure that the availability of geldanamycin, even at the highest concentrations used, was not a limiting factor in the experiments performed. A correct interpretation of the result would be more difficult, if not impossible, if geldanamycin were unstable in the culture medium employed, or its amount per cell would become a limiting factor in cultures where the number of cells was increasing with time. These are relevant issues for the use of ansamycins, since frequently for this category of drugs the biological effect is dependent not only on their concentration, but also on the number of cells, volume of the medium, and the total amount of the compound present [Chiosis *et al.*, 2003]. To address these possibilities, additional experiments were carried out, utilizing three different protocols.

Protocol 1: Jurkat and Jurkat IκBαM cells were cultured continuously for 48 hours. Every 12 hours, a small sample of cell suspension was withdrawn and analyzed. This protocol corresponds to the procedure used in all experiments discussed before.

Protocol 2: Jurkat and Jurkat IκBαM cells were cultured for 12 hours. A small sample of cell suspension was then withdrawn for analysis. The remaining cells were washed, resuspended in fresh medium, and geldanamycin was added to achieve the concentration of 150 nM. This procedure was repeated every 12 hours for 48 hours. Control cultures were treated identically, but geldanamycin was not added. This protocol minimized the possibility of depletion of the drug from the medium by the cells.

Protocol 3: Jurkat and Jurkat IκBαM cells were cultured for 12 hours. A small sample of cell suspension was then withdrawn for analysis. The remaining cells were washed, counted, and resuspended in a volume of fresh medium that yielded the original concentration of cells. Geldanamycin was added to achieve the concentration of 150 nM. This procedure was repeated every 12 hours up to 48 hours. Control cultures were treated identically, but geldanamycin was not added. This protocol minimized the possibility of decreasing the ratio of geldanamycin molecules to the number of cells due to cell proliferation during the course of the experiment.

The quantitative results are shown in **Figures 28** and **29**. The control cells not exposed to geldanamycin yielded comparable values with all three protocols and, therefore, were

combined in a single average. When the distribution of cells in the cell cycle and the fraction of apoptotic cells were compared, essentially no differences were noted between the three protocols. In experiments with Jurkat cells, only two groups showed statistically significant difference (cells in S phase in protocol 2 at 48 hours, **Figure 28G**, and apoptotic cells in protocol 3 at 36 hours, **Figure 28F**), and in Jurkat IκBαM statistically significant difference was found in seven cases (red symbols in **Figure 29**). The presence of these nine statistically significant differences does not prove the existence of dissimilarities between the outcomes of the three protocols; these differences most likely appeared by chance. Since a total of 192 comparisons were done in the entire set of data, and since the significance level was set at 0.05, it follows that in 5% of the comparisons (5% of 192 = 9.6) the statistical computation may assert the existence of a difference while, in reality, none exists. In qualitative terms, the overall pattern of the response to geldanamycin was similar with all three protocols and both types of cells. Thus, the obtained data do not support the possibility that altering the protocol by modifying access of cells to geldanamycin could affect the results of the experiments.

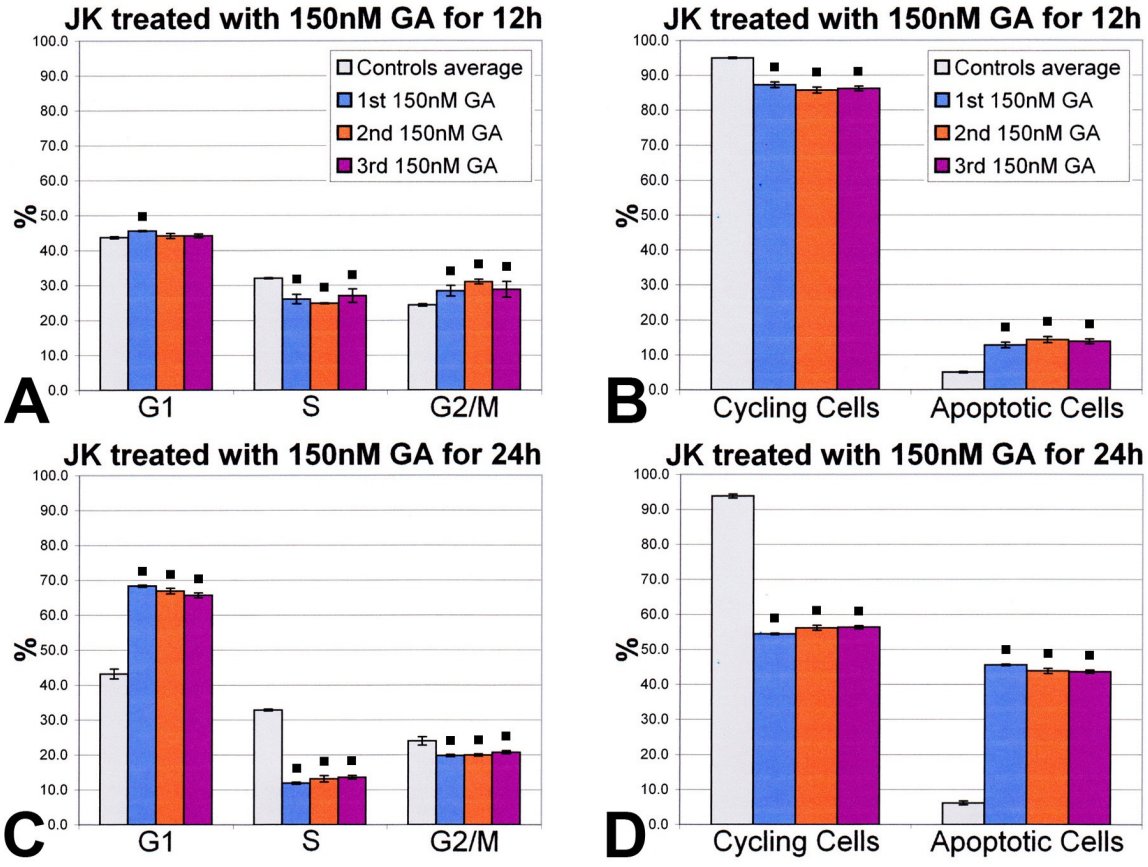

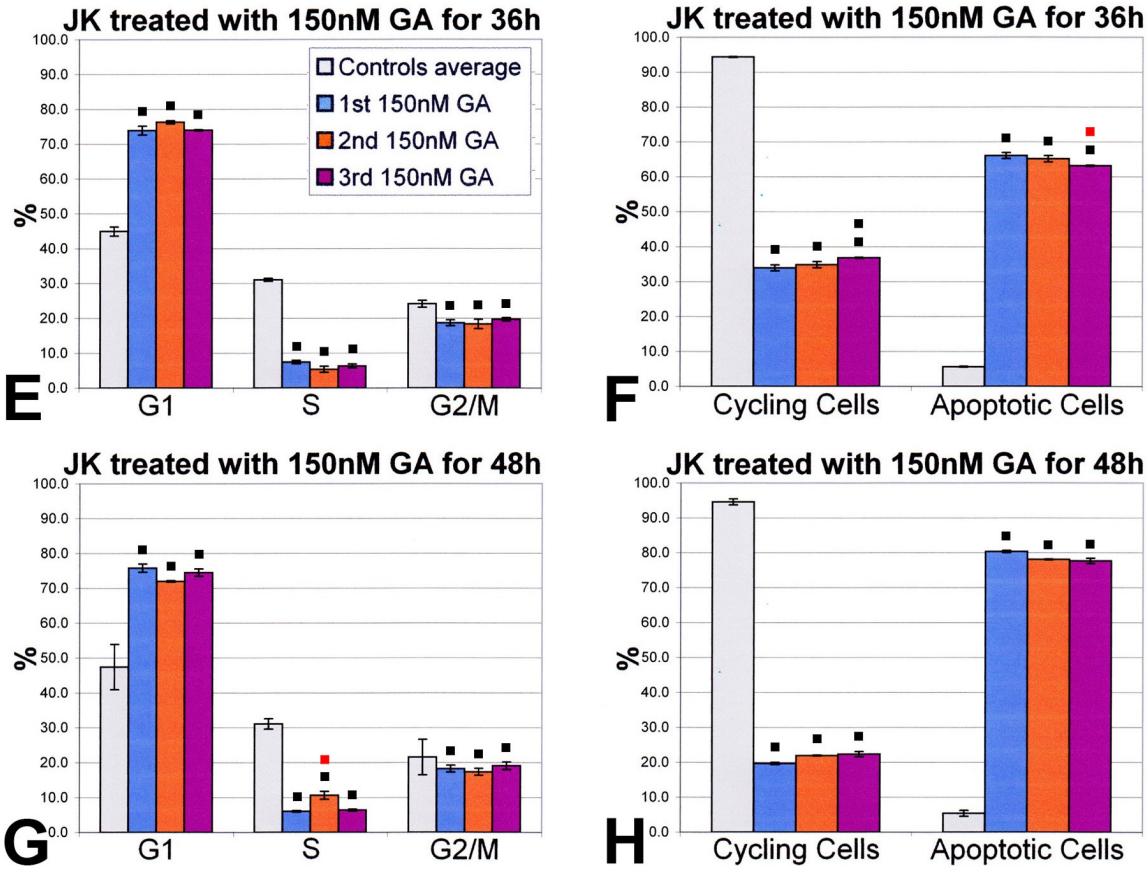

Figure 28. Alternative protocols of geldanamycin treatment: effects on Jurkat cells. Cells were cultured according to protocol 1 (1st), protocol 2 (2nd) and protocol 3 (3rd) in the presence of 150 nM geldanamycin. Bar graphs illustrate the distribution of cells in the cell cycle (A, C, E, G) and the proportion live cycling cells and cells undergoing apoptosis (B, D, F, H). ■ Indicates statistically significant ($P<0.05$) difference vs. control conditions (no geldanamycin). ■ Indicates statistically significant ($P<0.05$) difference vs. the two other protocols. JK, Jurkat cells; GA, geldanamycin.

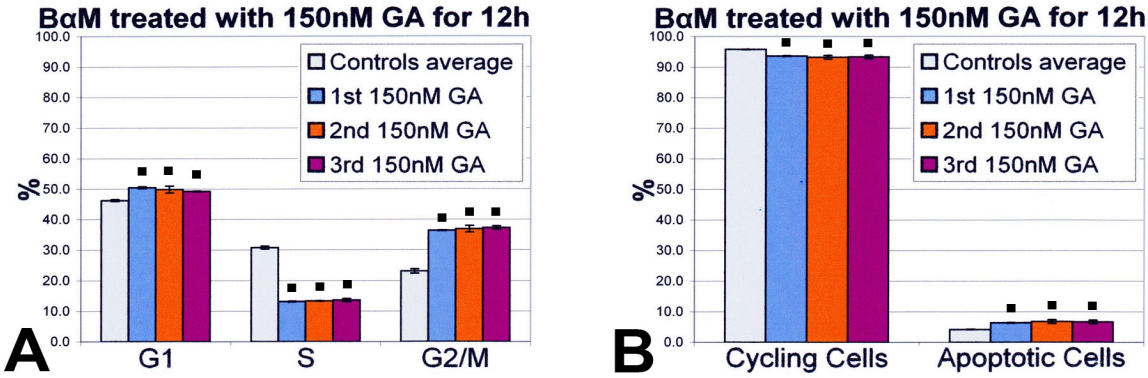

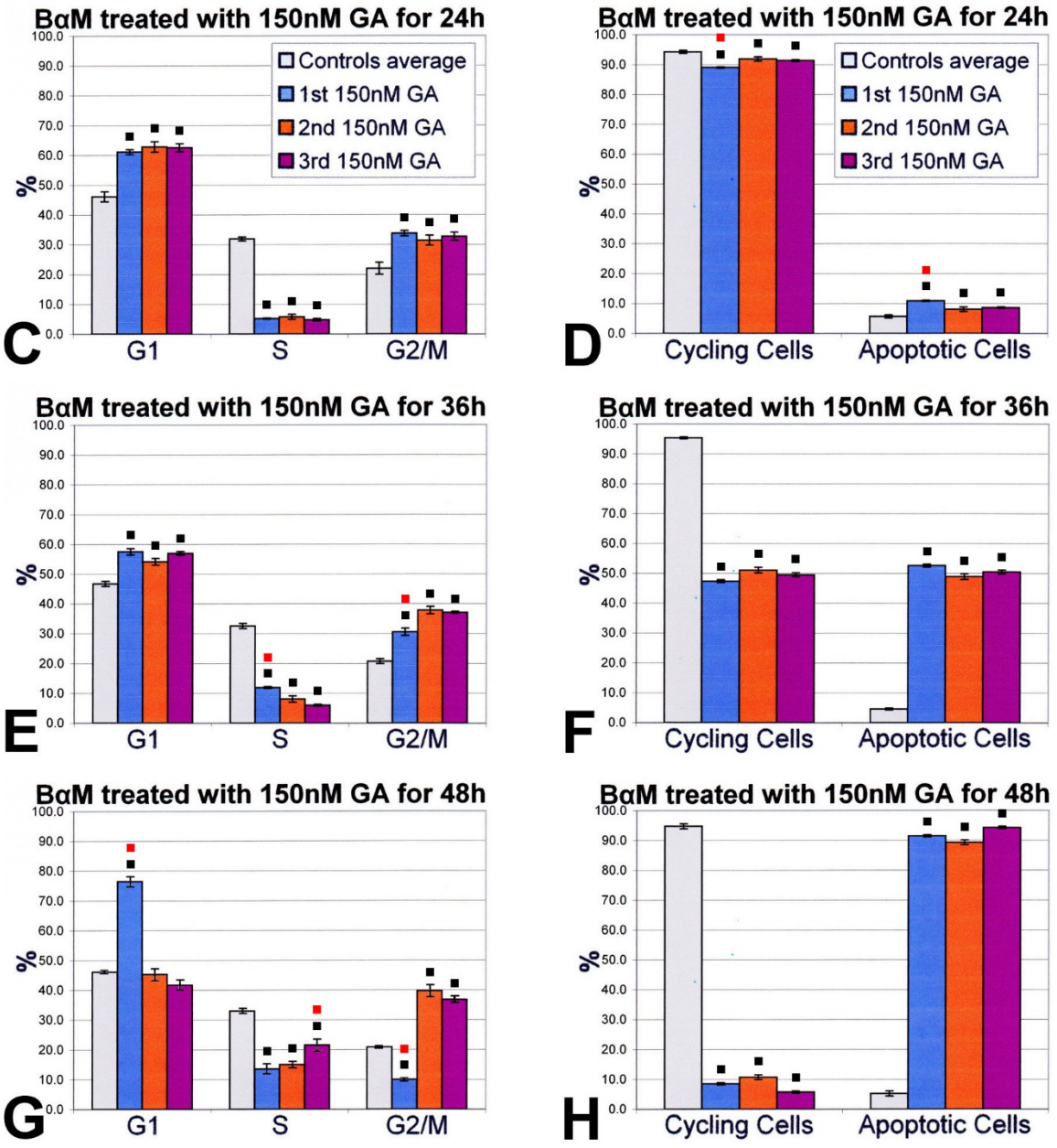

Figure 29. Alternative protocols of geldanamycin treatment: effects on Jurkat IκBαM cells. Cells were cultured according to protocol 1 (1st), protocol 2 (2nd) and protocol 3 (3rd) in the presence of 150 nM geldanamycin. Bar graphs illustrate the distribution of cells in the cell cycle (A, C, E, G) and the proportion live cycling cells and cells undergoing apoptosis (B, D, F, H). ■ Indicates statistically significant ($P<0.05$) difference vs. control conditions (no geldanamycin). ■ Indicates statistically significant ($P<0.05$) difference vs. the two other protocols. BαM, Jurkat IκBαM cells; GA, geldanamycin.

DISCUSSION

The results of the present study indicate that geldanamycin, an inhibitor of HSP90, induces exit from the cell cycle and transition to the G0 state, and, to a lesser extent, apoptosis in human lymphocytes. In Jurkat cells, an established cell line of a T cell leukemia, the drug induces block of cell cycle progression by arresting the cells in G1, and a significant degree of apoptotic cell death. The pro-apoptotic effect of geldanamycin is potentiated by simultaneous inhibition of NF-κB activity. These newly identified pathways of geldanamycin action are shown schematically in **Figure 30**.

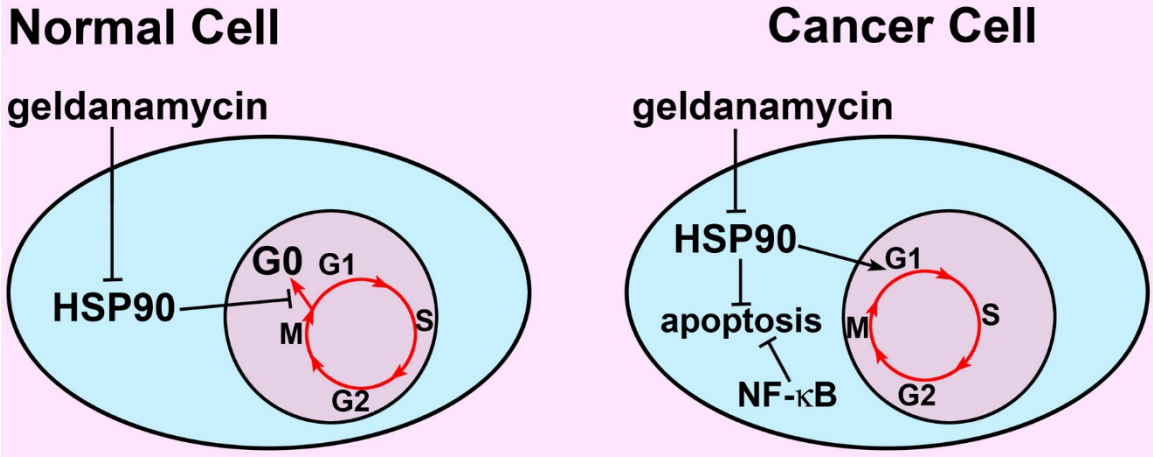

Figure 30. Schematic representation of the major findings of this study.

HSP90 and cancer

HSP90 is expressed at high levels in cells of solid tumors [Conroy *et al*., 1998] and hemopoietic malignancies [Yufu *et al*., 1992; Chant *et al*., 1995] and its client proteins are frequently overexpressed or mutated in cancer cells [Burrows *et al*., 2004, Whitesell and Lindquist, 2005]. Therefore, this chaperone protein attracts increasing attention as a target for anticancer drugs [Franke *et al*., 2013; Garcia-Carbonero *et al*., 2013; Proia and Bates, 2014, Chatterjee *et al*., 2016; Khandelwal *et al*., 2016; Chatterjee and Burns, 2017]. One of the compelling reasons for this interest is the mechanistic link of HSP90 to the so-called "six hallmarks of cancer", which include: 1. self-sufficiency in growth signals; 2. resistance to growth-inhibitory signals; 3. lack of sensitivity to apoptotic stimuli; 4. unlimited replicative potential; 5. promotion of angiogenesis; and 6. invasion of the surrounding tissue [Hanahan and Weinberg, 2000; Maloney and Workman, 2002; Hanahan and Weinberg, 2011; Miyata *et al*., 2013; Khandelwal *et al*., 2016]. The data collected in the last decade point to the involvement of HSP90 at several levels of oncogenesis. The increased

amounts of HSP90 in cancer cells may reflect the physiological cytoprotective response to the hostile milieu of the tumor, which is hypoxic, nutrient-deprived, and acidic [Petrulio *et al*., 2006; Lunt *et al*., 2009]. Molecularly, the activity of HSP90 may be implicated in the ability of tumor cells to overcome the deranged signaling associated with these aspects of tumorigenesis. As a result, cancer cells possess the capacity to resist programmed cell death that would ensue otherwise [Takayama *et al*., 2003; Mosser and Morimoto, 2004; Whitesell and Lindquist, 2005]. In the discussion below, I will focus on the potential interaction of HSP90 with the cell cycle and apoptosis, i.e., the first three of the six hallmarks of cancer.

HSP90 and cell cycle

The cell cycle is a tightly regulated by cyclin-dependent kinases (CDKs), which are activated by their associated proteins, cyclins [Deshpande *et al*., 2005]. CDKs exert their function by phosphorylation of multiple substrates, such as retinoblastoma protein (pRb) [Giacinti and Giordano, 2006; Dick and Rubin, 2013; Indovina *et al*., 2013; Uchida, 2016]. Two major checkpoints, G1 and G2/M, are present in the cell cycle; they prevent cells with DNA damage from undergoing cell division [Kastan and Bartek, 2004; Uchida, 2012; Sperka *et al*., 2012; Maes *et al*., 2017; Otto and Sicinski, 2017]. Crucial components of these checkpoints are deregulated in most types of cancer cells, resulting in loss of normal growth properties and evasion of cell cycle controls [Giacinti and Giordano, 2006; Lapenna and Giordano, 2009; Otto and Sicinski, 2017].

The tumor suppressor protein p53 is the most researched example of molecules involved in cell cycle checkpoints [Merkel *et al*., 2017; Kastenhuber and Lowe, 2017]. p53 induces arrest in the G1 phase of the cell cycle in order to initiate the process of DNA repair [Chen *et al*., 2010; Carvajal and Manfredi, 2013]. The pathway by which p53 can arrest the cell cycle in G1 involves pRb. The transition from G1 to S is conditioned by phosphorylation of Rb by a complex of CDK4 and cyclin D [Kato *et al*., 1993; Choi and Anders, 2014]. Phosphorylated Rb releases the transcription factor E2F-1, activating transcription of several genes involved in S phase progression, one of which is cyclin E. Subsequently, cyclin E activates cdk2, which continues to phosphorylate Rb protein, so that it reaches a hyperphosphorylated state [Geng *et al*., 1996; Lundberg and Weinberg, 1998] and allows the G1 to S transition [Donnellan and Chetty, 1999; Harbour and Dean, 2000]. Activated p53 inhibits this process at its onset by inducing expression of p21, an inhibitor of CDK4.

If p53 is inactivated by mutations present in cancer cells, this inhibitory mechanism is not triggered by DNA damage and the cell proceeds to S phase regardless of DNA integrity [Dick and Rubin, 2013; Indovina *et al*., 2013; Uchida, 2012; Sperka *et al*., 2012].

The question then concerns the mechanism by which HSP90 contributes to the control of the G1 cell cycle arrest. This is a relevant issue since the G1 arrest was documented in the experiments involving Jurkat cells carried out in the present study. Although the information available in the literature is limited, scattered evidence allows suggesting potential pathways by which geldanamycin inhibition of HSP90 could block the progression of the cell cycle. It is well documented that p53 is a client protein of HSP90 [Didenko *et al*., 2012; Calderwood and Gong, 2016]. Inhibition of HSP90 increases the stability of the p53 protein and sensitizes cancer cells to therapeutic interventions [Ayrault *et al*., 2009; Vaseva *et al*., 2011; Roh *et al*., 2013; McLaughlin *et al*., 2017]. Thus, the ability of geldanamycin to induce the G1 arrest may be due to direct interaction of HSP90 with p53 (see **Figure 31**). Alternatively, the arrest could be dependent on the interaction of HSP90 with its another client protein, Mdm2, which is a negative regulator of p53 [Karni-Schmidt *et al*., 2016]. Since inhibition of HSP90 causes a rapid loss of Mdm2 [Ayrault *et al*., 2009], p53 would be upregulated, and G1 cell cycle arrest could be effectuated.

Consistent with the role of pRb in cell cycle regulation, herbimycin A, an ansamycin antibiotic related to geldanamycin, fails to induce the G1 block in cancer cell lines which lack a functional Rb protein [Srethapakdi *et al.*, 2000]. Moreover, the drug promotes accumulation of hypophosphorylated Rb; this loss of phosphorylation of Rb protein is preceded by a rapid decrease in the level of cyclin D and ckd4 [Srethapakdi *et al*., 2000]. These results are consistent with the possibility that HSP90 acts upstream of the Rb protein, most likely by downregulation of cyclin D and cdk4, as those proteins belong to the clientele of the chaperone (see Table I). Fibroblasts exposed to geldanamycin also respond with downregulation of cyclin E and cdk2 [Bedin *et al*., 2004], which are both involved in Rb phosphorylation [Mazumder *et al*., 2004]. In addition, as shown in colon cancer cells, geldanamycin increases the ubiquitination of cyclin E and promotes its degradation via the proteasome pathway [Bedin *et al*., 2009]. Thus, the signaling pathways converging on pRb may represent another cluster of effectors mediating the impact of geldanamycin on cell cycle progression.

The multiple mechanisms by which HSP90 can control the G1 to S transition in Jurkat cells are summarized in **Figure 31**.

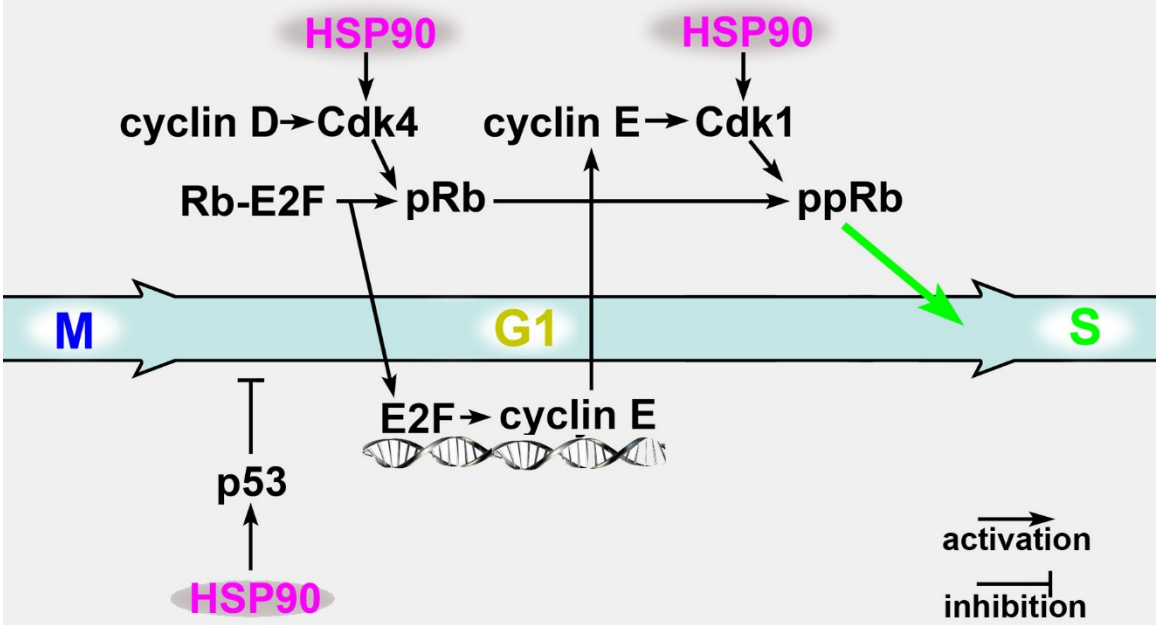

Figure 31. Potential mechanisms of geldanamycin-mediated G1 arrest. See text for detail. Rb, pRb, and ppRb denote hypo-phosphorylated, intermediately phosphorylated and hyper-phosphorylated Rb protein, respectively.

It is noteworthy that in normal human lymphocytes the treatment with geldanamycin caused a withdrawal from the cell cycle to G0, as opposed to the G1 block seen in leukemia Jurkat cells. The exact mechanism underlying this difference remains unknown, but it may be related to the fact that most non-cancerous adult cells assume residence in G0 state in the absence of appropriate growth stimulation [Zetterberg and Larson, 1985; Pelayo *et al*., 2006]. In this regard, it is important to emphasize that the mechanisms controlling the transition into G0 state are much less understood than those regulating the progression of the cell cycle [Yao, 2014; Miles and Breeden, 2017]. Similarly, the pathways leading to the activation of quiescent cells are characterized much better than those promoting the entry into the G0 state [Cheung and Rando, 2013; Richmond *et al*., 2016]. How geldanamycin promotes the transition of lymphocytes to the quiescent G0 state remains an unanswered question, but it is safe to postulate that HSP90 interacts with proteins regulating this process.

A phenomenon that occurred in both normal lymphocytes and Jurkat leukemia cells was a transient arrest in G2/M shortly after exposure of cells to geldanamycin. This block is not

dependent on pRb since this protein does not contribute to the control of the G2/M transition [Hostein *et al*., 2001]. The mechanism implicated in the G2/M arrest may involve any of the several G2 checkpoint kinases, which have been identified as HSP90 client proteins [http://www.picard.ch/downloads/Hsp90interactors.pdf]. They include Wee1, a protein kinase that regulates the G2 checkpoint in response to DNA damage [Do *et al*., 2013], Myt1, which controls the G2 checkpoint by phosphorylating CDK1 [Chow and Poon, 2013], and Polo-1 kinase [Liu *et al*., 2012]. The latter is regulated by HSP90 and its co-chaperone Sgt1 [Martins *et al*., 2009], and is required for kinetochore assembly, normal centrosome maturation, and entry and progression through mitosis [Sumara *et al*., 2004]. Additional work is required to identify which of this potential mechanisms was responsible for the transient G2/M arrest in both types of cells studied.

HSP90 and apoptosis

Programmed cell death is indispensable for the maintenance of a constant number of cells in any biological structure and constitutes a natural barrier to the development of cancer. However, tumor cells possess a broad spectrum of mechanisms that allow them to bypass this control process. This feature is so widespread among cancer cells that it was included in the list of the six 'hallmarks of cancer" [Hanahan and Weinberg, 2000; Hanahan and Weinberg, 2011].

A key molecule in the activation of the apoptotic program is tumor suppressor protein p53 [Brady and Attardi, 2010; Brady *et al*., 2011; Chen 2016]. The main function of p53 is the response to cellular stress such as DNA damage or hypoxia and interrupting the progression of cell cycle arrest until the damage is repaired [Kastan *et al*., 1991; Lane 1992]. If the injury cannot be appropriately rectified, activation of apoptosis takes place [Liebermann *et al*., 2007; Brown *et al*., 2007; Lago *et al*., 2011]. p53 is a non-kinase HSP90 client protein [Workman, 2004]; HSP90 can form an association with the DNA-binding domain of p53 and this interaction is essential for the stability of the tumor suppressor protein [Wang and Chen, 2003; Hagn *et al*., 2011]. HSP90 inhibitors reduce binding of p53 to its target DNA sequences, providing further evidence that the heat shock protein is necessary to ensure the transcriptionally active structural conformation of p53 [Muller *et al*., 2004; Walerych *et al*., 2010]. The mechanism by which p53 elicits apoptosis involves upregulation of the pro-apoptotic protein Bax [Zheng *et al*., 2015], thus making HSP90 an indispensable component of the initial steps in the apoptotic pathway.

The full understanding of the role that HSP90 plays in apoptosis is nevertheless much more difficult. The involvement of HSP90 in apoptosis is complicated by the fact that Bcl-2 and Bcl-xL, two proteins with potent pro-survival properties, are also clients of HSP90 [Cohen-Saidon *et al.*, 2006; Kurashina *et al.*, 2009; McNamara *et al.*, 2012]. Furthermore, the function of the receptor of IGF-1, a crucial pro-survival growth factor, is dependent on HSP90 as well [Takata *et al.*, 1997; Ramos *et al.*, 2007]. These apparently inconsistent roles of HSP90 in the activation of expression of both pro-apoptotic and anti-apoptotic proteins lead to the conclusion that a delicate balance must exist in the recruitment of HSP90 into one of these two mutually exclusive signaling pathways. What controls this balance, and how it is altered in cancer cells, remains a challenging question for future studies. In this regard, a hypothesis of "HSP90 addiction" exhibited by tumor cells has to be mentioned. It was proposed by Neckers [Myiata *et al.*, 2013] and states that HSP90 is expressed at permissive levels in both normal and cancer cells. However, since in cancer cells pro-growth and pro-survival genes are strongly activated, an inhibition of HSP90 activity will have a much higher impact on the growth and survival of cancer cells, while non-cancer cells may continue to function normally at lower levels of active HSP90. This is illustrated schematically in **Figure 32**.

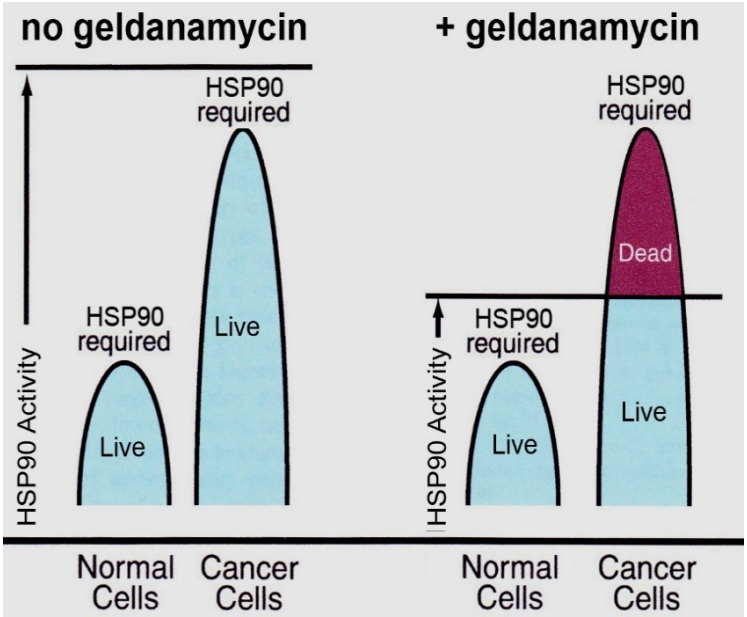

Figure 32. Scheme illustrating the "HSP90 addiction" of cancer cells. For detail see text. Modified from [Miyata *et al.*, 2013].

This hypothesis is consistent with the observations made in the current study. With comparable time and concentration of geldanamycin, leukemia Jurkat cells exhibited more than 2-fold higher levels of apoptosis than normal human lymphocytes (compare data included in **Figure 17H** with those in **Figure 8B**).

In summary, geldanamycin and its analogs may constitute a promising anti-cancer drug because of their preferential pro-apoptotic and anti-proliferative action on cancer cells. Several clinical trials are currently ongoing [Bhat *et al*., 2014; Khandelwal *et al*., 2016; Chatterjee and Burns, 2017], and the data presented here may elucidate some of the mechanisms of anti-cancer effects of this class of drugs. Additionally, understanding the downstream consequences of geldanamycin treatment at the cellular level will help in the interpretation of experiments with inhibition of HSP90 [Lilja *et al*., 2015; Prince *et al*., 2015; Zhang *et al*., 2015; Lee *et al*., 2016].

LITERATURE

Agah R, Kirshenbaum LA, Abdellatif M, Truong LD, Chakraborty S, Michael LH, Schneider MD. Adenoviral delivery of E2F-1 directs cell cycle reentry and p53-independent apoptosis in postmitotic adult myocardium in vivo. J Clin Invest. 1997;100:2722-2728.

Akahane K, Sanda T, Mansour MR, Radimerski T, DeAngelo DJ, Weinstock DM, Look AT. HSP90 inhibition leads to degradation of the TYK2 kinase and apoptotic cell death in T-cell acute lymphoblastic leukemia. Leukemia. 2016;30:219-228.

An WG, Schulte TW, Neckers LM. The heat shock protein 90 antagonist geldanamycin alters chaperone association with p210bcr-abl and v-src proteins before their degradation by the proteasome. Cell Growth Differ. 2000;11:355-360.

Arkan MC, Greten FR. IKK- and NF-κB-mediated functions in carcinogenesis. Curr Top Microbiol Immunol. 2011;349:159-169.

Ayrault O, Godeny MD, Dillon C, Zindy F, Fitzgerald P, Roussel MF, Beere HM. Inhibition of Hsp90 via 17-DMAG induces apoptosis in a p53-dependent manner to prevent medulloblastoma. Proc Natl Acad Sci U S A. 2009;106:17037-17042.

Bai L, Xu S, Chen W, Li Z, Wang X, Tang H, Lin Y. Blocking NF-κB and Akt by Hsp90 inhibition sensitizes Smac mimetic compound 3-induced extrinsic apoptosis pathway and results in synergistic cancer cell death. Apoptosis. 2011;16:45-54.

Baldwin AS. Regulation of cell death and autophagy by IKK and NF-κB: critical mechanisms in immune function and cancer. Immunol Rev. 2012;246:327-345.

Banerjee B, Kestner CA, Stukenberg PT. EB1 enables spindle microtubules to regulate centromeric recruitment of Aurora B. J Cell Biol. 2014;204:947-963.

Barrott JJ, Haystead TA. Hsp90, an unlikely ally in the war on cancer. FEBS J. 2013;280:1381-1396.

Bedin M, Catelli MG, Cabanié L, Gaben AM, Mester J. Indirect participation of Hsp90 in the regulation of the cyclin E turnover. Biochem Pharmacol. 2009;77:151-158.

Bedin M, Gaben AM, Saucier C, Mester J. Geldanamycin, an inhibitor of the chaperone activity of HSP90, induces MAPK-independent cell cycle arrest. Int J Cancer. 2004;109:643-652.

Belalcazar A, Shaib WL, Farren MR, Zhang C, Chen Z, Yang L, Lesinski GB, El-Rayes BF, Nagaraju GP. Inhibiting heat shock protein 90 and the ubiquitin-proteasome pathway impairs metabolic homeostasis and leads to cell death in human pancreatic cancer cells. Cancer. 2017 Aug 25. Epub ahead of print.

Beyer C, Pisetsky DS. Modeling nuclear molecule release during in vitro cell death. Autoimmunity. 2013;46:298-301.

Bhat R, Tummalapalli SR, Rotella DP. Progress in the discovery and development of heat shock protein 90 (Hsp90) inhibitors. J Med Chem. 2014;57:8718-8728.

Blagosklonny MV. Cell death beyond apoptosis. Leukemia. 2000;14:1502-1508.

Borkovich KA, Farrelly FW, Finkelstein DB, Taulien J, Lindquist S. hsp82 is an essential protein that is required in higher concentrations for growth of cells at higher temperatures. Mol Cell Biol. 1989;9:3919-3930.

Brady CA, Attardi LD. p53 at a glance. J Cell Sci. 2010;123:2527-2532.

Brady CA, Jiang D, Mello SS, Johnson TM, Jarvis LA, Kozak MM, Kenzelmann Broz D, Basak S, Park EJ, McLaughlin ME, Karnezis AN, Attardi LD. Distinct p53 transcriptional programs dictate acute DNA-damage responses and tumor suppression. Cell. 2011;145:571-583.

Brando B, Barnett D, Janossy G, Mandy F, Autran B, Rothe G, Scarpati B, D'Avanzo G, D'Hautcourt JL, Lenkei R, Schmitz G, Kunkl A, Chianese R, Papa S, Gratama JW. Cytofluorometric methods for assessing absolute numbers of cell subsets in blood. European Working Group on Clinical Cell Analysis. Cytometry. 2000;42:327-46.

Broemer M, Krappmann D, Scheidereit C. Requirement of Hsp90 activity for IkappaB kinase (IKK) biosynthesis and for constitutive and inducible IKK and NF-kappaB activation. Oncogene. 2004;23:5378-5386.

Brown L, Boswell S, Raj L, Lee SW. Transcriptional targets of p53 that regulate cellular proliferation. Crit Rev Eukaryot Gene Expr. 2007;17:73-85.

Burrows F, Zhang H, Kamal A. Hsp90 activation and cell cycle regulation. Cell Cycle. 2004;3:1530-1536.

Carvajal LA, Manfredi JJ. Another fork in the road--life or death decisions by the tumour suppressor p53. EMBO Rep. 2013;14:414-421.

Chang CH, Drechsel DA, Kitson RR, Siegel D, You Q, Backos DS, Ju C, Moody CJ, Ross D. 19-substituted benzoquinone ansamycin heat shock protein-90 inhibitors: biological activity and decreased off-target toxicity. Mol Pharmacol. 2014;85:849-857.

Chang Z, Lu M, Kim SS, Park JS. Potential role of HSP90 in mediating the interactions between estrogen receptor (ER) and aryl hydrocarbon receptor (AhR) signaling pathways. Toxicol Lett. 2014;226:6-13.

Chant ID, Rose PE, Morris AG. Analysis of heat-shock protein expression in myeloid leukaemia cells by flow cytometry. Br J Haematol. 1995;90:163-168.

Chatterjee S, Bhattacharya S, Socinski MA, Burns TF. HSP90 inhibitors in lung cancer: promise still unfulfilled. Clin Adv Hematol Oncol. 2016;14:346-356.

Chatterjee S, Burns TF. Targeting heat shock proteins in cancer: a promising therapeutic approach. Int J Mol Sci. 2017;18:E1978.

Chen G, Cao P, Goeddel DV. TNF-induced recruitment and activation of the IKK complex require Cdc37 and Hsp90. Mol Cell. 2002;9:401-410.

Chen F, Wang W, El-Deiry WS. Current strategies to target p53 in cancer. Biochem Pharmacol. 2010;80:724-730.

Chen B, Zhong D, Monteiro A. Comparative genomics and evolution of the HSP90 family of genes across all kingdoms of organisms. BMC Genomics. 2006;7:156.

Chen J. The cell-cycle arrest and apoptotic functions of p53 in tumor initiation and progression. Cold Spring Harb Perspect Med. 2016;6:a026104.

Cheung TH, Rando TA. Molecular regulation of stem cell quiescence. Nat Rev Mol Cell Biol. 2013;14:329-340.

Chiosis G, Huezo H, Rosen N, Mimnaugh E, Whitesell L, Neckers L. 17AAG: low target binding affinity and potent cell activity--finding an explanation. Mol Cancer Ther. 2003;2:123-129.

Choi YJ, Anders L. Signaling through cyclin D-dependent kinases. Oncogene. 2014;33:1890-1903.

Chow JP, Poon RY. The CDK1 inhibitory kinase MYT1 in DNA damage checkpoint recovery. Oncogene. 2013;32:4778-4788.

Cohen-Saidon C, Carmi I, Keren A, Razin E. Antiapoptotic function of Bcl-2 in mast cells is dependent on its association with heat shock protein 90. Blood. 2006;107:1413-1420.

Conroy SE, Sasieni PD, Fentiman I, Latchman DS. Autoantibodies to the 90kDa heat shock protein and poor survival in breast cancer patients. Eur J Cancer. 1998;34:942-953.

Cullinan SB, Whitesell L. Heat shock protein 90: a unique chemotherapeutic target. Semin Oncol. 2006;33:457-465.

Dai C, Whitesell L. HSP90: a rising star on the horizon of anticancer targets. Future Oncol. 2005;1:529-540.

Darzynkiewicz Z, Bedner E, Traganos F. Difficulties and pitfalls in analysis of apoptosis. Methods Cell Biol. 2001b;63:527-46.

Darzynkiewicz Z, Juan G, Bedner E. Determining cell cycle stages by flow cytometry. Curr Protoc Cell Biol. 2001a;Chapter 8:Unit 8.4.

Darzynkiewicz Z, Juan G, Srour EF. Differential staining of DNA and RNA. Curr Protoc Cytom. 2004;Chapter 7:Unit 7.3.

Darzynkiewicz Z, Traganos F, Sharpless T,Melamed MR. Lymphocyte stimulation: a rapid multiparameter analysis. Proc Natl Acad Sci USA. 1976;73:2881-2884.

Darzynkiewicz Z, Traganos F, Kapuscinski J, Staiano-Coico L, Melamed MR. Accessibility of DNA in situ to various fluorochromes: relationship to chromatin changes during erythroid differentiation of Friend leukemia cells. Cytometry. 1984;5:355-363.

DeBoer C, Meulman PA, Wnuk RJ, Peterson DH. Geldanamycin, a new antibiotic. J Antibiot. 1970;23:442-447.

Deshpande A, Sicinski P, Hinds PW. Cyclins and cdks in development and cancer: a perspective. Oncogene. 2005;24:2909-2915.

DeZwaan DC, Freeman BC. HSP90: the Rosetta stone for cellular protein dynamics? Cell Cycle. 2008;7:1006-1012.

DeZwaan DC, Freeman BC. HSP90 manages the ends. Trends Biochem Sci. 2010;35:384-391.

Dick FA, Rubin SM. Molecular mechanisms underlying RB protein function. Nat Rev Mol Cell Biol. 2013;14:297-306.

Didenko T, Duarte AM, Karagöz GE, Rüdiger SG. Hsp90 structure and function studied by NMR spectroscopy. Biochim Biophys Acta. 2012;1823:636-647.

Do K, Doroshow JH, Kummar S. Wee1 kinase as a target for cancer therapy. Cell Cycle. 2013;12:3159-3164.

Donnellan R, Chetty R. Cyclin E in human cancers. FASEB J. 1999;13:773-780.

Du YW, Chen JG, Bai HL, Huang HY, Wang J, Li SL, Liu GC, Jiang Q, Chai J, Zhao YP, Ma YF. A novel agonistic anti-human death receptor 5 monoclonal antibody with tumoricidal activity induces caspase- and mitochondrial-dependent apoptosis in human leukemia Jurkat cells. Cancer Biother Radiopharm. 2011;26:143-152.

Durand JK, Baldwin AS. Targeting IKK and NF-κB for therapy. Adv Protein Chem Struct Biol. 2017;107:77-115.

Eckl JM, Richter K. Functions of the Hsp90 chaperone system: lifting client proteins to new heights. Int J Biochem Mol Biol. 2013;4:157-165.

Eckl JM, Daake M, Schwartz S, Richter K. Nucleotide-free sB-Raf is preferentially bound by Hsp90 and Cdc37 in vitro. J Mol Biol. 2016;428:4185-4196.

Elia A, Powley IR, Macfarlane M, Clemens MJ. Modulation of the sensitivity of Jurkat T-cells to inhibition of protein synthesis by tumor necrosis factor α-related apoptosis-inducing ligand. J Interferon Cytokine Res. 2014;34:769-777.

Erlejman AG, Lagadari M, Toneatto J, Piwien-Pilipuk G, Galigniana MD. Regulatory role of the 90-kDa-heat-shock protein (Hsp90) and associated factors on gene expression. Biochim Biophys Acta. 2014;1839:71-87.

Eustace BK, Sakurai T, Stewart JK, Yimlamai D, Unger C, Zehetmeier C, Lain B, Torella C, Henning SW, Beste G, Scroggins BT, Neckers L, Ilag LL, Jay DG. Functional proteomic screens reveal an essential extracellular role for hsp90 alpha in cancer cell invasiveness. Nat Cell Biol. 2004;6:507-514.

Fang B, Boross PI, Tozser J, Weber IT. Structural and kinetic analysis of caspase-3 reveals role for s5 binding site in substrate recognition. J. Mol. Biol. 2006;360:654-666.

Flynn JM, Mishra P, Bolon DN. Mechanistic asymmetry in Hsp90 dimers. J Mol Biol. 2015;427:2904-2911.

Franke J, Eichner S, Zeilinger C, Kirschning A. Targeting heat-shock-protein 90 (Hsp90) by natural products: geldanamycin, a show case in cancer therapy. Nat Prod Rep. 2013;30:1299-1323.

Galea-Lauri J, Latchman DS, Katz DR. The role of the 90-kDa heat shock protein in cell cycle control and differentiation of the monoblastoid cell line U937. Exp Cell Res. 1996;226:243-254.

Garcia-Carbonero R, Carnero A, Paz-Ares L. Inhibition of HSP90 molecular chaperones: moving into the clinic. Lancet Oncol. 2013;14:e358-e369.

Gartner EM, Silverman P, Simon M, Flaherty L, Abrams J, Ivy P, Lorusso PM. A phase II study of 17-allylamino-17-demethoxygeldanamycin in metastatic or locally advanced, unresectable breast cancer. Breast Cancer Res Treat. 2012;131:933-937.

Gasparini C, Celeghini C, Monasta L, Zauli G. NF-κB pathways in hematological malignancies. Cell Mol Life Sci. 2014;71:2083-2102.

Geng Y, Eaton EN, Picón M, Roberts JM, Lundberg AS, Gifford A, Sardet C, Weinberg RA. Regulation of cyclin E transcription by E2Fs and retinoblastoma protein. Oncogene. 1996;12:1173-1180.

Giacinti C, Giordano A. RB and cell cycle progression. Oncogene. 2006;25:5220–5227.

Hagn F, Lagleder S, Retzlaff M, Rohrberg J, Demmer O, Richter K, Buchner J, Kessler H. Structural analysis of the interaction between Hsp90 and the tumor suppressor protein p53. Nat Struct Mol Biol. 2011;18:1086-1093.

Halicka HD, Smolewski P, Darzynkiewicz Z, Dai W, Traganos F. Arsenic trioxide arrests cells early in mitosis leading to apoptosis. Cell Cycle. 2002;1:201-209.

Hanahan D, Weinberg RA. The hallmarks of cancer. Cell. 2000;100:57-70.

Hanahan D, Weinberg RA. Hallmarks of cancer: the next generation. Cell. 2011;144:646-674.

Harbour JW, Dean DC. The Rb/E2F pathway: expanding roles and emerging paradigms. Genes Dev. 2000;14:2393-2409.

He W, Wu L, Gao Q, Du Y, Wang Y. Identification of AHBA biosynthetic genes related to geldanamycin biosynthesis in Streptomyces hygroscopicus 17997. Curr Microbiol. 2006;52:197-203.

Helbing CC, Wellington CL, Gogela-Spehar M, Cheng T, Pinchbeck GG, Johnston RN. Quiescence versus apoptosis: Myc abundance determines pathway of exit from the cell cycle. Oncogene. 1998;17:1491-1501.

Hickey E, Brandon SE, Smale G, Lloyd D, Weber LA. Sequence and regulation of a gene encoding a human 89-kilodalton heat shock protein. Mol Cell Biol. 1989;9:2615-2626.

Hill JA, Ammar R, Torti D, Nislow C, Cowen LE. Genetic and genomic architecture of the evolution of resistance to antifungal drug combinations. PLoS Genet. 2013;9:e1003390.

Hostein I, Robertson D, DiStefano F, Workman P, Clarke PA. Inhibition of signal transduction by the Hsp90 inhibitor 17-allylamino-17-demethoxygeldanamycin results in cytostasis and apoptosis. Cancer Res. 2001;61:4003-4009.

Hu Y, Bobb D, He J, Hill DA, Dome JS. The HSP90 inhibitor alvespimycin enhances the potency of telomerase inhibition by imetelstat in human osteosarcoma. Cancer Biol Ther. 2015;16:949-957.

Huang W, Ye M, Zhang LR, Wu QD, Zhang M, Xu JH, Zheng W. FW-04-806 inhibits proliferation and induces apoptosis in human breast cancer cells by binding to N-terminus of Hsp90 and disrupting Hsp90-Cdc37 complex formation. Mol Cancer. 2014;13:150.

Indovina P, Marcelli E, Casini N, Rizzo V, Giordano A. Emerging roles of RB family: new defense mechanisms against tumor progression. J Cell Physiol. 2013;228:525-535.

Iyer G, Morris MJ, Rathkopf D, Slovin SF, Steers M, Larson SM, Schwartz LH, Curley T, DeLaCruz A, Ye Q, Heller G, Egorin MJ, Ivy SP, Rosen N, Scher HI, Solit DB. A phase I trial of docetaxel and pulse-dose 17-allylamino-17-demethoxygeldanamycin in adult patients with solid tumors. Cancer Chemother Pharmacol. 2012;69:1089-1097.

Jackson SE. Hsp90: structure and function. Top Curr Chem. 2013;328:155-240.

Jeong J, Kim W, Kim LK, VanHouten J, Wysolmerski JJ. HER2 signaling regulates HER2 localization and membrane retention. PLoS One. 2017;12:e0174849.

Jérôme V, Vourc'h C, Baulieu EE, Catelli MG. Cell cycle regulation of the chicken hsp90 alpha expression. Exp Cell Res. 1993;205:44-51.

Jin X, Wang Z, Qiu L, Zhang D, Guo Z, Gao Z, Deng C, Wang F, Wang S, Guo C. Potential biomarkers involving IKK/RelA signal in early stage non-small cell lung cancer. Cancer Sci. 2008;99:582-589.

Juan G, Darzynkiewicz Z. Bivariate analysis of DNA content and expression of cyclin proteins. Curr Protoc Cytom. 2001;Chapter 7:Unit 7.9.

Juan G, Gruenwald S, Darzynkiewicz Z. Phosphorylation of retinoblastoma susceptibility gene protein assayed in individual lymphocytes during their mitogenic stimulation. Exp Cell Res. 1998;239:104-110.

Juan G, Traganos F, James WM, Ray JM, Roberge M, Sauve DM, Anderson H, Darzynkiewicz Z. Histone H3 phosphorylation and expression of cyclins A and B1

measured in individual cells during their progression through G2 and mitosis. Cytometry. 1998;32:71-77.

Jurczyszyn A, Zebzda A, Czepiel J, Perucki W, Bazan-Socha S, Cibor D, Owczarek D, Majka M. Geldanamycin and its derivatives inhibit the growth of myeloma cells and reduce the expression of the MET receptor. J Cancer. 2014;5:480-490.

Kancha RK, Bartosch N, Duyster J. Analysis of conformational determinants underlying HSP90-kinase interaction. PLoS One. 2013;8:e68394.

Karin M, Greten FR. NF-kappaB: linking inflammation and immunity to cancer development and progression. Nat Rev Immunol. 2005;5:749-759.

Karkoulis PK, Stravopodis DJ, Konstantakou EG, Voutsinas GE. Targeted inhibition of heat shock protein 90 disrupts oncogenic signaling pathways, thus inducing cell cycle arrest and programmed cell death in human urinary bladder cancer cell lines. Cancer Cell Intl. 2013;13:11-27.

Karni-Schmidt O, Lokshin M, Prives C. The roles of MDM2 and MDMX in cancer. Annu Rev Pathol. 2016;11:617-644.

Kastan MB, Onyekwere O, Sidransky D, Vogelstein B, Craig RW. Participation of p53 protein in the cellular response to DNA damage. Cancer Res. 1991;51:6304-6311.

Kastan MB, Bartek J. Cell-cycle checkpoints and cancer. Nature. 2004;432:316–323.

Kato J, Matsushime H, Hiebert SW, Ewen ME, Sherr CJ. Direct binding of cyclin D to the retinoblastoma gene product (pRb) and pRb phosphorylation by the cyclin D-dependent kinase CDK4.Genes Dev. 1993;7:331-342.

Katschinski DM, Le L, Heinrich D, Wagner KF, Hofer T, Schindler SG, Wenger RH. Heat induction of the unphosphorylated form of hypoxia-inducible factor-1alpha is dependent on heat shock protein-90 activity. J Biol Chem. 2002;277:9262-9267.

Ke X, Chen J, Peng L, Zhang W, Yang Y, Liao X, Mo L, Guo R, Feng J, Hu C, Nie R. Heat shock protein 90/Akt pathway participates in the cardioprotective effect of exogenous hydrogen sulfide against high glucose-induced injury to H9c2 cells. Int J Mol Med. 2017;39:1001-1010.

Khandelwal A, Crowley VM, Blagg BSJ. Natural product inspired N-terminal Hsp90 inhibitors: from bench to bedside? Med Res Rev. 2016;36:92-118.

Kim T, Keum G, Pae AN. Discovery and development of heat shock protein 90 inhibitors as anticancer agents: a review of patented potent geldanamycin derivatives. Expert Opin Ther Pat. 2013;23:919-943.

Kinzel L, Ernst A, Orth M, Albrecht V, Hennel R, Brix N, Frey B, Gaipl US, Zuchtriegel G, Reichel CA, Blutke A, Schilling D, Multhoff G, Li M, Niyazi M, Friedl AA, Winssinger N, Belka C, Lauber K. A novel HSP90 inhibitor with reduced hepatotoxicity synergizes with radiotherapy to induce apoptosis, abrogate clonogenic survival, and improve tumor control in models of colorectal cancer. Oncotarget. 2016;7:43199-43219.

Kitson RR, Moody CJ. Learning from nature: advances in geldanamycin- and radicicol-based inhibitors of Hsp90. J Org Chem. 2013;78:5117-5141.

Krukenberg KA, Street TO, Lavery LA, Agard DA. Conformational dynamics of the molecular chaperone Hsp90. Q Rev Biophys. 2011;44:229-255.
Kurashina R, Ohyashiki JH, Kobayashi C, Hamamura R, Zhang Y, Hirano T, Ohyashiki K. Anti-proliferative activity of heat shock protein (Hsp) 90 inhibitors via beta-catenin/TCF7L2 pathway in adult T cell leukemia cells. Cancer Lett. 2009;284:62-70.

Lago CU, Sung HJ, Ma W, Wang PY, Hwang PM. p53, aerobic metabolism, and cancer. Antioxid Redox Signal. 2011;15:1739-1748.

Lamoth F, Juvvadi PR, Fortwendel JR, Steinbach WJ. Heat shock protein 90 is required for conidiation and cell wall integrity in Aspergillus fumigatus. Eukaryot Cell. 2012;11:1324-1332.

Lancet JE, Gojo I, Burton M, Quinn M, Tighe SM, Kersey K, Zhong Z, Albitar MX, Bhalla K, Hannah AL, Baer MR. Phase I study of the heat shock protein 90 inhibitor alvespimycin (KOS-1022, 17-DMAG) administered intravenously twice weekly to patients with acute myeloid leukemia. Leukemia. 2010;24:699-705.

Lane DP. p53, guardian of the genome. Nature. 1992;358:15-16.

Lange BM, Bachi A, Wilm M, González C. Hsp90 is a core centrosomal component and is required at different stages of the centrosome cycle in Drosophila and vertebrates. EMBO J. 2000;19:1252-1262.

Lapenna S, Giordano A. Cell cycle kinases as therapeutic targets for cancer. Nat Rev Drug Discov. 2009;8:547-566.

Lavrik IN, Golks A, Krammer PH. Caspases: pharmacological manipulation of cell death. J. Clin. Invest. 2005;115:2665-2672.

Lee D, Lee K, Cai XF, Dat NT, Boovanahalli SK, Lee M, Shin JC, Kim W, Jeong JK, Lee JS, Lee CH, Lee JH, Hong YS, Lee JJ. Biosynthesis of the heat-shock protein 90 inhibitor geldanamycin: new insight into the formation of the benzoquinone moiety. Chembiochem. 2006;7:246-248.

Lee J, An YS, Kim MR, Kim YA, Lee JK, Hwang CS, Chung E, Park IC, Yi JY. Heat shock protein 90 regulates subcellular localization of Smads in Mv1Lu cells. J Cell Biochem. 2016;117:230-8.

Lee HG, Park WJ, Shin SJ, Kwon SH, Cha SD, Seo YH, Jeong JH, Lee JY, Cho CH. Hsp90 inhibitor SY-016 induces G2/M arrest and apoptosis in paclitaxel-resistant human ovarian cancer cells. Oncol Lett. 2017;13:2817-2822.

Lewis J, Devin A, Miller A, Lin Y, Rodriguez Y, Neckers L, Liu ZG. Disruption of hsp90 function results in degradation of the death domain kinase, receptor-interacting protein (RIP), and blockage of tumor necrosis factor-induced nuclear factor-kappaB activation. J Biol Chem. 2000;275:10519-10526.

Li YP, Chen JJ, Shen JJ, Cui J, Wu LZ, Wang Z, Li ZR. Synthesis and biological evaluation of geldanamycin analogs against human cancer cells. Cancer Chemother Pharmacol. 2015;75:773-782.

Li D, Marchenko ND. ErbB2 inhibition by lapatinib promotes degradation of mutant p53 protein in cancer cells. Oncotarget. 2017;8:5823-5833.

Liebermann DA, Hoffman B, Vesely D. p53 induced growth arrest versus apoptosis and its modulation by survival cytokines. Cell Cycle. 2007;6:166-170.

Lilja A, Weeden CE, McArthur K, Nguyen T, Donald A, Wong ZX, Dousha L, Bozinovski S, Vlahos R, Burns CJ, Asselin-Labat ML, Anderson GP. HSP90 inhibition suppresses lipopolysaccharide-induced lung inflammation in vivo. PLoS One. 2015;10:e0114975.

Liu XS, Song B, Tang J, Liu W, Kuang S, Liu X. Plk1 phosphorylates Sgt1 at the kinetochores to promote timely kinetochore-microtubule attachment. Mol Cell Biol. 2012;32:4053-4067.

Lockshin RA, Zakeri Z. Caspase-independent cell deaths. Curr Opin Cell Biol. 2002;14:727-733.

Lorenz VN, Schön MP, Seitz CS. c-Rel in Epidermal Homeostasis: A Spotlight on c-Rel in Cell Cycle Regulation. J Invest Dermatol. 2016;136:1090-1096.

Lundberg AS, Weinberg RA. Functional inactivation of the retinoblastoma protein requires sequential modification by at least two distinct cyclin-cdk complexes. Mol Cell Biol. 1998;18:753-761.

Lunt SJ, Chaudary N, Hill RP. The tumor microenvironment and metastatic disease. Clin Exp Metastasis. 2009;26:19-34.

Maes A, Menu E, Veirman K, Maes K, Vand Erkerken K, De Bruyne E. The therapeutic potential of cell cycle targeting in multiple myeloma. Oncotarget. 2017;8:90501-90520.

Mahony D, Parry DA, Lees E. Active cdk6 complexes are predominantly nuclear and represent only a minority of the cdk6 in T cells. Oncogene. 1998;16:603-611.

Maloney A, Workman P. HSP90 as a new therapeutic target for cancer therapy: the story unfolds. Expert Opin Biol Ther. 2002;2:3-24.

Martínez P, Blasco MA. Telomere-driven diseases and telomere-targeting therapies. J Cell Biol. 2017;216:875-887.

Martins T, Maia AF, Steffensen S, Sunkel CE. Sgt1, a co-chaperone of Hsp90 stabilizes Polo and is required for centrosome organization. EMBO J. 2009;28:234-247.

Mazumder S, DuPree EL, Almasan A. A dual role of cyclin E in cell proliferation and apoptosis may provide a target for cancer therapy. Curr Cancer Drug Targets. 2004;4:65-75.

McLaughlin M, Barker HE, Khan AA, Pedersen M, Dillon M, Mansfield DC, Patel R, Kyula JN, Bhide SA, Newbold KL, Nutting CM, Harrington KJ. HSP90 inhibition sensitizes head and neck cancer to platin-based chemoradiotherapy by modulation of the DNA damage response resulting in chromosomal fragmentation. BMC Cancer. 2017;17:86.

McNamara AV, Barclay M, Watson AJ, Jenkins JR. Hsp90 inhibitors sensitise human colon cancer cells to topoisomerase I poisons by depletion of key anti-apoptotic and cell cycle checkpoint proteins. Biochem Pharmacol. 2012;83:355-367.

Messaoudi S, Peyrat JF, Brion JD, Alami M. Heat-shock protein 90 inhibitors as antitumor agents: a survey of the literature from 2005 to 2010. Expert Opin Ther Pat. 2011;21:1501-1542.

Miles S, Breeden L. A common strategy for initiating the transition from proliferation to quiescence. Curr Genet. 2017;63:179-186.

Mitra S, Ghosh B, Gayen N, Roy J, Mandal AK. Bipartite role of heat shock protein 90 (Hsp90) keeps CRAF kinase poised for activation. J Biol Chem. 2016;291:24579-24593.

Miyata Y, Nakamoto H, Neckers L. The therapeutic target Hsp90 and cancer hallmarks. Curr Pharm Des. 2013;19:347-365.

Modi S, Saura C, Henderson C, Lin NU, Mahtani R, Goddard J, Rodenas E, Hudis C, O'Shaughnessy J, Baselga J. A multicenter trial evaluating retaspimycin HCL (IPI-504) plus trastuzumab in patients with advanced or metastatic HER2-positive breast cancer. Breast Cancer Res Treat. 2013;139:107-113.

Mosser DD, Morimoto RI. Molecular chaperones and the stress of oncogenesis. Oncogene. 2004;23:2907-2918.

Müller L, Schaupp A, Walerych D, Wegele H, Buchner J. Hsp90 regulates the activity of wild type p53 under physiological and elevated temperatures. J Biol Chem. 2004;279:48846-48854.

Muñoz MJ, Jimenez J. Genetic interactions between Hsp90 and the Cdc2 mitotic machinery in the fission yeast *Schizosaccharomyces* pombe. Mol Gen Genet. 1999;261:242-250.

Münster PN, Srethapakdi M, Moasser MM, Rosen N. Inhibition of heat shock protein 90 function by ansamycins causes the morphological and functional differentiation of breast cancer cells. Cancer Res. 2001;61:2945-2952.

Naderi J, Hung M, Pandey S. Oxidative stress-induced apoptosis in dividing fibroblasts involves activation of p38 MAP kinase and over-expression of Bax: resistance of quiescent cells to oxidative stress. Apoptosis. 2003;8:91-100.

Napetschnig J, Wu H. Molecular basis of NF-κB signaling. Annu Rev Biophys. 2013;42:443-468.

Neckers L, Ivy SP. Heat shock protein 90. Curr Opin Oncol. 2003;15:419-424.

Neckers L. Heat shock protein 90: the cancer chaperone. J Biosci. 2007;32:517-530.

Neckers L, Workman P. Hsp90 molecular chaperone inhibitors: are we there yet? Clin Cancer Res. 2012;18:64-76.

Nowakowski GS, McCollum AK, Ames MM, Mandrekar SJ, Reid JM, Adjei AA, Toft DO, Safgren SL, Erlichman C. A phase I trial of twice-weekly 17-allylamino-demethoxy-geldanamycin in patients with advanced cancer. Clin Cancer Res. 2006;12:6087-6093.

Otto T, Sicinski P. Cell cycle proteins as promising targets in cancer therapy. Nat Rev Cancer. 2017;17:93-115.

Pearl LH, Prodromou C. Structure and mechanism of the Hsp90 molecular chaperone machinery. Annu Rev Biochem. 2006;75:271-294.

Pelayo R, Miyazaki K, Huang J, Garrett KP, Osmond DG, Kincade PW. Cell cycle quiescence of early lymphoid progenitors in adult bone marrow. Stem Cells. 2006;24:2703-2713.

Petrulio CA, Kim-Schulze S, Kaufman HL. The tumour microenvironment and implications for cancer immunotherapy. Expert Opin Biol Ther. 2006;6:671-684.

Picard D. HSP90 Interactors. http://www.picard.ch/downloads/Hsp90interactors.pdf. Accessed December 15, 2017.

Piper PW, Millson SH. Spotlight on the microbes that produce heat shock protein 90-targeting antibiotics. Open Biol. 2012;2:120-138.

Pozarowski P, Grabarek J, Darzynkiewicz Z. Flow cytometry of apoptosis. Curr Protoc Cell Biol. 2004;Chapter 18:Unit 18.8.

Pozarowski P, Halicka DH, Darzynkiewicz Z. Cell cycle effects and caspase-dependent and independent death of HL-60 and Jurkat cells treated with the inhibitor of NF-kappaB parthenolide. Cell Cycle. 2003;2:377-383.

Prasad S, Ravindran J, Aggarwal BB. NF-kappaB and cancer: how intimate is this relationship. Mol Cell Biochem. 2010;336:25-37.

Prince TL, Kijima T, Tatokoro M, Lee S, Tsutsumi S, Yim K, Rivas C, Alarcon S, Schwartz H, Khamit-Kush K, Scroggins BT, Beebe K, Trepel JB, Neckers L. Client proteins and small molecule inhibitors display distinct binding preferences for constitutive and stress-induced HSP90 isoforms and their conformationally restricted mutants. PLoS One. 2015;10:e0141786.

Proia DA, Bates RC. Ganetespib and HSP90: translating preclinical hypotheses into clinical promise. Cancer Res. 2014;74:1294-1300.

Rajagopal D, Bal V, Mayor S, George A, Rath S. A role for the Hsp90 molecular chaperone family in antigen presentation to T lymphocytes via major histocompatibility complex class II molecules. Eur J Immunol. 2006;36:828-841.

Ramos RR, Swanson AJ, Bass J. Calreticulin and Hsp90 stabilize the human insulin receptor and promote its mobility in the endoplasmic reticulum. Proc Natl Acad Sci USA. 2007;104:10470-10475.

Ren Z, Aerts JL, Pen JJ, Heirman C, Breckpot K, De Grève J. Phosphorylated STAT3 physically interacts with NPM and transcriptionally enhances its expression in cancer. Oncogene. 2015;34:1650-1657.

Restall IJ, Lorimer IA. Induction of premature senescence by hsp90 inhibition in small cell lung cancer. PLoS One. 2010;5:e11076.

Richmond CA, Shah MS, Carlone DL, Breault DT. Factors regulating quiescent stem cells: insights from the intestine and other self-renewing tissues. J Physiol. 2016;594:4805-4813.

Richter K, Hendershot LM, Freeman BC. The cellular world according to Hsp90. Nat Struct Mol Biol. 2007;14:90-94.

Ritossa F. A new puffing pattern induced by temperature shock and DNP in Drosophila. Experientia. 1962;18:571–573.

Ritossa F. Discovery of the heat shock response. Cell Stress Chaperones. 1996;1:97-98.

Roh J-L, Kim EH, Park HB, Park JY. The Hsp90 inhibitor 17-(allylamino)-17-demethoxy-geldanamycin increases cisplatin antitumor activity by inducing p53-mediated apoptosis in head and neck cancer. Cell Death Dis. 2013;4:e956.

Rubini M, Panozzo M, Selvatici R, Baricordi OR, Mazzilli MC, Pozzan T, Gandini E. An anti-HLA class I monoclonal antibody alters the progression in the cell cycle of phytohemagglutinin-activated human T lymphocytes. Exp Cell Res. 1990;187:11-15.

Saif MW, Erlichman C, Dragovich T, Mendelson D, Toft D, Burrows F, Storgard C, Von Hoff D. Open-label, dose-escalation, safety, pharmacokinetic, and pharmacodynamic study of intravenously administered CNF1010 (17-(allylamino)-17-demethoxy-geldanamycin [17-AAG]) in patients with solid tumors. Cancer Chemother Pharmacol. 2013;71:1345-1355.

Sankhala KK, Mita MM, Mita AC, Takimoto CH. Heat shock proteins: a potential anticancer target. Curr Drug Targets. 2011;12:2001-2008.

Sawarkar R, Paro R. Hsp90@chromatin.nucleus: an emerging hub of a networker. Trends Cell Biol. 2013;23:193-201.

Schenk E, Hendrickson AE, Northfelt D, Toft DO, Ames MM, Menefee M, Satele D, Qin R, Erlichman C. Phase I study of tanespimycin in combination with bortezomib in patients with advanced solid malignancies. Invest New Drugs. 2013;31:1251-1256.

Schlenke P, Frohn C, Klüter H, Saballus M, Hammers HJ, Zajac SR, Kirchner H. Evaluation of a flow cytometric method for simultaneous leukocyte phenotyping and quantification by fluorescent microspheres. Cytometry. 1998;33:310-7.

Schneider U, Schwenk H, Bornkamm G. Characterization of EBV-genome negative "null" and "T" cell lines derived from children with acute lymphoblastic leukemia and leukemic transformed non-Hodgkin lymphoma. Int J Cancer. 1977;19:621–626.

Seo YH. Small molecule inhibitors to disrupt protein-protein interactions of heat shock protein 90 chaperone machinery. J Cancer Prev. 2015;20:5-11.

Sidera K, Gaitanou M, Stellas D, Matsas R, Patsavoudi E. A critical role for HSP90 in cancer cell invasion involves interaction with the extracellular domain of HER-2. J Biol Chem. 2008;283:2031-2041.

Sidera K, Patsavoudi E. Extracellular HSP90: conquering the cell surface. Cell Cycle. 2008;7:1564-1568.

Siegel D, Jagannath S, Vesole DH, Borello I, Mazumder A, Mitsiades C, Goddard J, Dunbar J, Normant E, Adams J, Grayzel D, Anderson KC, Richardson P. A phase 1 study of IPI-504 (retaspimycin hydrochloride) in patients with relapsed or relapsed and refractory multiple myeloma. Leuk Lymphoma. 2011;52:2308-2315.

Shalini S, Dorstyn L, Dawar S, Kumar S. Old, new and emerging functions of caspases. Cell Death Differ. 2015;22:526-539.

Southworth DR, Agard DA. Client-loading conformation of the Hsp90 molecular chaperone revealed in the cryo-EM structure of the human Hsp90:Hop complex. Mol Cell. 2011;42:771-781.

Speltz EB, Brown RS, Hajare HS, Schlieker C, Regan L. A designed repeat protein as an affinity capture reagent. Biochem Soc Trans. 2015;43:874-880.

Sperka T, Wang J, Rudolph KL. DNA damage checkpoints in stem cells, ageing and cancer. Nat Rev Mol Cell Biol. 2012;13:579-590.

Sreedhar AS, Csermely P. Heat shock proteins in the regulation of apoptosis: new strategies in tumor therapy: a comprehensive review. Pharmacol Ther. 2004;101:227-257.

Srethapakdi M, Liu F, Tavorath R, Rosen N. Inhibition of Hsp90 function by ansamycins causes retinoblastoma gene product-dependent G1 arrest. Cancer Res. 2000;60:3940-3946.

Stepanova L, Leng X, Parker SB, Harper JW. Mammalian p50Cdc37 is a protein kinase-targeting subunit of Hsp90 that binds and stabilizes Cdk4. Genes Dev. 1996;10:1491-1502.

Storie I, Sawle A, Goodfellow K, Whitby L, Granger V, Reilly JT, Barnett D. Flow rate calibration I: a novel approach for performing absolute cell counts. Cytometry B Clin Cytom. 2003;55:1-7.

Street TO, Lavery LA, Agard DA. Substrate binding drives large-scale conformational changes in the Hsp90 molecular chaperone. Mol Cell. 2011;42:96-105.

Sumara I, Giménez-Abián JF, Gerlich D, Hirota T, Kraft C, de la Torre C, Ellenberg J, Peters JM. Roles of polo-like kinase 1 in the assembly of functional mitotic spindles. Curr Biol. 2004;14:1712-1722.

Sun Y, St Clair DK, Fang F, Warren GW, Rangnekar VM, Crooks PA, St Clair WH. The radiosensitization effect of parthenolide in prostate cancer cells is mediated by nuclear factor-kappaB inhibition and enhanced by the presence of PTEN. Mol Cancer Ther. 2007;6:2477-2486.

Takata Y, Imamura T, Iwata M, Usui I, Haruta T, Nandachi N, Ishiki M, Sasaoka T, Kobayashi M. Functional importance of heat shock protein 90 associated with insulin receptor on insulin-stimulated mitogenesis. Biochem Biophys Res Commun. 1997;237:345-347.

Takayama S, Reed JC, Homma S. Heat-shock proteins as regulators of apoptosis. Oncogene. 2003;22:9041-9047.

Tetzlaff MT, Curry JL, Ivan D, Wang WL, Torres-Cabala CA, Bassett RL, Valencia KM, McLemore MS, Ross MI, Prieto VG. Immunodetection of phosphohistone H3 as a surrogate of mitotic figure count and clinical outcome in cutaneous melanoma. Mod Pathol. 2013;26:1153-1160.

Tsutsumi S, Scroggins B, Koga F, Lee MJ, Trepel J, Felts S, Carreras C, Neckers L. A small molecule cell-impermeant Hsp90 antagonist inhibits tumor cell motility and invasion. Oncogene. 2008;27:2478-2487.

Uchida C. The retinoblastoma protein: functions beyond the G1-S regulator. Curr Drug Targets. 2012;13:1622-1632.

Uchida C. Roles of pRB in the regulation of nucleosome and chromatin structures. Biomed Res Int. 2016;2016:5959721.

Umezawa K, Chaicharoenpong C. Molecular design and biological activities of NF-kappaB inhibitors. Mol Cells. 2002;14:163-167.

Uo T, Dvinge H, Sprenger CC, Bradley RK, Nelson PS, Plymate SR. Systematic and functional characterization of novel androgen receptor variants arising from alternative splicing in the ligand-binding domain. Oncogene. 2017;36:1440-1450.

Vaishampayan UN, Burger AM, Sausville EA, Heilbrun LK, Li J, Horiba MN, Egorin MJ, Ivy P, Pacey S, Lorusso PM. Safety, efficacy, pharmacokinetics, and pharmacodynamics of the combination of sorafenib and tanespimycin. Clin Cancer Res. 2010;16:3795-3804.

Van Antwerp DJ, Martin SJ, Kafri T, Green DR, Verma IM. Suppression of TNF-alpha-induced apoptosis by NF-kappaB. Science. 1996;274:787-789.

Vaseva AV, Yallowitz AR, Marchenko ND, Xu S, Moll UM. Blockade of Hsp90 by 17AAG antagonizes MDMX and synergizes with Nutlin to induce p53-mediated apoptosis in solid tumors. Cell Death Dis. 2011;2: e156.

Wagner AJ, Chugh R, Rosen LS, Morgan JA, George S, Gordon M, Dunbar J, Normant E, Grayzel D, Demetri GD. A phase I study of the HSP90 inhibitor retaspimycin hydrochloride (IPI-504) in patients with gastrointestinal stromal tumors or soft-tissue sarcomas. Clin Cancer Res. 2013;19:6020-6029.

Walerych D, Gutkowska M, Klejman MP, Wawrzynow B, Tracz Z, Wiech M, Zylicz M, Zylicz A. ATP binding to Hsp90 is sufficient for effective chaperoning of p53 protein. J Biol Chem. 2010;285:32020-32028.

Walker AR, Klisovic R, Johnston JS, Jiang Y, Geyer S, Kefauver C, Binkley P, Byrd JC, Grever MR, Garzon R, Phelps MA, Marcucci G, Blum KA, Blum W. Pharmacokinetics and dose escalation of the heat shock protein inhibitor 17-allyamino-17-demethoxygeldanamycin in combination with bortezomib in relapsed or refractory acute myeloid leukemia. Leuk Lymphoma. 2013;54:1996-2002.

Walter R, Pan KT, Doebele C, Comoglio F, Tomska K, Bohnenberger H, Young RM, Jacobs L, Keller U, Bönig H, Engelke M, Rosenwald A, Urlaub H, Staudt LM, Serve H, Zenz T, Oellerich T. HSP90 promotes Burkitt lymphoma cell survival by maintaining tonic B-cell receptor signaling. Blood. 2017;129:598-608.

Wan F, Lenardo MJ. The nuclear signaling of NF-kappaB: current knowledge, new insights, and future perspectives. Cell Res. 2010;20:24-33.

Wandinger SK, Richter K, Buchner J. The Hsp90 chaperone machinery. J Biol Chem. 2008;283:18473-18477.

Wang C, Chen J. Phosphorylation and hsp90 binding mediate heat shock stabilization of p53. J Biol Chem. 2003;278:2066-2071.

Wang X, Ju W, Renouard J, Aden J, Belinsky SA, Lin Y. 17-allylamino-17-demethoxygeldanamycin synergistically potentiates tumor necrosis factor-induced lung cancer cell death by blocking the nuclear factor-kappaB pathway. Cancer Res. 2006;66:1089-1095.

Wang R, Shao F, Liu Z, Zhang J, Wang S, Liu J, Liu H, Chen H, Liu K, Xia M, Wang Y. The Hsp90 inhibitor SNX-2112, induces apoptosis in multidrug resistant K562/ADR cells through suppression of Akt/NF-κB and disruption of mitochondria-dependent pathways. Chem Biol Interact. 2013;205:1-10.

Wang DH, Zhang YJ, Zhang SB, Liu H, Liu L, Liu FL, Zuo J. Geldanamycin mediates the apoptosis of gastric carcinoma cells through inhibition of EphA2 protein expression. Oncol Rep. 2014;32:2429-2436.

Watanabe G, Behrns KE, Kim JS, Kim RD. Heat shock protein 90 inhibition abrogates hepatocellular cancer growth through cdc2-mediated G2/M cell cycle arrest and apoptosis. Cancer Chemother Pharmacol. 2009;64:433-443.

Wen J, You KR, Lee SY, Song CH, Kim DG. Oxidative stress-mediated apoptosis. The anticancer effect of the sesquiterpene lactone parthenolide. J Biol Chem. 2002;277:38954-38964.

Whitesell L, Lin NU. HSP90 as a platform for the assembly of more effective cancer chemotherapy. Biochim Biophys Acta. 2012;1823:756-766.

Whitesell L, Lindquist SL. HSP90 and the chaperoning of cancer. Nat Rev Cancer. 2005;5:761-772.

Whitesell L, Mimnaugh EG, De Costa B, Myers CE, Neckers LM. Inhibition of heat shock protein HSP90-pp60v-src heteroprotein complex formation by benzoquinone ansamycins: essential role for stress proteins in oncogenic transformation. Proc Natl Acad Sci USA. 1994;91:8324-8328.

Workman P. Combinatorial attack on multistep oncogenesis by inhibiting the Hsp90 molecular chaperone. Cancer Lett. 2004;206:149-157.

Workman P, Burrows F, Neckers L, Rosen N. Drugging the cancer chaperone HSP90: combinatorial therapeutic exploitation of oncogene addiction and tumor stress. Ann N Y Acad Sci. 2007;1113:202-216.

Wu J, Liu T, Rios Z, Mei Q, Lin X, Cao S. Heat shock proteins and cancer. Trends Pharmacol Sci. 2017;38:226-256.

Xie H, Lee MH, Zhu F, Reddy K, Peng C, Li Y, Lim do Y, Kim DJ, Li X, Kang S, Li H, Ma W, Lubet RA, Ding J, Bode AM, Dong Z. Identification of an Aurora kinase inhibitor specific for the Aurora B isoform. Cancer Res. 2013;73:716-724.

Yamaki H, Iguchi-Ariga SM, Ariga H. Inhibition of c-myc gene expression in murine lymphoblastoma cells by geldanamycin and herbimycin, antibiotics of benzoquinoid ansamycin group. J Antibiot. 1989;42:604-610.

Yamaki H, Nakajima M, Shimotohno KW, Tanaka N. Molecular basis for the actions of Hsp90 inhibitors and cancer therapy. J Antibiot. 2011;64:635-644.

Yang YC, Cheng TY, Huang SM, Su CY, Yang PW, Lee JM, Chen CK, Hsiao M, Hua KT, Kuo ML. Cytosolic PKM2 stabilizes mutant EGFR protein expression through regulating HSP90-EGFR association. Oncogene. 2016;35:3387-3398.

Yao G. Modelling mammalian cellular quiescence. Interface Focus. 2014;4:20130074.

Ye M, Huang W, Wu WW, Liu Y, Ye SN, Xu JH. FM807, a curcumin analogue, shows potent antitumor effects in nasopharyngeal carcinoma cells by heat shock protein 90 inhibition. Oncotarget. 2017;8:15364-15376.

Yufu Y, Nishimura J, Nawata H. High constitutive expression of heat shock protein 90 alpha in human acute leukemia cells. Leuk Res. 1992;16:597-605.

Zetterberg A, Larsson O. Kinetic analysis of regulatory events in G1 leading to proliferation or quiescence of Swiss 3T3 cells. Proc Natl Acad Sci USA. 1985;82:5365-5369.

Zhang H, Burrows F. Targeting multiple signal transduction pathways through inhibition of Hsp90. J Mol Med. 2004;82:488-499.

Zhang Z, Ding Y, Li W, Song B, Yang R. Interleukin-17A- or tumor necrosis factor α-mediated increase in proliferation of T cells cocultured with synovium-derived mesenchymal stem cells in rheumatoid arthritis. Arthritis Res Ther. 2013;15:R169.

Zhang C, Yang C, Feldman MJ, Wang H, Pang Y, Maggio DM, Zhu D, Nesvick CL, Dmitriev P, Bullova P, Chittiboina P, Brady RO, Pacak K, Zhuang Z. Vorinostat suppresses hypoxia signaling by modulating nuclear translocation of hypoxia inducible factor 1 alpha. Oncotarget. 2017;8:56110-56125.

Zhao S, Li H, Jiang C, Ma T, Wu C, Huo Q, Liu H. 17-Demethoxy-reblastatin, an Hsp90 inhibitor, induces mitochondria-mediated apoptosis through downregulation of Mcl-1 in human hepatocellular carcinoma cells. J Bioenerg Biomembr. 2015;47:373-381.

Zheng JH, Viacava Follis A, Kriwacki RW, Moldoveanu T. Discoveries and controversies in BCL-2 protein-mediated apoptosis. FEBS J. 2016;283:2690-2700.